

COMPARING THE TIDALLY INFLUENCED FACIES IN THE
TONGANOXIE SANDSTONE IN NORTHEASTERN KANSAS WITH
MODERN ANALOGS FROM TURNAGAIN ARM OF COOK INLET,
ALASKA, USA

by

MANSOUR H. AL-HASHIM

B.S., King Saud University, 2001

A THESIS

Submitted in partial fulfillment of the
requirements for the degree

MASTER OF SCIENCE

Department of Geology
College of Arts and Sciences

KANSAS STATE UNIVERSITY
Manhattan, Kansas

2009

Approved by:

Major Professor
Allen W. Archer

Abstract

This study compares the tidally influenced facies found within the Tonganoxie Sandstone Member (Stranger Formation, Douglas Group) (Upper Pennsylvanian) of northeastern Kansas with similar facies directly observed in the upper intertidal mudflats of Turnagain Arm of Cook Inlet (Alaska, USA). The two settings contain strikingly similar facies that are characteristic of upper macrotidal estuaries with a strong influence of tidal activities. Identical aspects and features found within both settings include rhythmic vertical variation in stratum thicknesses (cyclic tidal rhythmities), high estimated sedimentation and aggradation rates, and biogenic and physical sedimentary structures (e.g., drag marks, raindrop impressions, arthropod traces and tetrapod trackways, zigzag burrows, runoff washouts, and upright trees, among others). Tidal rhythmities are the most important evidence that is indicative of the tidal influence on the depositional processes of these two study areas. Such cyclic tidal rhythmities have been reported and described from several Carboniferous settings in the eastern USA. Modern analogs to these Carboniferous rhythmities are usually found within upper macrotidal estuarine depositional environments, especially within fluvio-estuarine transitional zones. These environments are distributed over a wide range of modern latitudes. Using cyclic tidal rhythmities as modern analogs for interpreting similar ancient facies is a powerful tool for paleogeographic and paleoenvironmental reconstructions, although it is somewhat a new approach.

Table of Contents

List of Figures v

List of Tables x

Acknowledgments..... xi

Introduction..... 1

Statement of Problem..... 10

Importance of Investigation 11

Previous Work-The Pennsylvanian System of Kansas..... 17

Paleogeography of the U.S. Mid-Continent during the Carboniferous 19

Methods.....25

Study Area 29

Douglas Group 32

Geologic Setting..... 36

Sandstone Bodies of the Tonganoxie Sequence 37

Facies Assemblages of the Tonganoxie Sandstone Member..... 38

Depositional Environment of the Tonganoxie Sandstone Member 46

Ichnofossils of the Tonganoxie Sandstone Member 47

Evidence of Tidal Influence within the Tonganoxie Sandstone Succession at the Buildex
Quarry 50

Facies of the Tonganoxie Succession at Buildex Quarry 50

 Planar-Bedded-and-Laminated Facies (PBL)..... 50

 Unit A1 of the PBL Facies..... 55

 Unit A2 of the PBL Facies..... 55

Unit A3 of the PBL Facies.....	56
Channel-and-Levee Facies (CL).....	56
Discussion and Interpretation	64
Stratigraphic Sections	66
The Modern Analog.....	76
Location and General Information.....	76
Climate and Precipitation Rates.....	78
Depositional Zones	83
Tidal Influence within the Turnagain Arm.....	91
Tidal System of the Cook Inlet and Turnagain Arm.....	91
Biogenic and Physical Sedimentary Structures in Turnagain Arm	94
Internal Facies within Turnagain Arm Sediments	106
Discussion and Interpretation	107
Observations of Cyclic Tidal Rhythmites.....	110
Soft-Sediment Deformation Structures.....	120
Conclusions.....	135
References Cited	137
APPENDIX A.....	145
APPENDIX B	150
APPENDIX C	160

List of Figures

Figure 1. Fisk's (1944) model for valley development during a single eustatic cycle.	6
Figure 2. Schematic cross section of an incised valley showing the typical ranges of valley depth and width and the important role of the base level in the formation of incised valleys..	7
Figure 3. Diagram showing different types of incised-valley systems such as the piedmont and coastal plain systems along with a valley associated with alluvial plain.	8
Figure 4. Diagram showing the effect of the relative shelf position on sizes and geometries of incised valley-fills.	9
Figure 5. Percentages of oil production from different reservoirs in Kansas area.	14
Figure 6. Percentages of gas production from a number of reservoirs in Kansas.	15
Figure 7. Age and stratigraphic position of primary oil and gas producing IVF reservoirs in Kansas.	16
Figure 8. Stratigraphy of the upper Pennsylvanian System with special focus on the stratigraphy of the Douglas Group and Stranger Formation.	21
Figure 9. Diagram showing the stratigraphy of the upper Carboniferous succession in eastern Kansas.	22
Figure 10. Diagram showing the estimated eustatic sea-level changes along with global temperature variations through the Phanerozoic Eon.	23
Figure 11. Diagram showing the degree of frequency of Carboniferous glaciations.	24
Figure 12. A row of surveyor's flags along with steel washers placed on the surface of an intertidal flat.	28
Figure 13. Map of study area showing the distribution of the Douglas Group outcrop and location of Buildex Quarry.	30
Figure 14. Map of Tonganoxie paleovalley and Douglas Group outcrop.	31
Figure 15. A photo showing the north wall at Buildex Quarry.	34
Figure 16. Photo of a sandstone unit that is mineralogically dominated by quartz and muscovite described from Aelschlaeger core of Tonganoxie paleovalley fill.	35
Figure 17. Schematic cross section of the Tonganoxie incised paleovalley fill in	

northeastern Kansas showing the different types of sandstone units along with other components that comprise the filling of the paleovalley.	40
Figure 18. Block diagram representing a model of Carboniferous incised valley-fill of western Kansas and southeastern Colorado.....	41
Figure 19. Two bar charts showing bed and laminae thickness vs. bed number that were constructed based on data from the planar-stratified siltstone and the upper part of the planar cross-bedded assemblages of the Tonganoxie Sandstone.....	43
Figure 20. Photo showing a thick coal unit described from Aelschlaeger core taken from the Tonganoxie paleovalley fill succession.	44
Figure 21. Photo showing a thick paleosol from Aelschlaeger core taken from the Tonganoxie paleovalley fill succession. Note the impact of weathering on this paleosol.	45
Figure 22. Photo of tidal rhythmites taken from a roadcut exposure northeast of the Buildex Quarry.....	48
Figure 23. Two segments taken from a complete Buildex Quarry core	49
Figure 24. General view of the quarry exposure showing two walls or faces.....	51
Figure 25. View of the Tonganoxie succession at Buildex Quarry showing the Weston Shale and the Ottawa Coal.	52
Figure 26. Stratigraphic section showing the complete succession of the Tonganoxie expousre at Buildex Quarry	53
Figure 27. Two figures showing the cyclic thickening and thinning of strata in an upward direction	57
Figure 28. Bar chart showing a clear pattern of cyclicity through the lower part of the Tonganoxie succession at the Buildex Quarry.....	58
Figure 29. Three figures showing the vertical sedimentary-structure sequences (VSS) within Unit A2.	59
Figure 30. Some sedimentary structures from bedding planes of the Tonganoxie laminated siltstones, including drag marks, raindrop impacts, fish-fin drag marks, arthropod traces, and very small runnels.	60
Figure 31. Sedimentary structures and biogenic traces found on bedding planes, including fish-fin drag marks, tetrapod footprint trackway with tail drag mark, dendritic runnels, and standing-water mark.....	61

Figure 32. Physical and biogenic sedimentary structures that include foam marks, <i>Haplotichnus</i> trace fossils, <i>Treptichnus bifurcus</i> , and <i>Treptichnus pollardi</i>	62
Figure 33. More sedimentary structures, including dendritic runnel marks taken from Unit A2, irregular network on a bed surface, and several zigzag burrows.....	63
Figure 34. Stratigraphic Section Legend	67
Figure 35. Stratigraphic section of Mechaskey core.....	68
Figure 36. Photos of shales and mudstones within Mechaskey core showing variation in thickness as well as in lithology and development of lamination and planar bedding.....	69
Figure 37. Photos of fine-grained deposits from Mechaskey showing well-developed planar lamination and interlamination of mud and very fine sand.	70
Figure 38. Small section representing unit 9 of Mechaskey core and showing some details.....	71
Figure 39. Small section representing unit 12 of Mechaskey core and showing some details.....	72
Figure 40. Stratigraphic column constructed based on part of Aelschlaeger core.....	73
Figure 41. Photos of clastic coarse-grained sediments from Aelschlaeger core.....	74
Figure 42. Limestone units within described Aelschlaeger core	75
Figure 43. Map showing the location of the Cook Inlet on the south-central coast of Alaska, USA. It also shows Knik and Turnagain Arms	79
Figure 44. Location of the Cook Inlet along with some other world’s highest tide areas	80
Figure 45. Photos showing a huge area of spruce forests affected by the Great Alaskan Earthquake of 1964	81
Figure 46. Chart showing mean monthly temperature and monthly rainfall of the Turnagain Arm area	82
Figure 47. Aerial photo showing the six distinct depositional zones of Turnagain Arm .	87
Figure 48. Aerial photo showing some transitional zones within the depositional zonation of the Turnagain Arm, Cook Inlet, Alaska, USA	88
Figure 49. A view of a laterally extensive tidal mudflat at Bird Point in the Turnagain	

Arm	89
Figure 50. A cutbank exposure of soft sediment deformation and rhythmites along with an excavation showing vertically stacked cyclic alternations of silt/sand-rich and mud-drape laminae, or tidal rhythmites	90
Figure 51. Photos showing the occurrence of tidal bores and the turbulence created by such vigorous currents	93
Figure 52. Photos showing different types of ripples such as straight-crested ripples, complex ripples, and ebb-directed ripples.	96
Figure 53. Several features from upper intertidal mudflats, including zigzag burrows and fish-fin drag marks	97
Figure 54. Tetrapod trackways and footprints produced by different animals	98
Figure 55. Photos of upright trees in Turnagain Arm that are encased in upper intertidal mudflats and are underlain by thick peat layers.....	100
Figure 56. Arenicola type bioturbation and burrows along with wrinkle marks.	101
Figure 57. Some physical sedimentary structures on tidal flat sediment surfaces that include foam marks, raindrop imprints, and drip marks	102
Figure 58. Photos of mud volcanoes and drag marks that are produced by leaves and dead bugs.	103
Figure 59. Superficial burrows and traces within the Turnagain Arm, including <i>Plangtichnus</i> type burrows and traces, <i>Treptichnus</i> like traces, and arthropod tracks. ..	104
Figure 60. More structures that include swirly biogenic features, looping biogenic features, and dewatering and degassing caverns at Bird Creek.	105
Figure 61. Images of X-rayed box cores showing planar laminations within Facies A and a combination of high-flow parallel lamination and intermediate-flow cross bedding within Facies B.	108
Figure 62. Images of X-rayed box cores showing Facies C and D with high percentages of voids and rootlets.....	109
Figure 63. Tidal deposits of Upper Carboniferous Mansfield Formation and Brazil Formation of Indiana, USA.....	112
Figure 64. Photograph of a segment of Tonganoxie Sandstone core (Mechaskey), exhibiting what is believed to be tidal cycles	113

Figure 65. Photograph of two outcrops that contain strikingly similar rhythmites taken from the Carboniferous Tonganoxie Sandstone, Kansas, USA; and the Bay of Mont Saint Michel, France 114

Figure 66. Two excavations within upper intertidal flats of Turnagain Arm showing relatively thick rhythmites from 20 Mile Creek along with some thin neap-spring cycles 117

Figure 67. Excavations within upper intertidal deposits at Glacier Creek showing neap-spring cycles within mud-dominated rhythmites and neap-spring cycles consisting of flat-laminated, silty laminae interbedded with thin clayey laminae. 118

Figure 68. Two photos of thin rhythmites and thick rhythmites that exhibit thick-thin pairing known as couplets..... 119

Figure 69. Photos of the Tonganoxie Sandstone core showing different types of load structures 124

Figure 70. Two photos of the Tonganoxie Sandstone core showing slump structures... 125

Figure 71. Two segments of the Tonganoxie Sandstone core showing different types of distorted bedding..... 126

Figure 72. Photos showing convolute bedding in cutbanks within Turnagain Arm..... 129

Figure 73. Convolute bedding within Turnagain Arm rhythmites, Alaska, USA 130

Figure 74. Load structures caused by unequal loading of sands over finer-grained deposits 131

Figure 75. Load structures in uppermost intertidal flats along with some ball and flame structures 132

Figure 76. Contorted bedding within Turnagain Arm rhythmites 133

Figure 77. Ball-and-pillow structures within Turnagain Arm rhythmites 134

List of Tables

Table 1. The four types of sandstone bodies within the Tonganoxie sequence.....	42
Table 2. Protozoan assemblages yielded by shale samples from the Tonganoxie sequence	42
Table 3. The sedimentary facies of the Tonganoxie Sandstone succession exposed at the Buildex Quarry	58

ACKNOWLEDGMENTS

I would like to thank Dr. Allen Archer for his help and guidance. I am eternally grateful to him for all the time spent in the field, especially the great Alaska field trip, and for giving me the opportunity to work with him and to use his resources and lab facilities. I would also like to record my gratitude to Dr. Mary Hubbard and Dr. Jack Oviatt for their encouragement and support and for their critical suggestions. I extend my gratitude to the other members of my thesis committee, Dr. George Clark and Dr. Matthew Totten, for their help. I am indebted to Kansas Geological Survey for providing me with all the necessary cores and data.

Thanks to my best and beloved friends for their friendship and love; Ben Deaver, Maris Deaver, Mitch Trumpp, Amanda Cashman, Kody Kramer, Jessi Puyear, Christina Jones, Juli Moore, John Myers, and Kevin Unrein.

Introduction

Two types of features are generated as a result of river activities. Channels are one of those features. They usually occur as single or separate channels that have dimensions of about 10's to 100's of meters in width and up to 10 m or slightly more in depth (Van Wagoner and others, 1990). Autocyclic processes like channel avulsion, stream capture, and normal coastal progradation control these channels. However, the autocyclic processes act within each individual channel. In other words, such channels are not affected by or directly related to any regional changes in accommodation space. Therefore, these small channels typically have a limited regional extent; hence, they are not considered valleys, at least not the valleys we are considering herein. In addition, randomly distributed channels within a sedimentary sequence are also not incised valleys in the sense of sequence stratigraphy. The other types of features that are created by river systems are known as incised valleys. Many workers define these incised valleys as being elongate, erosional features that have a prominent regional extent, are larger than single channels in terms of width and depth, and are formed and incised by the action of rivers during relative sea-level fall accompanied by changes in the accommodation space (Figure 1). The precise definition, therefore, is that incised valleys are incisions formed by fluvial erosion during drop of relative base level and were subsequently filled with sediments as relative base level rises again during transgressive times (Dalrymple et al., 1994) (Figure 1, 2). They usually range in depth from few to several hundreds of feet and in width from about a half mile to tens of miles (Figure 2). Incised valley fill system (IVF) is the term being used to refer to an incised valley with its sedimentary fill.

Over the last two decades, many studies of incised valley-fill deposits have been conducted (e.g., Posamentier and Vail, 1988; Posamentier et al., 1988; Van Wagoner et al., 1990; Dalrymple et al., 1992, 1994; Blum and Törnqvist, 2000). The model suggested by Zaitlin et al. (1994) is the most accepted and widely applied model for the development of incised valley-fill systems during a transgression and the subsequent regression. Incised valleys have been known and recognized for more than 70 years, but it was not until the 1980's when these incised valleys became very well recognized and widely accepted, with some exceptions, as independent stratigraphic entities (Zaitlin et al., 1994). In particular, the development of sequence stratigraphic models in the late

1970s and 1980s caused a huge curiosity of how fluvial and other continental settings fit into a mostly marine-derived conceptual framework (Blum and Törnqvist, 2000). As a result, incised valleys rose as a focus of attention because they truncate older units, juxtapose fluvial or estuarine facies on marine deposits, and delineate an important basinward change of facies due to relative sea level drop (Van Wagoner et al., 1990). In earlier times, in contrast, incised valleys and their deposits were usually put and included within other stratigraphic units. They have been dealt with either as deltaic distributaries or as merely fluvial channels (Zaitlin and others, 1994). In addition, there was no mention about any estuarine origin or influence within their fills much less any mention regarding any tidally influenced deposits within their successions. The only exception in this regard was Wilson's study (1948) on valley fill deposits of Tennessee where he did talk about some sort of estuarine nature of the deposits, which implies an interaction or transition between marine and fluvial systems. In recent years, more attention is being directed towards estuarine paleovalley systems and tidally-influenced facies within incised valley-fill deposits because these facies provide strong evidence for relative sea-level changes or maximum flooding (e.g. Dalrymple et al., 1990, 1992, 1994; Zaitlin et al., 1994). Due to these intensive studies, the concept of incised valley-fill system is now very popular in the sequence stratigraphic framework.

Some main rationales have drawn attention to incised valley-fill systems. One of them is the growing interest in how changes in accommodation space may affect a specific stratigraphic organization, especially if we take into account that incised valleys themselves represent important decreases in the accommodation space. The second reason is the association of these incised valleys with sequence-bounding unconformities. This association makes them powerful tools for identifying important unconformities, and makes them useful even as dating means, particularly before the advent of radiometric dating techniques (Zaitlin et al., 1994). The third reason is the fact that these IVFs are excellent hosts for hydrocarbon accumulations due to their high porosity and permeability. In fact, these fills are very good hydrocarbon reservoir units in both shallow marine and nonmarine settings (Van Wagoner et al., 1990). For example, a number of oil fields in western Kentucky produce from conglomeratic sandstone reservoirs that belong to the Pennsylvanian paleovalley systems in the Illinois Basin. The Lower Pennsylvanian

Morrow sandstone units in southwestern Kansas are another example where they have produced hydrocarbons for more than six decades and are still an attractive target for more hydrocarbon exploration and development. Valley fills may also form updip seals for reservoirs within laterally adjacent strata (Wood and Hopkins, 1989). Above all, there is a scientific motivation promoting the growing investigation of IVFs such as sequence stratigraphic interpretations and environmental applications concerning global warming and associated flooding, which may negatively affect people living at the banks of huge rivers.

Fills occupying incised valleys are of two types: (1) simple fills and (2) compound fills. A simple fill means that the valley has a single depositional sequence, whereas a compound or a complex fill indicates that the valley contains multiple depositional sequences or cycles. This stratigraphic disparity is mainly controlled by depth of incision and rate of sediment input (Zaitlin and others, 1994). Deeper valleys and lower rates of sedimentation are commonly associated with compound fills while shallower incisions with rapid sedimentation rates usually yield single or simple sequences. The mechanism of deposition by which incised valleys are filled can be divided into three different kinds of processes: progressive backfilling, progressive downfilling, and vertical aggradation filling. A significant rise in base level produces a progressive backfilling valley. On the other hand, a major increase in sediment supply, either caused by uplift in the source area or by a change in climatic conditions, produces a progressive downfilling valley. The vertical aggradation filling occurs when there is an increase in sediment production caused by many tributaries feeding into the valley, which is also related somehow to climatic variations (Schumm, 1977).

Incised valleys are classified into two major types. The first types are incised valleys that develop as a response to the fall of relative sea level which, in turn, caused by eustatic sea-level fall or tectonic uplift of the coastal zone (Figure 1, 2). The other types are incised valleys that form as a result of erosion caused by either tectonic uplift of an inland area or by an increase in fluvial discharge due to climatic changes (Schumm and Brakenridge, 1987). In other words, there are valleys that are related to relative sea-level changes such as Piedmont and coastal-plain incised valley systems, and there are systems that are not related to relative sea-level changes such as those associated with alluvial

plains (Figure 3). In fact, most of the work has been done on incised valleys that belong to the first class, and less attention was paid to incised valleys of the second class, although both of them are common at present time. The main reason of this bias is ascribed to the difference in the stratigraphic importance between these two types of incised valleys. For example, incised valleys related to relative sea-level fall are connected with regional sequence-bounding unconformities of type 1 (Van Wagoner and others, 1990); in addition, they are affected by marine processes along some of their parts. These two advantages are very useful especially when applied to sequence stratigraphic interpretations. On the other side, incised valleys that are not related to and not generated by relative sea-level fluctuation lack such association with sequence-bounding unconformities, and they usually occur within fluvial successions and contain terrestrial deposits, which makes their recognition somewhat difficult especially in older successions (Zaitlin et al., 1994). Therefore, incised valleys of the first class are stratigraphically more important than those of the second category according to Van Wagoner et al. (1990), and their identification is dependent on the recognition of sequence-bounding unconformities.

Based on sequence stratigraphic models, the formation of incised valley fills (IVFs) relates directly to sea-level changes over time. This fluctuation in sea level is considered the main control of the formation of valley fill deposits (Figure 1). Simply, when sea level falls, rivers erode and incise rapidly and deeply into the underlying beds, leaving elongate channels and valleys that extend basinward. Then, as sea level rises again, these incised valleys become flooded and filled with sediments making continuous sand bodies that usually acquire the geometric shapes of previously formed valleys (Figure 1, 2). However to cause incisions, the fall of the sea level must cause subaerial exposure of surfaces such as shelves that are steeper than the longitudinal gradient of the river system itself (Figure 3) (Posamentier et al., 1992). If the sea level did not drop sufficiently to expose the shelf, river incision may not occur. Other controls contributing to the formation of IVFs include climate, lithology of the underlying strata, and basement structure (Archer and Feldman, 1995). For example, rivers erode more deeply during wetter periods than during drier times. Thus, the development of incised valleys is not expected during middle and late Permian, which is famously known to be a dry period.

Climate, therefore, can be seen as a temporal indicator to the existence of incised valley fills while eustatic sea level fluctuation is a geometric control. Nevertheless, variations in climate can be powerful to the degree that they may have influenced the sizes of some incised paleovalleys as well as their fills. The best example of that comes from the Upper Carboniferous of eastern Kansas where large-scale paleovalleys with basal conglomerates and quartz-rich sandstones have been related to wetter intervals while smaller-scale paleovalleys that lack such basal terrigenous deposits were associated with drier climates (Archer, in press). The relative position on the depositional shelf has also a great impact on the scale of paleovalleys. Large-scale paleovalleys usually characterize foreland basins, whereas smaller paleovalleys are formed on the shelf (Figure 4). In addition, incised valleys become wider and deeper as we move from the upper shelf basinward (Archer and Greb, 1995) (Figure 4). Even though it seems as if there is only one process responsible for the formation and existence of incised valleys, a fluvial valley undergoes several processes and evolves from a small-incised channel to a huge valley in an evolutionary style (Figure 1).

This thesis will be dealing with tidally influenced facies found within a Pennsylvanian incised valley fill succession. Such facies are usually observed near the upper parts of incised valley sequences (Figure 2). Tidally influenced deposits are of high interest because they represent a transitional depositional environment between fluvial environments that affect the lower deposits of the successions and estuarine and marine environments that dominate and influence the uppermost facies. We will then support our observations and results with examples taken from a modern macrotidal setting. A question might arise about the relationship between modern macrotidal environments and incised paleovalleys. It appears that incised paleovalley systems were dominated by macrotidal conditions exactly like the conditions that are now taking place in modern macrotidal systems (Archer 2004).

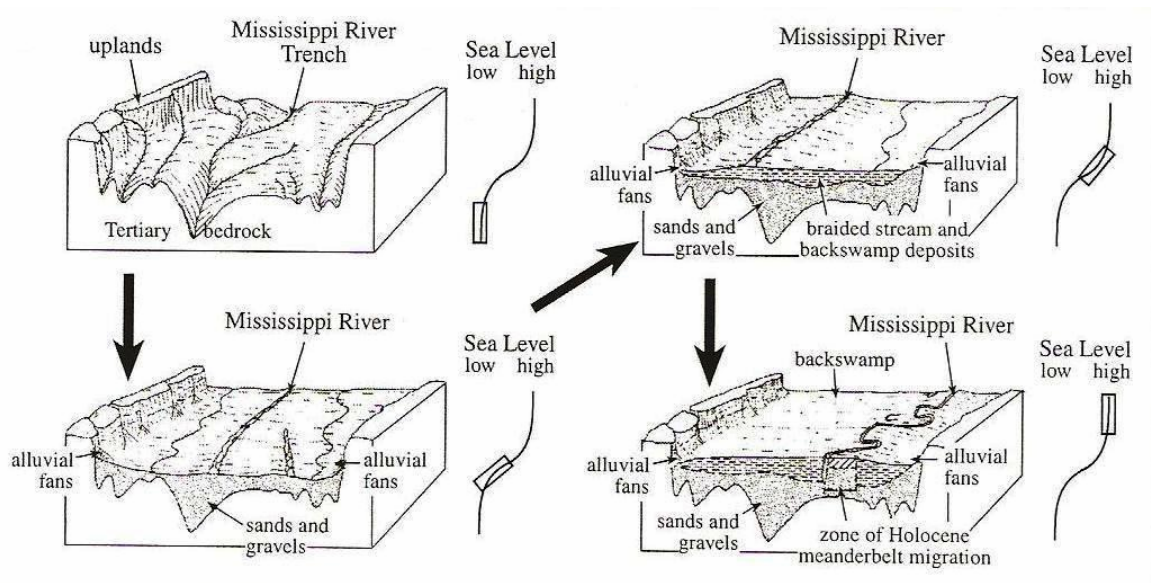


Figure 1. Fisk's (1944) model for valley development during a single eustatic cycle, based on the Mississippi river system. Note the incision during sea-level fall and the subsequent filling during sea-level rise and highstand. Also, note that the filling takes place in different stages (from Blum and Törnqvist, 2000).

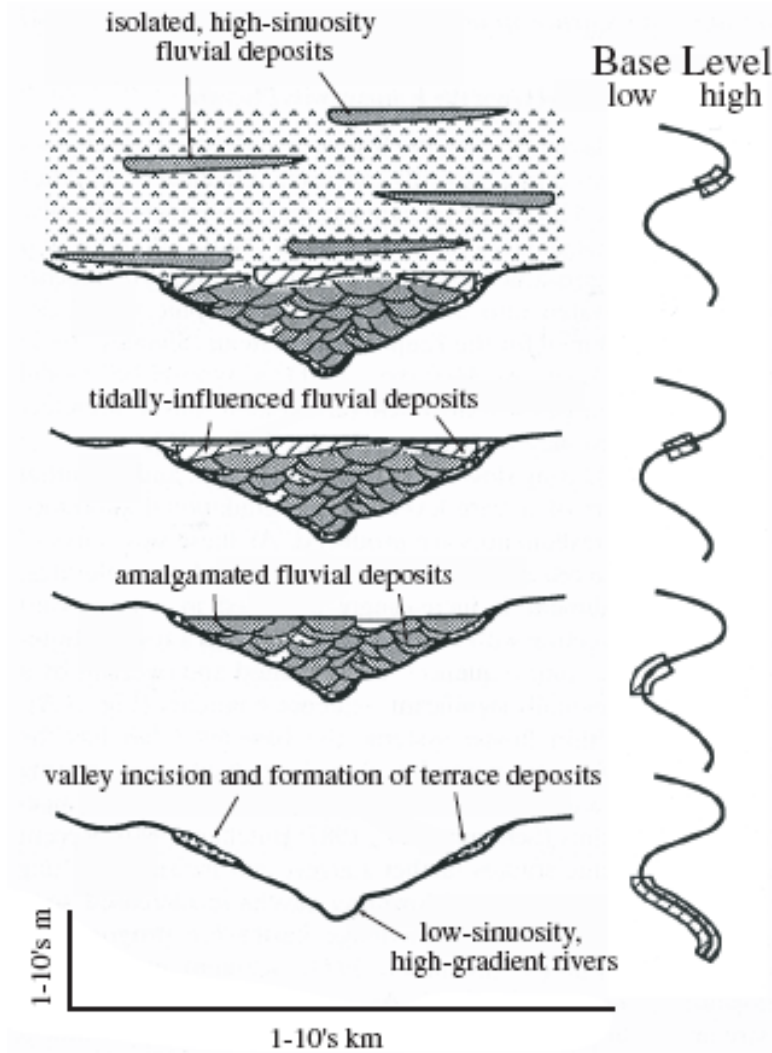


Figure 2. Schematic cross section of an incised valley showing the typical ranges of valley depth and width and the important role of the base level in the formation of incised valleys. Note the incision during base level fall and the subsequent filling during base level rise (from Blum and Törnqvist, 2000).

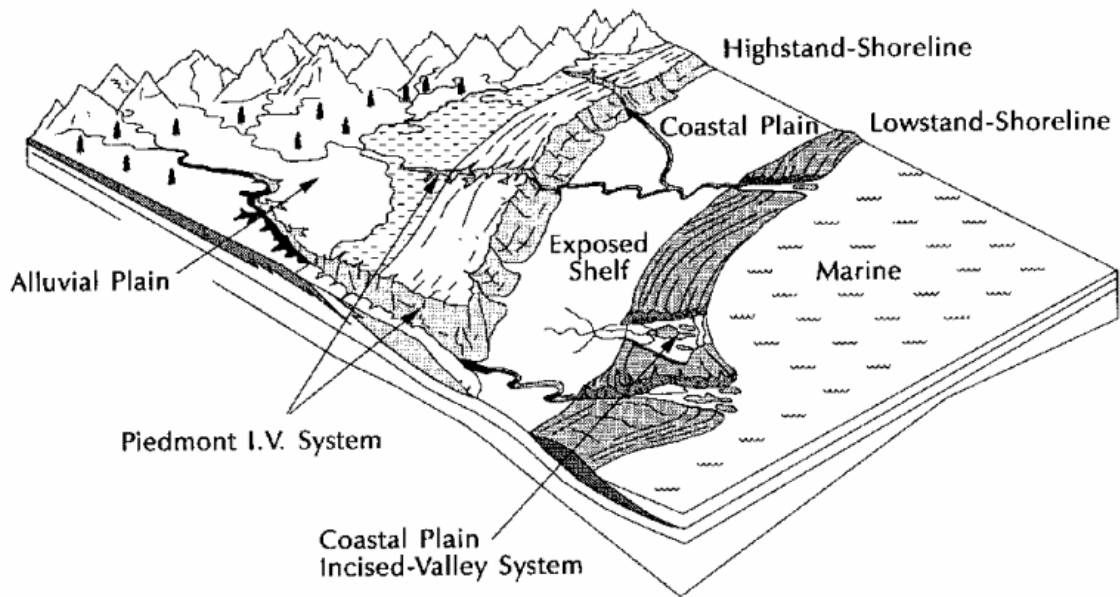


Figure 3. Diagram showing different types of incised-valley systems such as the piedmont and coastal plain systems along with a valley associated with the alluvial plain. Note the exposed shelf that implies a sufficient drop in the sea level (from Zaitlin et al., 1994).

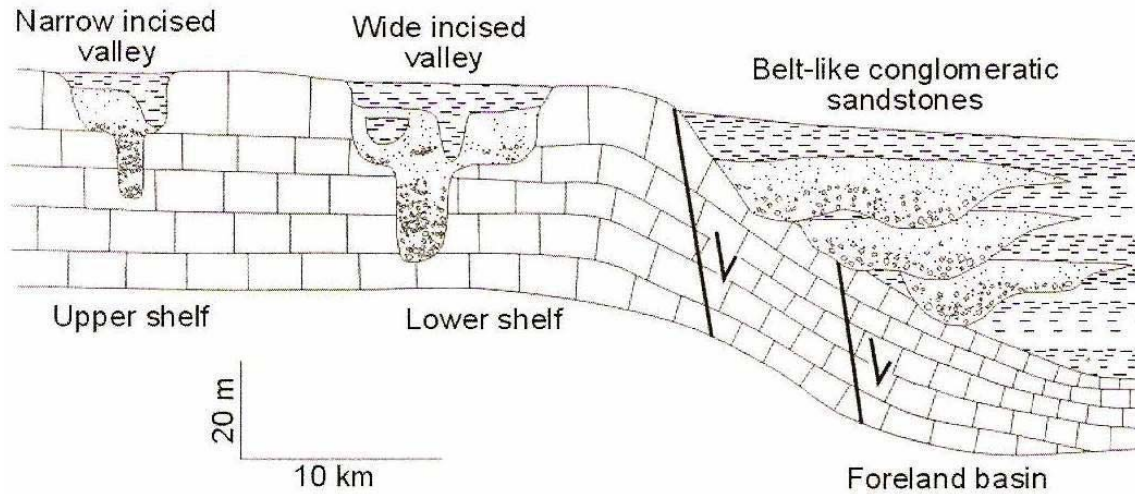


Figure 4. Diagram showing the effect of the relative shelf position on sizes and geometries of incised valley-fills. Note the increase in valleys' width and depth as we move basinward. Also, note the relationship between the fluvial deposits that fill the valleys and the underlying marine units (adapted from Archer and Greb, 1995).

Statement of Problem

Incised valley fill systems are very important as hydrocarbon reservoirs, but they also may exhibit internal heterogeneities. This local heterogeneity could minimize the overall hydrocarbon production and recovery rates because as mud content varies so does reservoir quality. In other words, production rates and recovery efficiencies of hydrocarbons depend mainly on the spatial distribution of reservoir properties which, in turn, depend on the presence and quality of porosity and permeability, among others. It is no secret that these two reservoir properties, especially the porosity, are highly affected by mud content. We also know that valley-fill successions gradually become muddier upward; hence, the upward increase of mud content within valley-fill systems is expected. However, the problem arises when reservoir sandstones of valley fills shift laterally into muddy sandstone facies or shales in seemingly unpredictable way. What makes the problem even more complicated is that seismic reflection data usually cannot resolve reservoir from nonreservoir valley-fill deposits because although modern three-dimensional reflection seismic data surveys are very good at delineating paleovalleys, the recognition of facies changes remains beyond the limits of seismic resolution (Feldman et al., 1995; Bowen et al., 1993). The difficulty of predicting reservoir heterogeneities by using log and seismic data comes also from the resolution of these techniques, which is usually insufficient to image reservoir-scale variability. Besides heterogeneity, the distribution, continuity, and location of sandstone bodies within each particular paleovalley fill succession may also affect the production rate, secondary recovery, and overall reservoir quality (Bowen et al., 1993). The other problem is that paleovalley facies interpretations resulting from field studies usually suffer from limited core data and lack of core control. Outcrop investigations lack three-dimensional controls as well (Feldman et al., 1995).

Many models have been proposed in order to figure out these problematic issues and to better understand the stratigraphic complexities of these systems for the sake of enhancing the performance of paleovalley reservoirs and, hence, maximizing the output from these valuable resources. These models are considered as an attempt to understand the depositional context and internal architecture of these paleovalley systems (e.g. Dalrymple et al., 1992, and Zaitlin et al., 1994). Fortunately, these valley fill systems that

we have been talking about have many similarities in common with valley-fill models, but they have important differences as well (Bowen et al., 1993). Some of these models have highlighted the potential sources of the heterogeneity. For example, several proposed models have suggested that the heterogeneity within complex paleovalley fills could be the result of multiple incisions where new incisions cut apart the previously formed continuous sandstones. Nevertheless, most of these models agreed upon the fact that the valley incision took place during a lowstand, and a subsequent transgression was responsible for valley filling, creating a succession of fluvial and/or estuarine facies at the base passing upward into more marine-influenced facies (Figure 2, 17). The local heterogeneity within incised valley reservoirs can be overcome by integrating outcrop stratigraphic models to subsurface log and seismic data, which means integrating rock properties and well log signatures. Better understanding of reservoirs in general and IVF reservoirs in particular depends on application of new ideas, advanced technologies, and traditional knowledge. We believe that comparison of ancient IVF systems to modern analogs is a promising approach not only to predict their internal architecture and facies changes but also to have insights about their origin, nature, depositional environments, and all the processes involved in their development.

Importance of Investigation

Incised valley fills are very important constituents of the stratigraphic record especially as petroleum exploration targets in spite of the fact that they represent only a volumetrically small segment of the sedimentary record (VanWagoner et al., 1990; Dalrymple et al., 1994). In Kansas, for instance, Pennsylvanian sandstone reservoirs that fall into the category of incised valley deposits have produced more than 220 million bbl of oil and 1.7 tcf of gas (Feldman et al., 1995). It is estimated that 15% of all oil-producing reservoirs and 28% of all gas-producing reservoirs in the state of Kansas are of IVF type (Figure 5, 6). Moreover, around 50% of lately discovered oil reservoirs and 70% of gas bearing reservoirs are within incised valley fill deposits. However, this production rate can be further enhanced with new discoveries and by using advanced production techniques. IVF reservoirs in Kansas are primarily Mississippian to Permian in age, and they range in depth from 2,000 to 6,000 feet (Figure 7). Although both oil and

gas reservoirs are commonly found in Morrowan rocks, oil reservoirs are particularly hosted within Cherokee and Chester rocks while gas reservoirs tend to concentrate in Atoka and Cherokee deposits. Sediments of these IVF reservoirs are described as porous and permeable rocks confined in fine-grained marine sediments, making a characteristic reservoir deposits. To put it in the context of the Tonganoxie sequence, as we shall see, the conglomeratic and trough-and-planar cross-bedded assemblages represent excellent reservoir facies because they are interconnected very well in addition to their lack of mud, which means having high porosity. This scenario has been documented also in Pennsylvanian Morrowan valley-fill deposits where most of the production comes from coarse-grained, permeable fluvial deposits that filled a paleovalley incised into the underlying fine-grained and less permeable estuarine and marine facies. Several oil fields in western Kentucky also produce from coarse-grained conglomeratic sandstone reservoirs within Pennsylvanian incised valley fills. In fact, IVF reservoirs are not just important and widespread within the Pennsylvanian but also within other geologic periods. For example, valley-fill deposits of the Lower Cretaceous Muddy Sandstone contain significant hydrocarbon accumulations and represent an important exploration target in Wyoming's Bighorn, Powder River, and eastern Wind River basins. Examples of incised valley fills containing hydrocarbon accumulations are abundant and widespread both spatially and temporally. To emphasize this importance, the Lower Pennsylvanian Morrow sandstone units in southwestern Kansas have been producing hydrocarbons for more than six decades, and still represent an attractive target for hydrocarbon exploration and development (Salcedo and Carr, 2003). Incised valley fill reservoirs are not restricted only to Kansas area and some other neighboring states, but are found throughout North America, accounting for billions of barrels of oil and trillions of cubic feet of gas (Bowen et al. 1993).

Besides having porous and permeable deposits that are so important as reservoirs, these paleovalleys contain shales that could form seals for other adjacent reservoirs (Bowen et al., 1993). This is another reason to make them attractive drilling targets. Pennsylvanian incised valleys have also been connected with economic coal deposits that further enhance their economic importance (Bowsher and Jewett 1943; Archer et al., 1994a). In addition, they contain valuable information on regional depositional processes

and sea-level changes. The good news about these IVF reservoirs is that their stratigraphic occurrence can be predicted based upon paleogeographic studies together with observations of modern depositional analogs and, of course, with the help of advanced 3-D seismic techniques. Precisely, incised valleys and their sedimentary fills have been associated with rapid sea level falls; hence, an important factor when exploring for IVF reservoirs is the recognition of such rapid drops in the sea level within the stratigraphic record. Moreover, theoretical considerations and direct observations of numerous modern incised valley systems suggest that it is possible to predict the stratigraphic organization of the entire valley fill, especially its estuarine deposits that have a complex three-dimensional nature (Zaitlin et al. 1994).

Sequence stratigraphic studies have suggested fluvial to estuarine origin of these IVF reservoirs. This implies that even though these incised valleys are filled with sediments that possess reservoir properties, they may still have some important internal inconsistencies. For instance, fluvial facies found in incised valleys are more permeable than estuarine sediments, and they have lower clay content. Yet, these fluvial deposits are laterally and vertically very heterogeneous which means they could unexpectedly pass from sandy (highly productive) facies into more muddy (nonreservoir) facies (Figure 9, 17). This is usually referred to as local heterogeneity, and it may result even from short-distance changes in the sandstone units and pore geometries. This internal heterogeneity is of particular concern when it comes to oil production, reservoir development, and secondary recovery. Therefore, better understanding of the depositional environment and internal architecture of these deposits is critically needed for continuing success in exploration for new IVF reservoirs and for increasing recovery from already discovered reservoirs of this type.

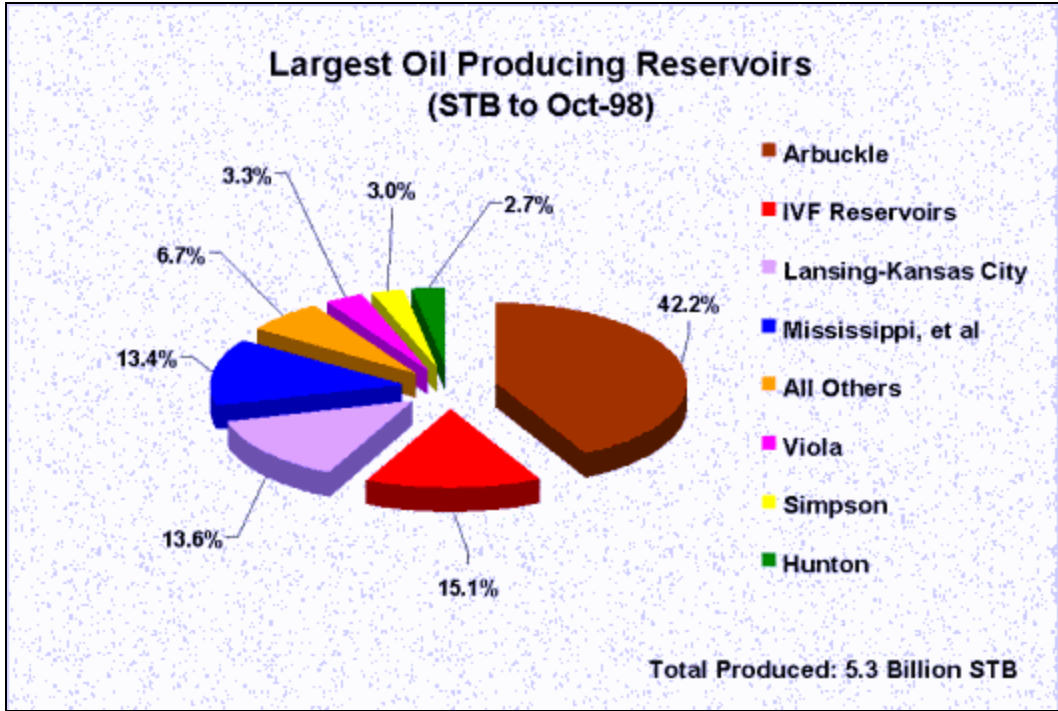


Figure 5. Percentages of oil production from different reservoirs in Kansas area. According to this diagram, the IVF reservoirs are the second major oil-producing reservoirs in Kansas (Gerlach, 2000).

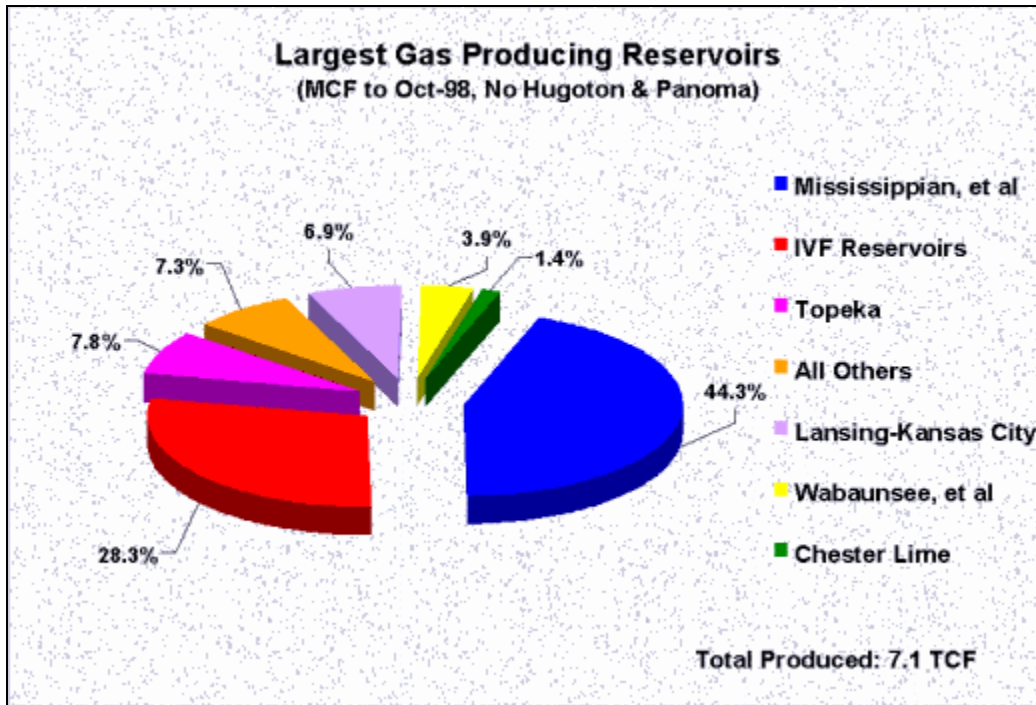


Figure 6. Percentages of gas production from a number of reservoirs. The production of gas from IVF reservoirs in Kansas is the second highest according to this diagram (Gerlach, 2000).

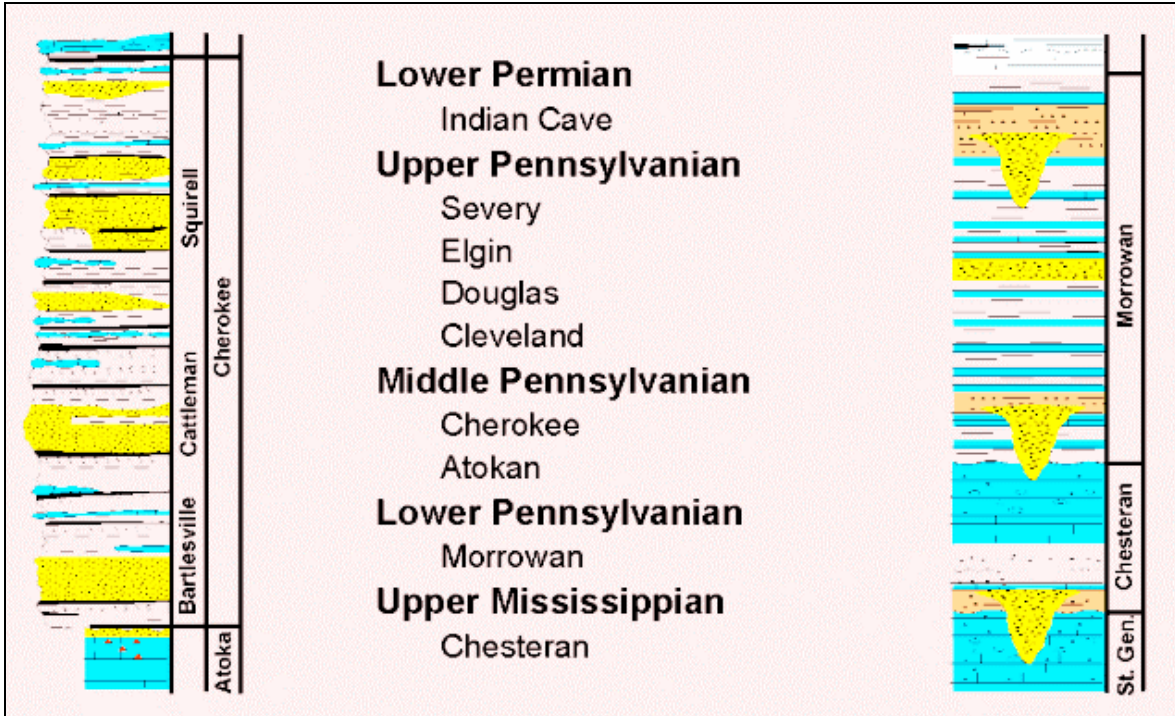


Figure 7. Age and stratigraphic position of primary oil and gas producing IVF reservoirs in Kansas. Producing IVF reservoirs range in age from Upper Mississippian (Chesteran) up to Lower Permian (Indian Cave) (Gerlach, 2000).

Previous Work-The Pennsylvanian System of Kansas

Pennsylvanian system is grouped into five series, and the Missourian and Virgilian Series represent the topmost parts of this system. These five series include both exposed Pennsylvanian rocks in Kansas and subsurface deposits that underlie all areas of central and western Kansas. Virgilian rocks are very well and extensively exposed especially in eastern Kansas. Virgilian Series encompasses three main groups (in an ascending order): Douglas, Shawnee, and Wabaunsee (Figure 8, 9). The accessibility and continuity of Virgilian rocks make the Upper Pennsylvanian System attractive to many workers in Kansas, and in some neighboring states as well ,because they can easily trace and recognize the cyclic sedimentation within these successions. In addition, the Upper Pennsylvanian also has noticeable facies variations and characteristic assemblages of faunas compared to adjacent strata and older parts of the system (Moore, 1949).

Organized stratigraphic work on Carboniferous rocks dates back to the middle of the nineteenth century, when Meek & Hayden (1859) first studied Pennsylvanian rocks of the Kansas River Valley. Ever since, Pennsylvanian rocks in the state of Kansas, including siliciclastic units, have been studied extensively by many workers (e.g. Bass, 1936; Mudge, 1956; Tarr, 1934). Among these studies were many focusing on the depositional and environmental aspects of these rock units both in Kansas and in adjacent states such as Moore (1950); Wanless and Weller (1932); and Lins (1950). We can conclude that the main reasons for conducting the majority of these studies were environmental and paleogeographic along with stratigraphic motivations. Part of that work can also be attributed to the economical importance of these rocks especially regarding their association with coal resources in Kansas (Bowsher and Jewett, 1943).

Based on analyses of their sedimentary features, Pennsylvanian rocks in Kansas are believed to have been deposited on stable regions or platform areas of the continent (Moore, 1949), which explains the fact that most of these units are thin and laterally continuous (Figure 9). These rocks have cyclic successions of limestones, shales, and thin sandstones along with some coal beds (Figure 8). The limestones and the majority of the shales, especially organic-rich laminated black shales, are of marine origin and are believed to have been deposited during intervals of higher sea level (Figure 10). Therefore, they are interpreted as being the highstand components of the depositional

succession. This interpretation is largely based on studying the fossils of these units and their assumed paleoecology. Subsequently, sequence-stratigraphic studies have supported this assumption as well. On the other hand, the sandstones, coals, and some of the shales are of non-marine origin. They were most likely deposited within tidal-estuarine and deltaic depositional environments (Archer et al., 1994a). From a sequence-stratigraphic point of view and compared to the marine facies, these siliciclastic facies represent the lowstand components of the sequence. Generally, marine strata are less prominent than their non-marine counterparts. Despite the thinness of these marine units, they are very important components of the Pennsylvanian section in eastern Kansas and other areas of the northern mid-continent. This kind of alternation between marine and nonmarine strata within Carboniferous rocks demonstrates the type of cyclic sedimentation that is very well known as Pennsylvanian or Carboniferous Cyclothems of the U.S. Mid-Continent (Wanless and Weller, 1932).

Cyclothems typically range in thickness from a few meters to tens of meters, although some of them cover much of the mid-western USA (Heckel, 1986). This cyclic sedimentation was first documented in the Illinois Basin within upper Paleozoic strata in the state of Illinois; then, it was noted within age-equivalent rocks of Kansas and elsewhere. Consequently, several cyclothem models have been derived from these basins such as the Illinois-Basin Cyclothem and Kansas Cyclothem. A special attention was given to the contribution of glacio-eustasy, climate, and tectonism to the development of cyclothems (Heckel 1986; Cecil 1990). These cyclothems have been interpreted to be the result of Gondwana glaciations, which generated sea level changes estimated to be tens of meters over time intervals of a few hundred thousand years or even less (Figure 10). In addition, there were relative sea level changes induced by tectonism (Heckel, 1986; Gibling and Wightman, 1994). Later, however, many workers became more interested in studying these Carboniferous units and cyclothems by using concepts of sequence stratigraphy rather than the cyclothem concept. This is because although standard cyclothem models have served as good models for marine, carbonate-dominated portions of the Pennsylvanian succession, they have significant limitations and drawbacks when it comes to the study of terrigenous portions due to their lack of lateral continuity caused by unconformities (Archer, in press). In this research, however, we will not concentrate on

describing the cyclothem model or investigating its suitability, applicability, or even validity. Instead, we will try to focus on tidal rhythmites found within the Upper Pennsylvanian Douglas Group of Kansas. Fortunately, Kansas has almost a complete succession of these Upper Pennsylvanian units. The Pennsylvanian rock record also reveals some significant non-deposition or erosion periods. These periods usually manifest as disconformities that are almost always associated with sequence boundaries that separate the subdivisions of the Pennsylvanian System. In fact, the Upper Pennsylvanian System itself is confined by an underlying disconformity and an overlying disconformity to angular unconformity that separates Pennsylvanian beds from Permian strata (Moore, 1949).

Paleogeography of the U.S. Mid-Continent during the Carboniferous

Paleogeography and palaeoclimate of the U.S. Mid-Continent during the Carboniferous, especially during the Pennsylvanian, are very important in order to fully understand and make sense of the cyclic nature of Pennsylvanian rocks. Paleogeographic reconstructions show that the U.S. Mid-Continent was located very close to the equatorial paleolatitudes (Archer and Feldman, 1995; Archer and Greb, 1995). As a result, several conditions existed during the Carboniferous and affected the deposystems of the U.S. Mid-Continent. The most important and influential conditions and events are the large-scale continental glaciations, valley incisions resulting from sea-level changes, and the possibility of extremely high coastal tides. During the time interval of early Carboniferous (Mississippian) to the Permian, there were major glaciations taking place (Figure 10, 11). Very high rates of recurrence characterized these glaciations especially during the upper Carboniferous and lower Permian (Figure 11). The overall conditions during the Pennsylvanian along with glacio-eustatic cycles resulted in alternations between exposures during regression times caused by glaciations and flooding during succeeding transgression periods generated by deglaciation and melting (Figure 10). This Carboniferous glacio-eustacy has affected a huge area of the Mid-Continent known as the craton. This is very similar to the glacial-interglacial oscillations that characterized the Pleistocene-Recent interval. When a regression takes place, fluvial systems start to incise into the underlying strata, and they carry with them massive amounts of sediments. These

sediments eventually fill valleys as deep as 40 m. However, at the same time, weathering, especially chemical weathering, was acting intensively due to the tropical, humid climate that was prominent during the Pennsylvanian throughout the U.S. Mid-Continent (Archer and Feldman, 1995). This type of weathering is responsible for generating mud-rich sediments that filled the drainage networks of the previously incised valleys. This wet climate assumption is supported by the abundance of surfaces with raindrop impressions found within the exposure of the Tonganoxie Sandstone Member at the Buildex Quarry. During transgression periods, incised valleys get flooded, and muddy estuaries develop. These floodings are believed to have been caused by Pennsylvanian shallow seas known as epi-continental or epeiric seas (Wells et al., 2005). Thus, the succession undergoes a transition from fluvial to estuarine facies, and further transgression can form marine facies as well (Archer et al., 1994a). These estuarine successions contain thick mud-draped bedforms, which require very high tidal ranges in order to form. Based on modern observations, such high tidal ranges usually occur in environments where macrotidal conditions are the main controlling agents of deposition. One of these high-tide areas is the Cook Inlet of Alaska, USA.

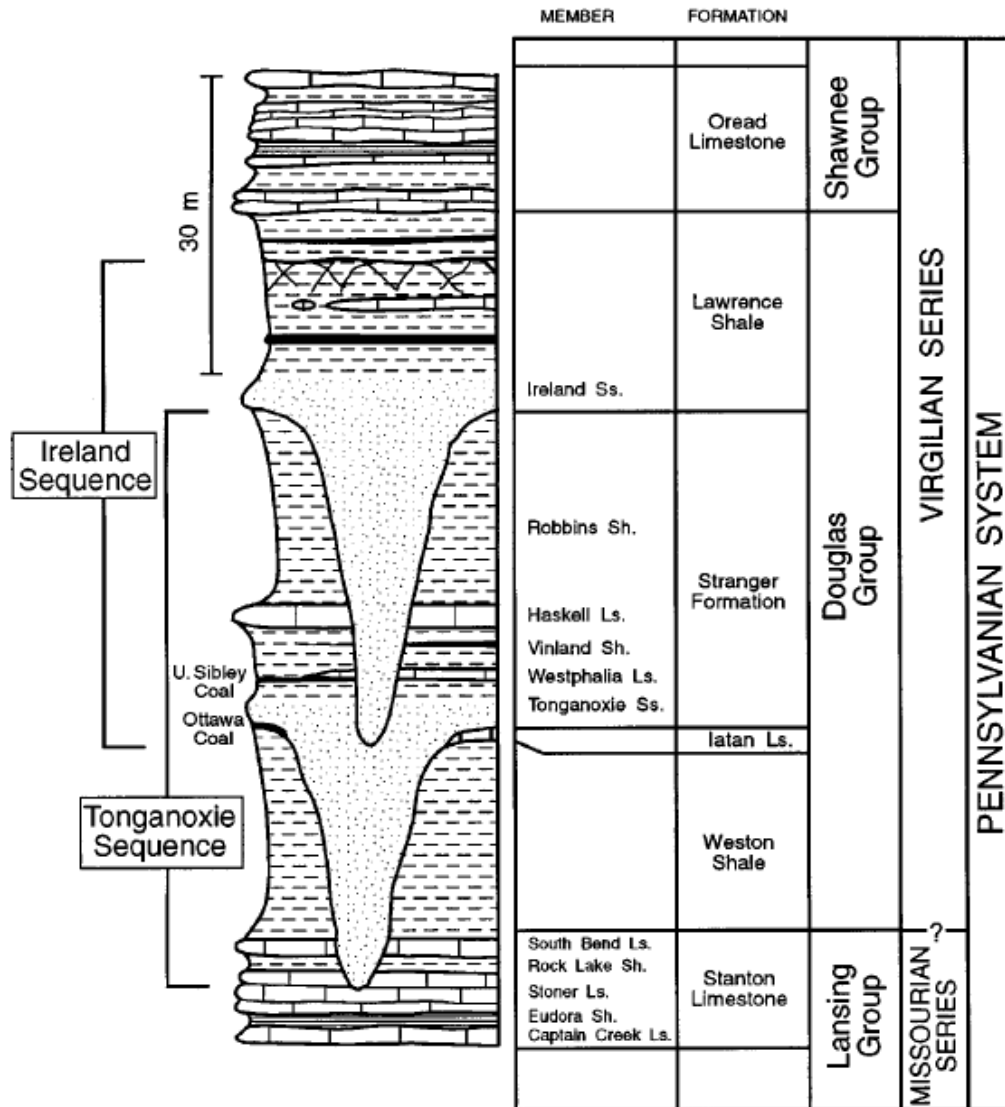


Figure 8. Stratigraphy of the upper Pennsylvanian System with special focus on the stratigraphy of the Douglas Group and Stranger Formation. Note the two valley-fill sequences (Tonganoxie and Ireland) (adapted from Feldman et al., 1994b).

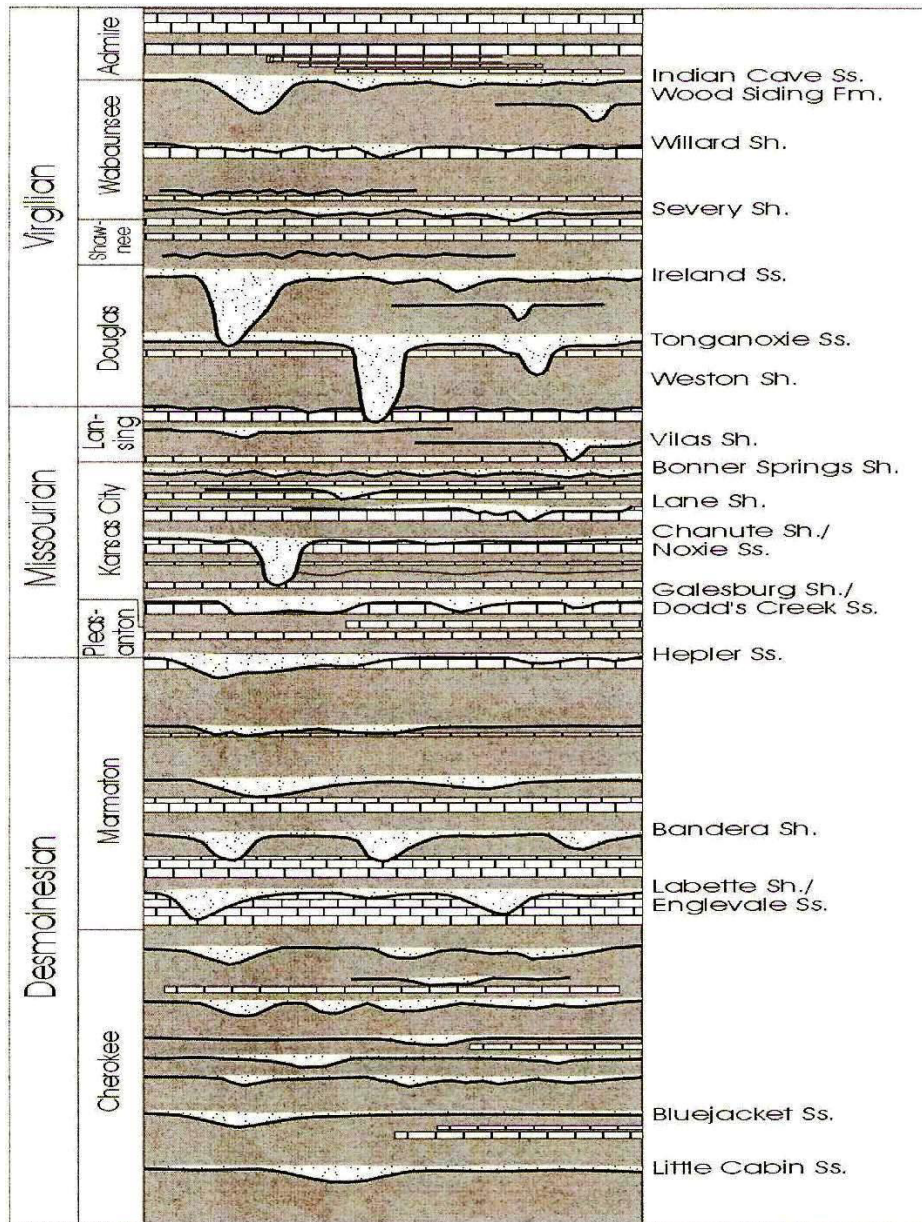


Figure 9. Diagram showing the stratigraphy of the upper Carboniferous succession in eastern Kansas. Note the difference between marine limestone units and nonmarine sandstone units. The limestone-rich strata are laterally continuous while there is a high degree of lateral heterogeneity within the sandstones. Also note the disconformable relationship between sandstone-rich units and the underlying units (from Archer, in press).

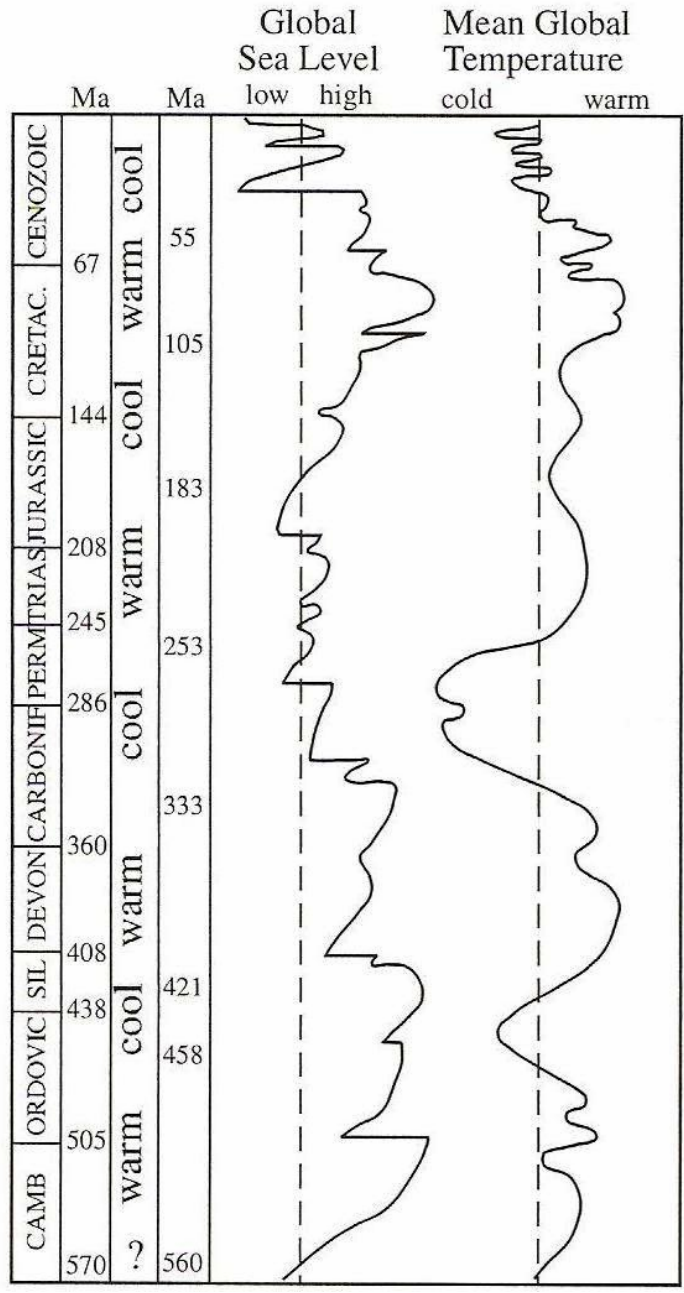


Figure 10. Diagram showing the estimated eustatic sea-level changes along with global temperature variations through the Phanerozoic Eon. Note the fluctuation of sea level during the Carboniferous especially during the Pennsylvanian due to Gondwana glaciations and deglaciations (from Blum and Törnqvist, 2000).

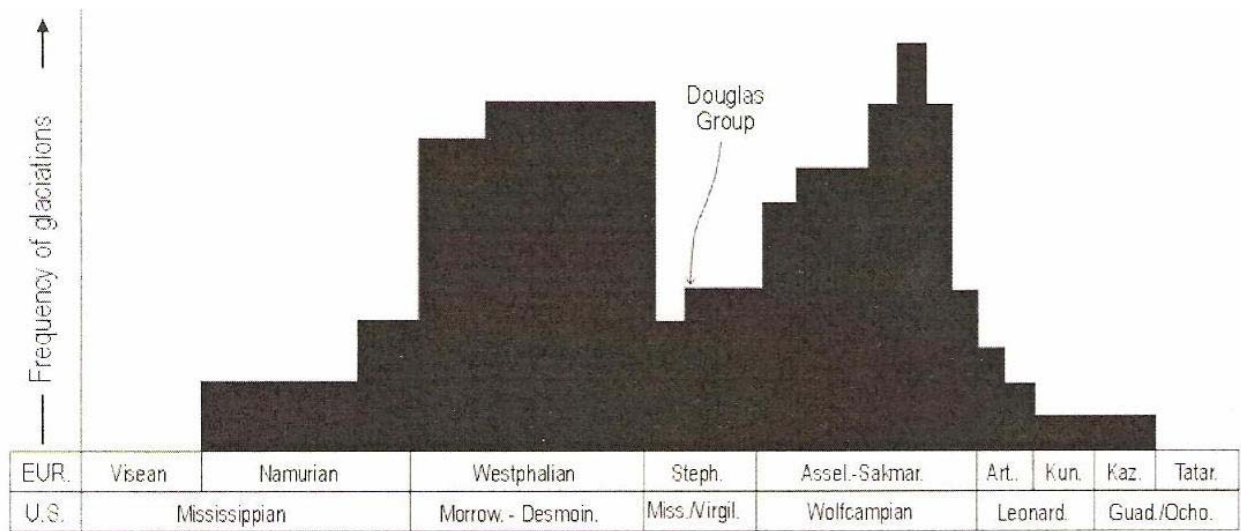


Figure 11. Diagram showing the degree of frequency of Carboniferous glaciations. Note the highest frequency glaciations that took place during the Morrow through Desmoinsian and during the Wolfcampian time. Note also the Douglas Group of Lower Virgilian that was formed during a low frequency of glaciation events (from Archer, in press).

Methods

This work is an attempt to compare the results of the processes that were acting during the deposition of the Tonganoxie Sandstone Member of upper Pennsylvanian (Late Carboniferous) with similar features found in a modern depositional environment where sedimentation mechanism is almost fully understood or at least can be observed and modeled (see Archer 1995, Archer and Johnson 1997). Thus, the concept of uniformitarianism, which is usually summarized in the statement: the present is the key to the past, is our basic theoretical method. The second step towards conducting an accurate and fair comparison is to clearly define the criteria that can be used to select the most suitable modern analog from several available and applicable ones. In general, the best modern environments that appear to be analogous to the Tonganoxie Sandstone are located within upper tidal flats of macrotidal settings especially at or near fluvial-estuarine zones (Archer, 2004). Interestingly, coastal geometric shape of some modern settings can be indicative of such potential analogous environments; for instance, most of the modern estuaries that seem analogous to the Tonganoxie are funnel-shaped entities. This sort of geometry allows for significant tidal range amplification at fluvial-estuarine transitions (Lanier et al., 1993). The Tonganoxie has been previously compared to some modern macrotidal settings such as the Bay of Fundy, Canada, and Bay of Mont Saint-Michel, France (Dalrymple et al. 1991, Archer and Johnson 1997, Archer 2004, and Tessier et al. 1995). However, essential differences have been found between these two modern estuaries and the Tonganoxie of Kansas. Therefore, the Turnagain Arm of Cook Inlet, Alaska, has become an option. Just to emphasize the scattered nature of such environments, the Changjiang (Yangtze) River of China was also considered at first but then excluded.

This investigation of Tonganoxie Sandstone facies is based on laboratory core studies and some comprehensive previous work that was conducted on this Pennsylvanian paleovalley fill. Many workers have studied the Tonganoxie Member of Kansas especially with regard to its ichnology, depositional environment, stratigraphic architecture, and palaeotidal system. The most thorough and detailed studies that are essential to ongoing research are Lanier et al. (1993), Feldman et al. (1995), Archer (2004), Archer et al. (1994b), and Buatois et al. (1998). During laboratory work, a total of

285 feet of subsurface cores were measured, described, and photographed on unit-by-unit basis (Appendix B). These cores were provided by Kansas Geological Survey, and were taken from two wells within the trunk paleovalley. The total thickness of Mechaskey core is about 145 feet, and the thickness of Aelschlaeger core exceeds 140 feet. Two major stratigraphic sections have been constructed afterward based on these core investigations (Figure 35, 40). In addition, two small columnar sections have been also constructed (Figure 38, 39). The aim of these minor sections is to closely show the systematic vertical variations in laminae thicknesses that were found within some units of the Mechaskey core (Figure 37). Adobe Illustrator 8.0 was used for this purpose.

Three procedures were adopted during the course of this investigation of the modern analog. They include direct observations, direct measurements, and subsequent analysis, discussion, and interpretation. A field trip to the Turnagain Arm of Alaska was conducted in the summer of 2006 (August 3-18, 2006). In Turnagain Arm area, particularly on top of its upper intertidal mudflats, we have observed a variety of biogenic and physical sedimentary structures such as burrows, wrinkle marks, foam marks, raindrop imprints, drip marks, mud volcanoes, and drag marks. The following structures have been observed: *Plangtichnus* type burrows and traces, *Treptichnus* like traces, arthropod trails and tracks, Swirly biogenic features, looping biogenic features, and dewatering and degassing caverns. In addition to these shallow surficial features, spectacular cyclic tidal rhythmites and soft-sediment deformation structures (SSD) have been documented within upper intertidal flats of Turnagain Arm. Most importantly, observations have documented the impact of some forces acting within this tide-dominated estuary, such as tidal bores and associated high current velocities on the deposition. This first-hand observation of all these features right from their original depositional environment and not so long after their formation coupled with subsequent comparison to similar ancient structures from the Tonganoxie Sandstone is very important and useful approach for understanding the depositional conditions of both the modern and the ancient settings. In fact, this fieldwork provides real insights into modern macrotidal estuaries in general.

Some direct measurements have been taken during the fieldwork. Accumulation rates were evaluated at several sites, including Tidal Bore, Bird Point, Peterson Creek, Girdwood, and Portage Creek. Measured rates within these sites range from zero or no

accumulation data up to one foot. The average ranges from about 6 to 8 inches at some locations and from 2 to 4 inches at others (Appendix A). For the purpose of measuring sedimentation rates within intertidal flats of Turnagain Arm, a series of small metal disks with inner holes have been employed. These disks are known as steel washers. Several washers were distributed on the surface of every targeted tidal flat right before the onset of tidal bores and associated flood tides. Then, at the same time, we inserted a small, short surveyor's flag through the opening of every distributed washer down to the surface of the mudflat (Figure 12A). Successive flags were separated by a constant distance of about 1m to ensure highly accurate sedimentation rate measurements. The same sites were rechecked about one to two days later, and were excavated from the point where the newly accumulated sediments contact the flags to the levels of the washers (Figure 12B). Excavation is very necessary here not just to measure accumulation rates but also to observe cyclic tidal rhythmites and soft-sediment deformation, especially within cut banks. However, the high liquefaction potential of intertidal sediments could make flagging and excavation somewhat difficult or even hazardous particularly when recently deposited sediments are disturbed, say, by walking across them (Figure 12A).

Latitudes and longitudes have been recorded for each location using a handheld GPS unit (Appendix C). For further and careful laboratory investigation of the internal facies of some upper intertidal flats within Turnagain Arm, shallow cores have been collected from almost every site we have visited, using plastic cylindrical tubes. This sampling process was conducted with extra caution because the sediments were very wet and thixotropic. The sampling also was restricted only to those areas exposed at low tide.

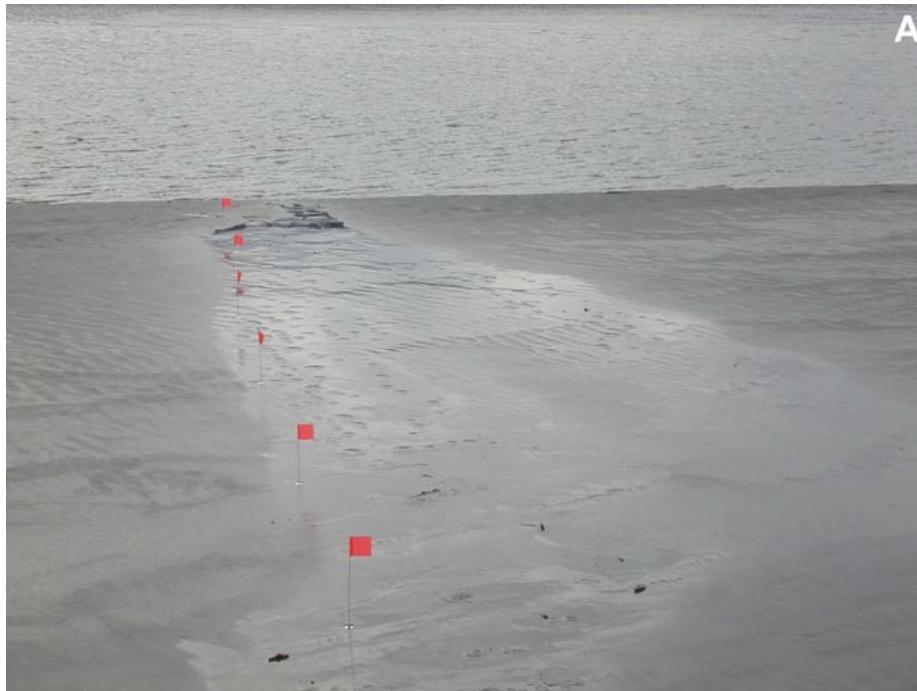


Figure 12. (A) A straight row of surveyor's flags along with steel washers placed on the surface of an intertidal flat. Note the constant distance between the flags. Note as well how the flat became thixotropic by walking across it. Few days later, excavations were made down to washers' levels for the sake of measuring sedimentation rates (B).

Study Area

One of the goals of this research is to observe a modern depositional environment in order to understand and be able to accurately interpret and make predictions about the controls, either allogenic or autogenic, that might have dominated a specific ancient depositional environment. Thus, the study area can be divided into two areas: modern and ancient. The ancient study area will be the Tonganoxie Sandstone Member (Stranger Formation, Douglas Group) of northeastern Kansas (Figure 13). The Tonganoxie paleovalley belongs to the lowest Virgilian (Stephanian) of the Upper Pennsylvanian System (Feldman et al., 1995) (Figure 8, 9). Pennsylvanian rock units in Kansas, including formations that belong to the Douglas Group, tend to outcrop in a south-southwest direction (Figure 13, 14) with an average thickness of about 2,500 feet, and they dip westward at about 25 feet per mile (Moore, 1949). In particular, the focus will be more on interpreting and describing tidally- influenced facies within the Tonganoxie Sandstone, especially those previously documented at its outcrop in Buildex Quarry. The exposure at Buildex Quarry is located in the southwest of Ottawa town in Franklin County, Kansas (NW 1/4 Sec. 23 T17S R19 E.) (Lanier et al., 1993) (Figure 13). The Buildex Quarry succession itself is on the eastern edge of the Tonganoxie paleovalley.

The good thing about the Tonganoxie Sandstone is that it represents an important and major paleovalley fill within the Pennsylvanian System (Figure 8, 9). Therefore, special attention will also be directed towards incised paleovalleys and their fills in general and within the Pennsylvanian System in particular. Sandstones were selected for other reasons as well. First, although intense studies were conducted on cyclic alternations of Pennsylvanian shales and limestones of the North American Midcontinent, as an attempt to interpret black shales and carbonates (e.g., Heckel 1977, 1983, 1986; Coveney et al. 1991), sandstone sequences within the same cycles have not been the focus of such intense studies. Second, the sediments of the Tonganoxie Sandstone are well exposed at that particular locality (Figure 15) and are interpreted as having been deposited in fluvio-estuarine settings or macrotidal settings (Bandel, 1967; Lanier, 1993; Lanier et al., 1993). These macrotidal settings are very suitable for the formation of tidal rhythmites. In fact, tidal rhythmites are widespread within these siliciclastic successions, especially within planar stratified siltstone assemblages exposed at the Buildex quarry. Carboniferous-age

tidal rhythmites have been recognized not just in the Tonganoxie Sandstone of Stranger Formation but also within other formations in the eastern USA such as the Mansfield Formation and Hindostan whetstone beds of Indiana (Kvale et al., 1999; Archer, 2004). These silt-rich tidal rhythmites have been described and analyzed by some workers (Kvale et al., 1989; Kvale and Archer, 1991; Lanier et al., 1993; Archer and Kvale, 1993; Archer et al., 1994; Archer and Johnson, 1997). Using these tidal rhythmites as interpretation and reconstruction tools is considered a significant development and relatively new approach in understanding Midcontinent Pennsylvanian siliciclastic rocks, especially when taking into account the complex array of facies found within these rocks (Lanier et al., 1993). The modern macrotidal setting to be used as the counterpart to the Tonganoxie is the Turnagain Arm of Cook Inlet, Alaska, USA.

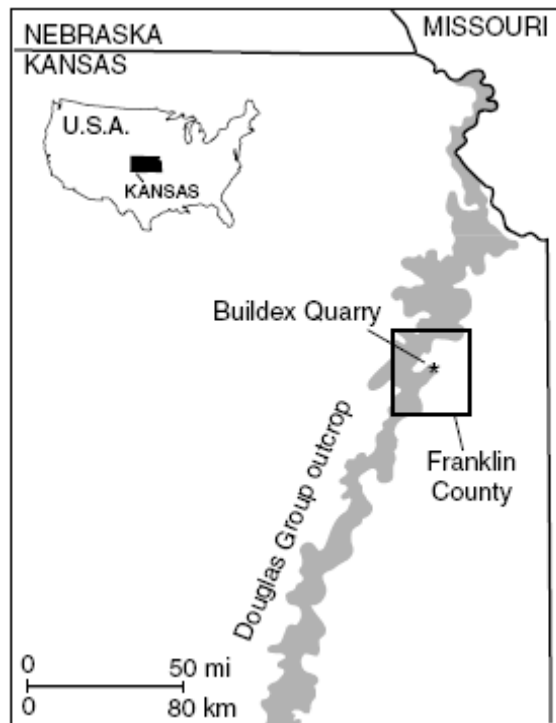


Figure 13. Map of study area showing the distribution of the Douglas Group outcrop and location of Buildex Quarry (from Lanier et al., 1993).

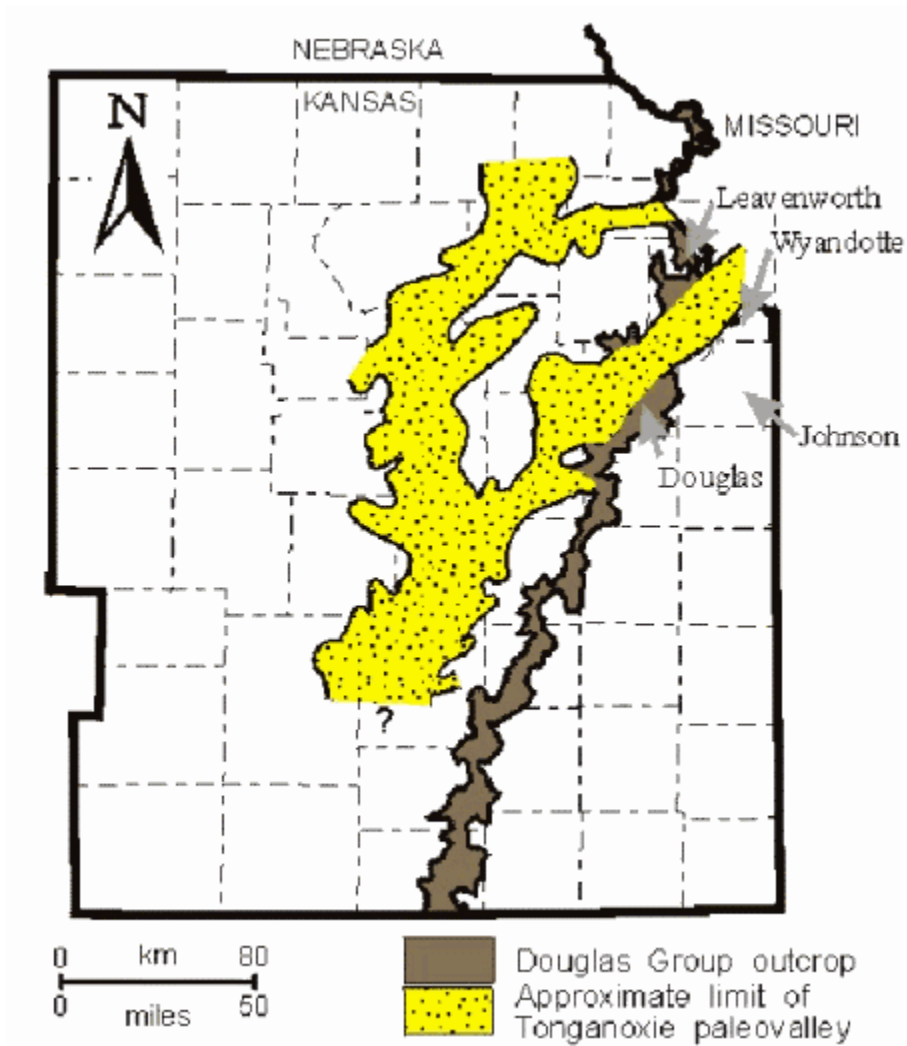


Figure 14. Map of Tonganoxie paleovalley and Douglas Group outcrop. The trend of both the Tonganoxie paleovalley and the Douglas Group is south-southwest. Note the question mark that indicates the difficulty in following the Tonganoxie paleovalley south of Greenwood County (modified from Feldman et al., 1995).

Douglas Group

The Douglas Group is Lower Virgilian (Upper Pennsylvanian). It is underlain by the Lansing Group (Upper Missourian) and overlain by the Shawnee Group (Upper Virgilian) (Figure 8). The most noticeable character that can be used to differentiate the underlying Lansing Group and the overlying lower Shawnee Group from the Douglas Group is that the first two groups contain relatively thick, laterally extensive limestones (marine units) while the Douglas Group in Kansas lacks such thick limestones and platy black shales (Figure 8, 9). The Douglas Group is composed mostly of siliciclastic facies with a few thin limestones and some minor beds of coals and conglomerates (Ball, 1964) (Figure 8). Douglas Group thickness ranges from 50 feet in southeastern Nebraska up to 700 feet in southern Kansas. In northeastern Kansas, Douglas units range in thickness from about 150 to 250 feet (Moore, 1949). Strata of this group are exposed in eastern Kansas in an outcrop belt (Figure 13, 14).

The Douglas Group is predominantly formed of non-marine terrigenous sediments such as sandstone, shaly sandstone, and sandy, silty, and clayey shales. The Tonganoxie and Ireland Members constitute the bulk of these sandstones in form of huge incised valley fills (Figure 8, 9). The siliciclastic deposits may also exist as sandstone tongues, sandstone lentils, and very small local channel fillings usually found within the shales such as Vilas Shale and Chanute Shale (Figure 9). The marine deposits include limestones and black shales. They are minor components within the Douglas Group, and represented mainly by the Haskell Limestone and the Westphalia Limestone Members (Figure 8). They occur as thin limestone beds compared to those thick siliciclastic units (Archer and Feldman, 1995). Nonetheless, these marine limestone units are persistent and laterally continuous which makes them very useful and important stratigraphic markers (Figure 9). For example, all of the four sequences within the uppermost Lansing Group up to the lower Shawnee Group were named after their prominent and thickest marine limestone and shale units (Archer and Feldman, 1995). In addition, marine black shales by large are organic-rich units; hence, they can be used in subsurface correlations due to their radioactive attributes (Archer and Feldman, 1995). Conglomerates in the Douglas Group are locally derived, and they have been interpreted as erosional products from the underlying strata. These conglomerates are usually associated with unconformities within

the Douglas Group (Stephens et al., 1999). Generally, the conglomeratic facies consist of limestone, siltstone, shale, clay, and coal pebbles and fragments (Bowsher and Jewett, 1943; Archer and Feldman, 1995). In fact, lithology of these conglomerates is highly dependant on the lithology of the underlying strata. Therefore, basal conglomerates of the Ireland Sandstone, for example, could slightly differ than those observed at the base of the Tonganoxie Sandstone Member (Bowsher and Jewett, 1943).

There are some different opinions among workers who worked on the Douglas Group about the possible source area of the terrigenous sediments. A primary investigation of facies relationships, thickness of sedimentary beds, and regional relationships has convinced many workers to assume a southern source for the terrigenous material (Moore, 1949). However, subsequent studies of directional sedimentary features and paleocurrent analyses have shown that the main potential sources for the clastic deposits of the Douglas Group were likely situated to the northeast. These source areas could include the metasedimentary rocks in the Wisconsin arch, the Appalachians, or the Canadian Shield in the Lake Superior region (Lins 1950; Bower 1961; Minor 1969). The evidence of distant source areas of these deposits comes from the fact that sandstone units within larger-scale paleovalleys of the Douglas Group such as the Tonganoxie and Ireland paleovalleys are dominated by quartz and muscovite (Archer, in press) (Figure 16). Further petrographic work would be needed to confirm the source area of these extrabasinal deposits with high degree of confidence. What matters for us here is that the Douglas Group contains estuarine facies that are very similar to the facies found throughout the Pennsylvanian siliciclastic rocks of the mid-continent (Archer et al., 1994a).



Figure 15. A photo showing the north wall at Buildex Quarry. The laterally continuous Tonganoxie Sandstone Member disconformably overlies the Weston Shale Member. Note the Ottawa coal that exists between these two strata (from Buatois et al., 1998).



Figure 16. Photo of a sandstone unit that is mineralogically dominated by quartz and muscovite described from Aelschlaeger core, which belongs to the Tonganoxie paleovalley fill. Note the shiny muscovite particles.

Geologic Setting

The Tonganoxie paleovalley was incised during the late Missourian sea level fall and then filled with sediment during the subsequent sea level rise or transgression (Lanier et al. 1993). Detailed studies have shown that this paleovalley is about 41 m deep and 11 km wide (Figure 17). It is about 240 km long trending northeast-southwest (Feldman et al., 1995, and Lanier et al., 1993) (Figure 14). In addition, isopach maps along with subsurface data and outcrop observations suggest that the trunk valley of this funnel-shaped incision has a U-shaped cross-valley profile filled with fining-upward succession of conglomerate, sandstone, and mudstone (Lins, 1950) (Figure 17). The succession also exhibits an increasing marine influence upward, just like regular incised valley-fill models for Carboniferous facies of western Kansas and southeastern Colorado (Figure 18). Paleovalley walls are bounded by shale, mostly the Weston Shale, with slopes of 15m/km, and its base is subhorizontal with relief of no more than 4m/km (Feldman et al., 1995) (Figure 17). Associated with the trunk valley are several tributary valleys extending northwest-southeast and feeding into the main valley. It is believed that all these tributary valleys were incised by minor tributary rivers, but tributary valleys on the northern edge of the paleovalley are far better defined than those on the southern edge. Based on its size and other considerations, it seems that the Tonganoxie paleovalley has drained a huge watershed, and probably the paleovalley was an important topographic feature during the early Virgilian time (Feldman et al., 1995).

The Tonganoxie sequence is one of two major sequences of the Douglas Group that are bounded by unconformities (Figure 8). This sequence includes recognized formation members from the base of the Tonganoxie Sandstone up to the erosional surface that forms the base of the Ireland sequence, which represents the second major sequence within the Douglas Group. The Tonganoxie sequence includes the Tonganoxie Sandstone Member of mostly fluvial and estuarine sandstones and mudstone facies. The Upper Sibley Coal is supposed to cap the Tonganoxie Sandstone, but it has been found only within limited areas. The Westphalia Limestone Member erosively overlies the Upper Sibley Coal, suggesting a widespread transgression (Buatois et al., 1998). Where the Upper Sibley Coal is absent, however, the Westphalia Limestone sits directly on the underlying mudstone and sandstone facies. Moving further upward within the

Tonganoxie sequence, there are also Vinland Shale, Haskell Limestone, and Robbins Shale Members (Figure 8). The Westphalia Limestone, Vinland Shale, and Haskell Limestone Members are considered as stacked retrogradational parasequence sets, whereas the Robbins Shale Member, especially its uppermost part, is judged to represent the highstand system tract (Archer, Lanier et al., 1994). At the base of the Robbins Shale Member, there is an open-marine, condensed section that represents the maximum flooding surface (mfs) (Figure 17). Regardless of all that, there are still some difficulties and problems when it comes to the recognition of system tracts within the Tonganoxie incised valley system (Archer and Feldman, 1995). It should be mentioned that the uppermost units of the Tonganoxie sequence are all of marine origin and contain fine-grained sediments. This is consistent with the general fining-upward nature of the sequence (Figure 17). The inference of marine origin for these uppermost units is based on their highly diverse suite of trace fossils and their dense marine fossil content. The high degree of bioturbation within these members suggests marine conditions as well (Feldman et al., 1995). This upward increase of marine influence is also consistent with the general model proposed for similar sequences found elsewhere (Figure 18).

Sandstone Bodies of the Tonganoxie Sequence

Sandstone bodies within the Tonganoxie sequence are of four types (Table 1) (Figure 17). Type I is an extensive belt of braided fluvial conglomerate and sandstone that lies mainly on the trunk valley and covers significant segments of the tributary valleys. This broad basal sandstone belt ranges in thickness from 3 to 18.3 m. Type II sandstone bodies are sinuous to arcuate estuarine deposits with mud drapes, and they maintain thickness of 18.3 m. These sandstones overlie type I sandstone bodies, and they are overlain and bounded by shale or mudstone deposits (Figure 17). Although type III sandstone bodies are elongate and their thickness may reach up to 12 m, their distribution is limited within the paleovalley, and they usually tend to exist near the heads of the tributaries. Type III sandstones are of high interest because they contain fine-grained sandstone and siltstone rhythmites (Archer, in press). Immediately underlying the Haskell Limestone Member, which tops the Tonganoxie paleovalley-fill succession, is type IV sandstone. This bioturbated marine sandstone is very extensive but not continuous (Figure 17) with

average thickness of only 3 m (Table 1) (Feldman et al., 1995). The deposition of these sandstones represents successive stages of transgression.

Facies Assemblages of the Tonganoxie Sandstone Member

Siliciclastic facies of the Tonganoxie sequence are mainly represented by the Tonganoxie Sandstone Member. These largely coarse-grained facies were put into several facies assemblages (Lanier et al., 1993; and Feldman et al., 1995). The facies assemblages include: conglomeritic assemblage, trough cross-bedded assemblage, planar cross-bedded assemblage, ripple cross-laminated assemblage, planar-stratified siltstone assemblage, sheet sandstone facies, and mudstone facies. This arrangement was based on recent outcrop studies along with core investigation, and many aspects were observed in these facies during lab work as well. Moreover, an attempt of using data from trace fossils and protozoan assemblages to determine any marine control during sedimentation of these facies was done by Feldman et al. (1995) (Table 2). These assemblages of protozoan and trace fossils have indicated the existence of brackish water conditions during late stages of deposition in a fluvial environment (Wightman et al., 1993; Feldman et al., 1995).

Since this investigation of the evidence for tidal influence within the Tonganoxie sequence is focused more on the planar-stratified siltstone assemblage, it will be described in some detail. The other assemblages will be mentioned briefly whenever needed. The reason is that the planar-bedded siltstone assemblage contains the most prominent evidence for a strong tidal influence on the deposition of the Tonganoxie sequence (Figure 19A). This evidence of tidal influence is particularly evident within the lower 3m of assemblage's outcrop at Buildex quarry in Franklin County, Kansas (Lanier et al., 1993) (Figure 13). To be fair, however, some of the other assemblages do exhibit slight evidence of tidal influence. The upper part of the planar cross-bedded assemblage, for instance, has clay drapes along with some paired laminae and shows some sort of cyclic variation in bed thickness (Figure 19B). All of these features, especially the mud drapes, point to the existence of tidal influence within the overall fluvial conditions under which the sequence is believed to have been deposited. Fauna and protozoan assemblages of this sequence are in agreement with this assumption as well (Table 2) (see Feldman et

al., 1995, and Lanier et al., 1993). The other evidence of prevailing tidal conditions comes from the ripple cross-laminated assemblage where flaser bedding is common along with rhythmic variation in laminae thicknesses, although these rhythmites are less developed compared to those of the previous assemblage. As an additional evidence of tidal impact on this assemblage, the ripple cross-laminated facies has also a bimodal paleoflow pattern in the northeast of the Tonganoxie. Well-developed rhythmic bedding is also contained in fine-grained facies such as mudstone and shale facies, but these facies are not exposed clearly in the Tonganoxie sequence as they are in the overlying Ireland sequence.

It is almost impossible to discuss the Tonganoxie sequence without mentioning coal deposits. Several coal units have been documented in the Tonganoxie Sandstone Member. The best studied and documented ones are the Upper Sibley Coal and the Ottawa Coal (Bowsher and Jewett, 1943). The Upper Sibley Coal usually lies on mudstone facies of the Tonganoxie Sandstone with thickness of about 33 cm. The Ottawa Coal, on the other hand, occurs close to or at the base of the Tonganoxie sequence, and it is rooted in the Weston Shale (Figure 15). At Buildex Quarry, the rooted Ottawa coal marks the basal erosion surface, which is a type 1 sequence boundary according to Van Wagoner et al. (1990), indicating that the paleovalley walls have been subaerially exposed (Lanier et al., 1993; Buatois et al., 1998) (Figure 15). The thickness of the Ottawa Coal unit almost matches that of the Upper Sibley Coal with the average being about 30 cm. However, at the Buildex Quarry, it is about 10-15 cm and laterally discontinuous, and possibly accumulated on the floodplain of the Tonganoxie fluvial system (Lanier et al., 1993). Subsurface data, especially the density logs, have shown that there are other discrete coal units within the Tonganoxie sequence, such as the thin silty coals at the top of the channel and levee facies at the quarry exposure. We did encounter many such coal units during our lab investigations of Tonganoxie cores (Figure 20). Recent models suggest a relationship between wetter climates and peat formation (Cecil, 1990). Regarding paleosols, there is a thick, extremely weathered paleosol found on the Iatan Limestone. At the Buildex quarry, there is also a complex paleosol formed on the Weston Shale, overlain by a coal unit (Feldman et al., 1995). The lab investigation has revealed similar paleosol intervals as well (Figure 21).

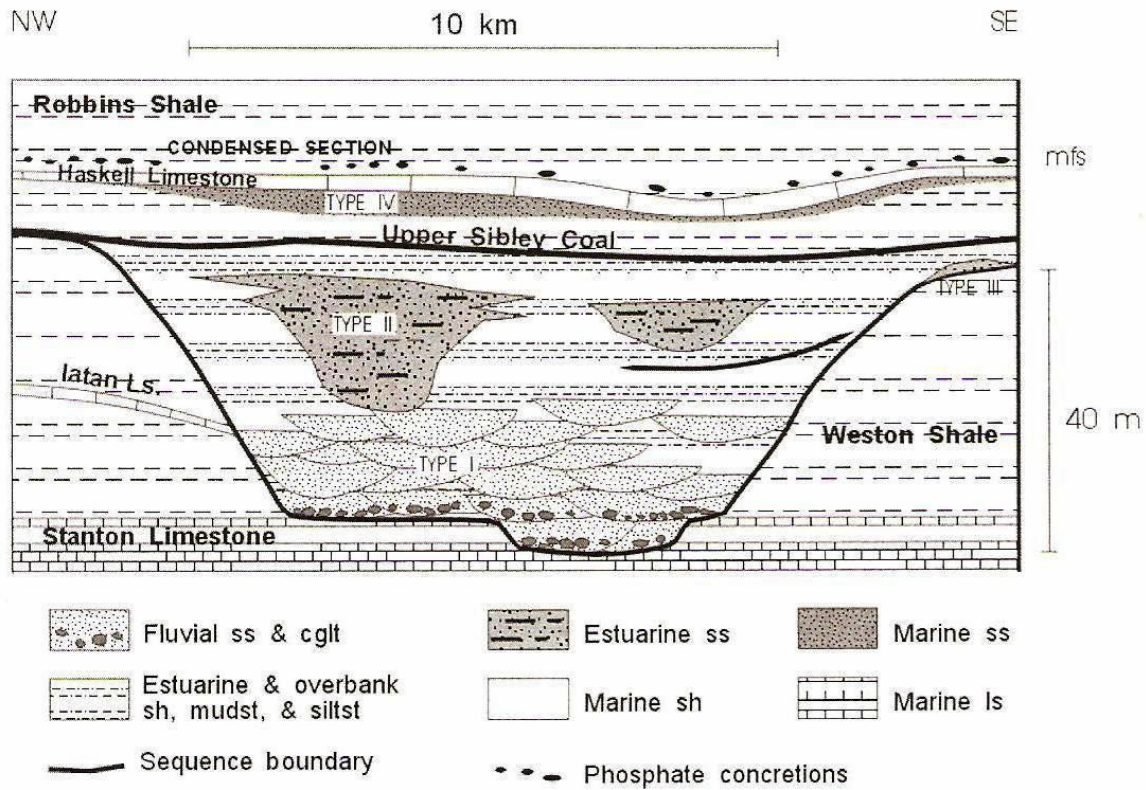


Figure 17. Schematic cross section of the Tonganoxie incised paleovalley fill in northeastern Kansas showing the different types of sandstone units along with other components that comprise the filling of the paleovalley. It also shows the underlying and overlying units. mfs = maximum flooding surface, sb = sequence boundary, ss = sandstone, cgl = conglomerate, sh = shale, mudst = mudstone, siltst = siltstone, and ls = limestone (from Archer, in press).

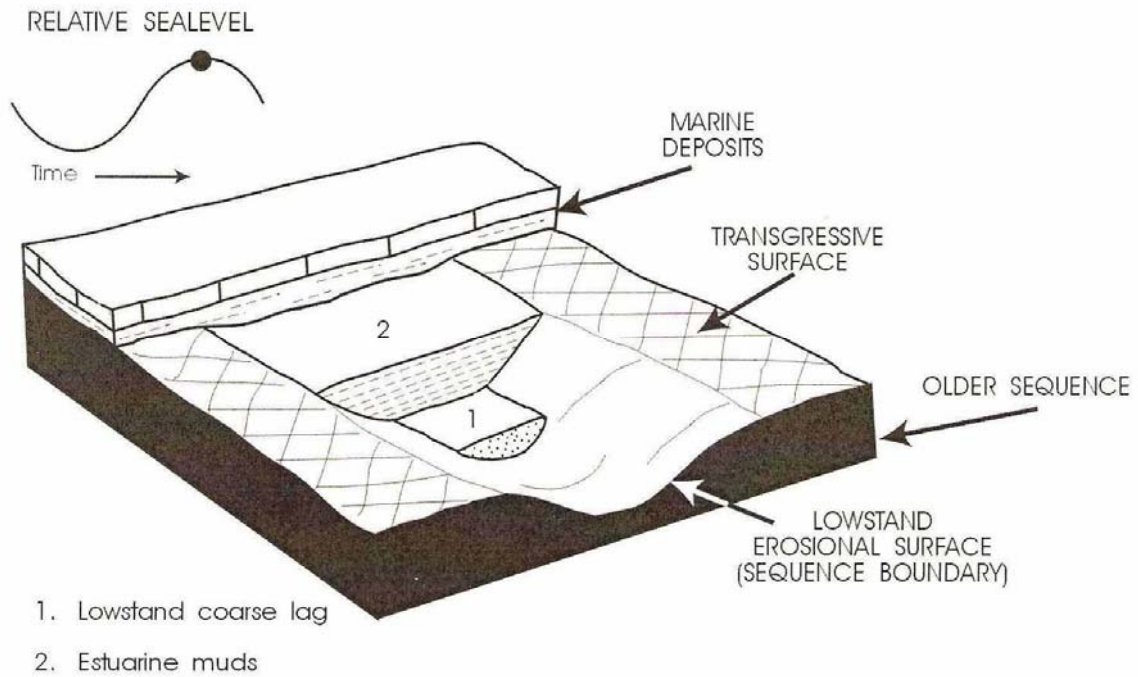


Figure 18. Block diagram representing a model of Carboniferous incised valley-fill of western Kansas and southeastern Colorado. The Tonganoxie succession is very similar to this model both in terms of the processes that formed it and in terms of the general upward fining of its deposits and the increase of marine influence (from Archer, in press).

Table 1. The four types of sandstone bodies within the Tonganoxie sequence. Note their thickness ranges and depositional settings (from Feldman et al., 1995)

Geometric Element	Thickness (m)	Depositional Setting
Type I sandstone: basal conglomerate and sandstone sheet.	3-18.3	Braided fluvial to upper estuarine
Type II sandstone: sinuous to arcuate sandstone bodies within muddy facies.	Up to 18.3	Estuarine point bars and channels
Muddy facies and siltstone valley fill above type I sandstone and surrounding type II sandstones.	Up to ~45	Tidal flats to muddy estuary
Type III sandstone: sandstone pods at upstream limits of tributary paleovalleys.	Up to 12.2	Valley-head delta
Type IV sandstone: sheet of rippled and burrowed sandstone below Haskell Limestone.	Up to 9.1	Shallow marine

Table 2. Supplementary table showing protozoan assemblages yielded by shale samples from the Tonganoxie sequence. Note their associated facies assemblages (from Feldman et al., 1995).

Facies Assemblage and Stratigraphic Position	Comments	Protozoan Fossils
Trough cross-bedded assemblage, type I sandstone	10-15 m above paleovalley floor	<i>Trochammina</i> predominant, one tubular foram, possibly <i>Hyperammina</i> , one thecamoebian
Planar cross-bedded assemblage, Tonganoxie Sandstone	-	Barren
Planar cross-bedded assemblage with clay drapes, type I sandstone	10.5 m above paleovalley base, directly above conglom. and trough cross-bedded assemblages	<i>Trochammina</i> predominant, well-preserved thecamoebians, forms resemble modern <i>Arcella</i> , <i>Centropyxis</i> , <i>Difflugia</i> , and <i>Nebela</i>
Planar cross-bedded assemblage with clay drapes, Tonganoxie Sandstone, type II sandstone	-	Single specimens of <i>Ammottum</i> and <i>Trochammina</i>
Ripple cross-laminated assemblage, Tonganoxie Sandstone	-	Single specimen of <i>Difflugia</i>
Ripple cross-laminated assemblage, Tonganoxie Sandstone	-	Barren
Ripple cross-laminated assemblage, Tonganoxie Sandstone	-	Possible <i>Ammottum</i> and <i>Trochammina</i> (poorly preserved)
Ripple cross-laminated assemblage, Vinland Shale	0.5 m below Haskell Limestone	<i>Difflugia</i> and indeterminate thecamoebians, <i>Trochammina</i> , <i>Hyperammina</i> , <i>Textularia</i>
Shale, Vinland Shale	1 m above Westphalia(?) Limestone	<i>Hyperammina sappingtonensis</i> , <i>H. contca</i> , <i>H. nitida</i> , <i>H. rockfordensis</i> , <i>Ammotiscus semiconstrictus</i> , <i>A. annularis</i> , <i>Ammotiscella vitigilensis</i> , <i>Thuramminoides sphaerodalis</i> , <i>Thurammina?</i> sp., <i>Glomospira</i> (?) sp., indeterminate specimens

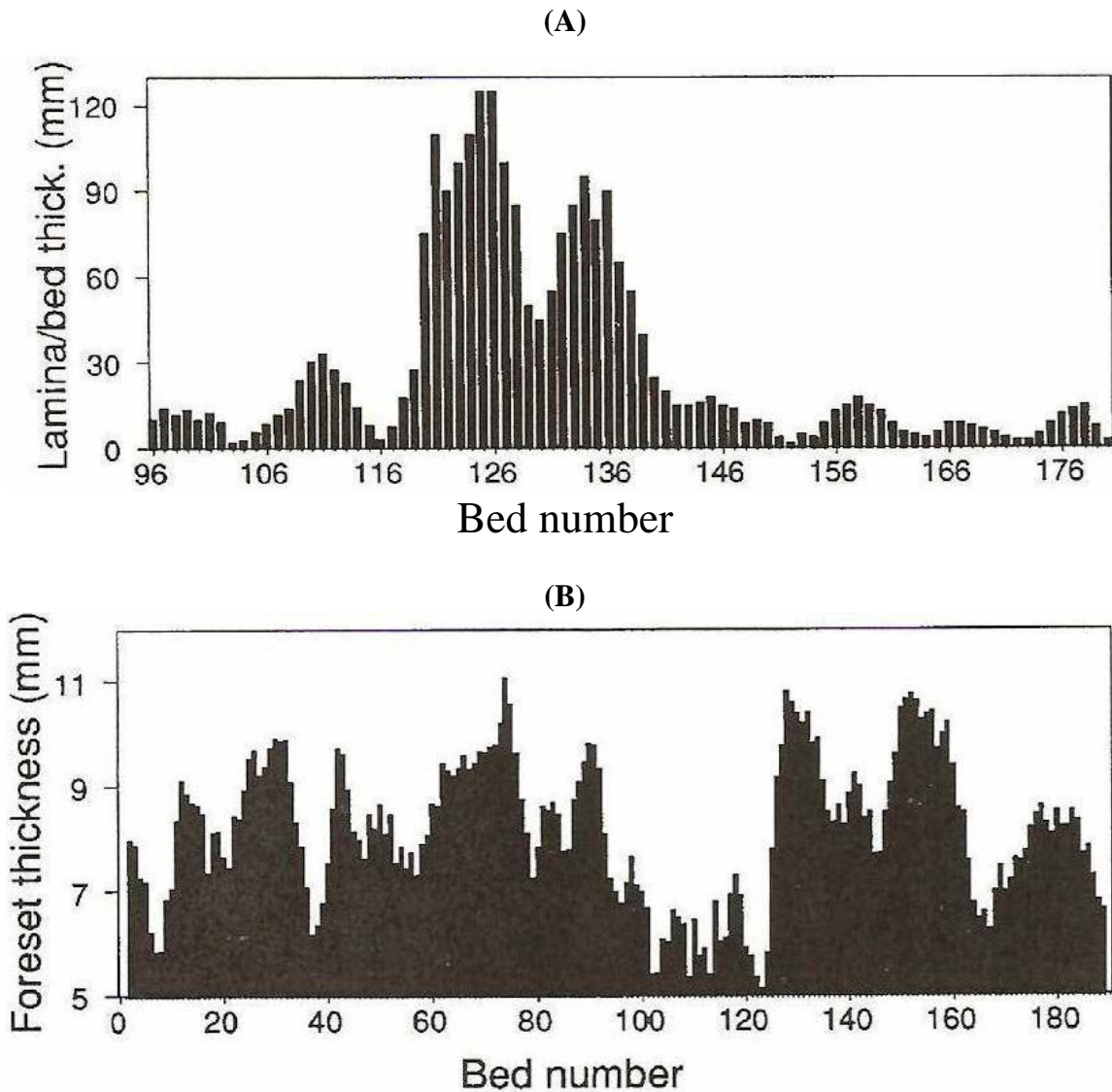


Figure 19. Two bar charts showing bed and laminae thickness vs. bed number that were constructed based on data from (A) the planar-stratified siltstone. Note its strong rhythmic pattern caused by tidal cycles. (B) the upper part of the planar cross-bedded assemblage, within type I sandstone. Note its less developed rhythmic pattern (modified from Feldman et al., 1995).

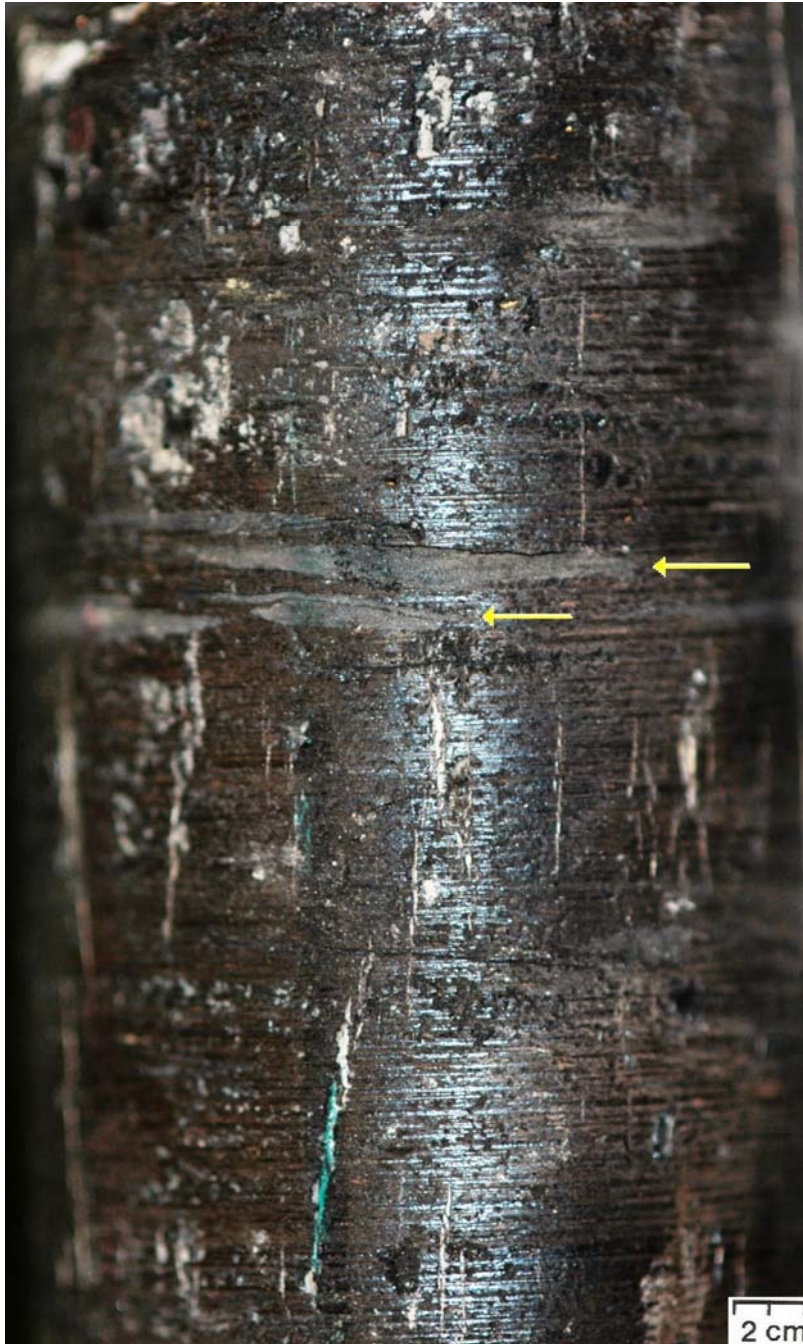


Figure 20. Photo showing a thick coal unit described from Aelschlaeger core taken from the Tonganoxie paleovalley fill succession. Note the existence of mud stripes (yellow arrows).



Figure 21. Photo showing a thick paleosol from Aelschlaeger core taken from the Tonganoxie paleovalley fill succession. Note the impact of weathering on this paleosol.

Depositional Environment of the Tonganoxie Sandstone Member

The depositional environment of the Tonganoxie Sandstone Member has been the focus of many studies (e. g. Lins, 1950; Lanier et al., 1993; Archer, Lanier et al., 1994; Archer and Feldman, 1995; Feldman et al., 1995). As mentioned earlier, the Tonganoxie Sandstone of eastern Kansas represents sedimentation within an estuarine paleovalley that was incised during a late Missourian drop in sea level and then filled by an early Virgilian transgressive event. A study by Bandel (1967), which was based on the analysis of Buildex ichnofauna, has suggested deposition in a river valley close to the river's mouth (Buatois et al., 1998). However, the well-exposed deposits of the Tonganoxie Sandstone Member at the Buildex Quarry are believed to have been deposited in a fluvio-estuarine transitional setting (Lanier, 1993; Lanier et al., 1993). According to Lanier et al. (1993), sediments of the Buildex succession were deposited on a tidal flat positioned near or even at the fluvial-estuarine transition within a macrotidal estuarine paleovalley. They also suggested that tidal processes have influenced the depositional environment of this part of the Tonganoxie Sandstone Member, and labeled the deposits as tidal rhythmites. This conclusion was based on the analysis of systematic vertical variations in laminae thicknesses where thicker strata represent deposition during spring tides and thinner laminae and beds reflect deposition during neap tides (Figure 19, 22).

The presence of certain bedding surface structures such as raindrop impressions, rill marks, and runnel marks and the absence of desiccation cracks and oxidized horizons are both considered as evidence of brief periods of subaerial exposure within the Buildex strata (Lanier et al., 1993). This evidence of brief subaerial exposure following almost every sedimentation event is, in turn, suggestive of fluvial overbank floodplain deposition. In fact, this part of the Tonganoxie Sandstone has many other features that are very similar to those of floodplain deposits such as sheetlike geometry, dominance of silt, upright plant remains, and absence or lack of bioturbation and body fossils (Lanier et al., 1993). Furthermore, the high preservation potential of bedding-plane features on both bed tops and bed soles suggests a non-erosive nature of this depositional setting with very high sedimentation rates. For example, convolutions and water-escape structures found within some of the bedsets indicate that the sediment contained high percentage of water content, which supports the high sedimentation rate interpretation (Lanier, 1993).

However, these high sedimentation rates, about 4 m/yr, are the result of extremely brief depositional events.

Ichnofossils of the Tonganoxie Sandstone Member

There is an increasing interest in studying the ichnology of estuarine depositional systems (e.g., Benyon and Pemberton, 1992; Pemberton and Wightman, 1992; Ranger and Pemberton, 1992; MacEachern and Pemberton, 1994). This intense research is due to the fact that investigating the organism-sediment interactions in these environments gives important information about the role of salinity as a controlling agent of the distribution of organisms and, hence, the distribution of trace fossil assemblages produced by these organisms. In addition, such studies could also offer high-resolution results that are very useful in delineating fluvio-estuarine transitions and may even assist in refining facies models based merely on physical sedimentary structures (Buatois et al., 1998). Although detailed discussion of the ichnofauna of the Tonganoxie Sandstone Member at Buildex Quarry is beyond this project, it is important to discuss briefly this ichnofauna as to provide an evidence of the dominant depositional conditions especially regarding salinity and tidal influence.

The ichnofossil assemblage of the Tonganoxie Sandstone Member at Buildex Quarry includes arthropod locomotion, resting and feeding traces, feeding structures, grazing traces, fish traces, tetrapod trackways, and root traces that represent plant biogenic structures. These trace fossils are limited to soles and tops of bedding planes, reflecting activity of a surface and near surface benthic fauna. A very few and shallow escape burrows of infaunal animals have been also reported (Figure 22). This scarcity of infaunal organisms has increased the preservation potential of fragile biogenic structures and original stratification (Figure 23A), with the exception of root traces which can be abundant especially within levee deposits (Figure 23B). Compared with typical trace-fossil assemblages of brackish-water and marginal-marine depositional environments, the Buildex ichnofauna lacks virtually all of the brackish water features (Buatois et al., 1997). Instead, the Buildex ichnofauna contains features that are indicative of terrestrial and freshwater faunas. These characteristics include ichnodiversity, taxonomic composition, dominance of surface and shallow subsurface trace fossils, lack or even

absence of infaunal burrows, and the mixture of arthropod trackways and grazing traces. Moreover, some of the forms found in the Buildex are typical of nonmarine environments such as *Undichna*, *Stiaria*, *Stiallia*, and *Dendroidichnites* (Buatois et al., 1998). The freshwater-terrestrial nature of the Buildex ichnofauna may appear as inconsistent with signatures of tidal influence found in the same succession. This inconsistency diminishes, however, when we take into account the fact that in estuarine systems; tidal effects usually extend landward well beyond the intrusion of saltwater (Dalrymple et al. 1992). In fact, this scenario is not an exception, and it was noted in the Cobequid Bay-Salmon River estuary of the Bay of Fundy, Canada, where most of the upper estuary region is affected by freshwater conditions with no marine or brackish faunas (Dalrymple et al., 1991).

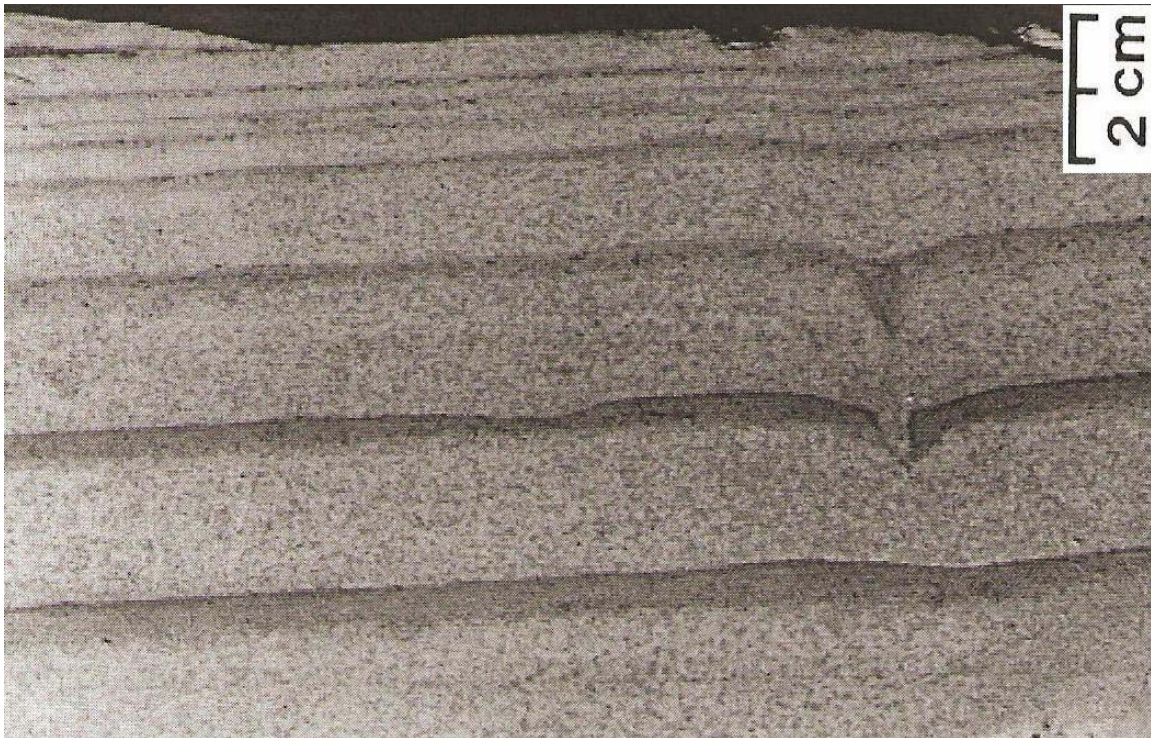


Figure 22. Photo of tidal rhythmites taken from a roadcut exposure northeast of the Buildex Quarry. Thicker strata represent deposition during spring tides and thinner laminae reflect deposition during neap tides. Note the escape structure (middle right) that disturbs some of the beds (adapted from Buatois et al., 1998).

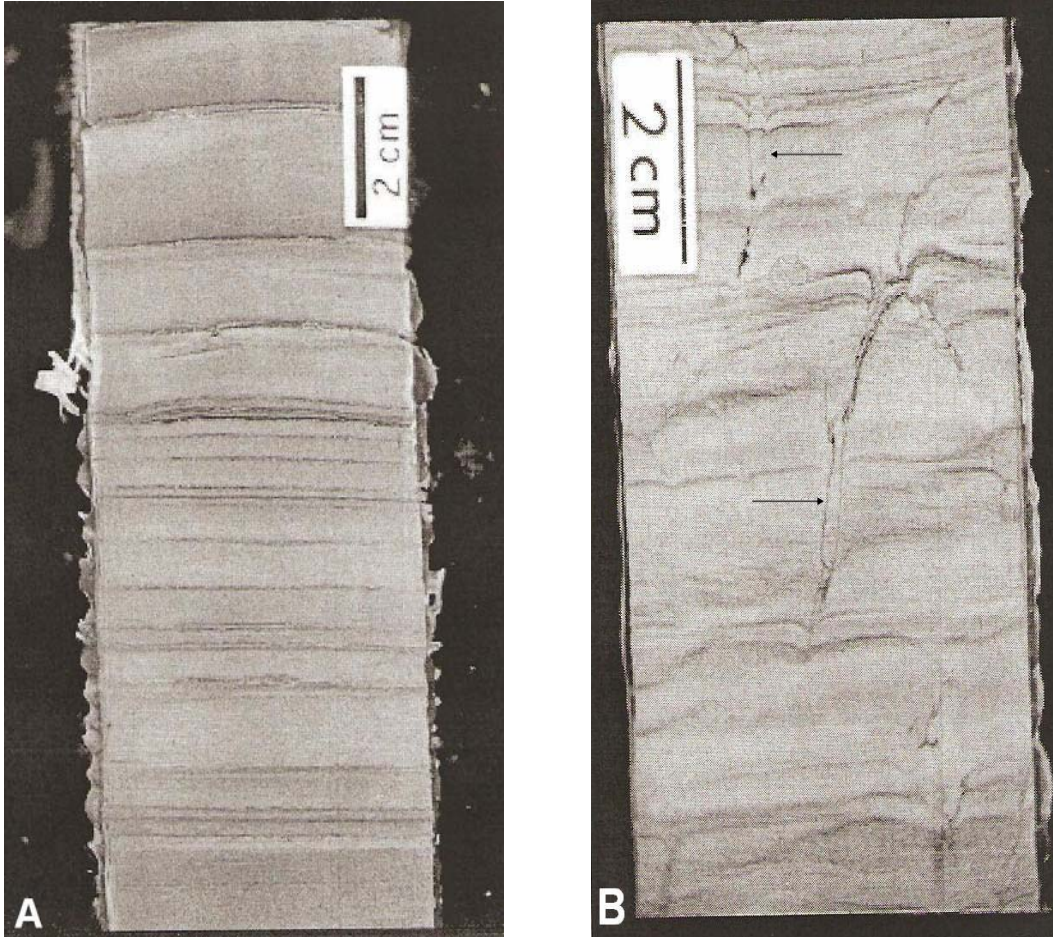


Figure 23. Two segments taken from a complete Buildex Quarry core. (A) The primary stratification is well preserved, indicating absence of any infaunal animal activities. (B) The original stratification is affected by root traces (black arrows), representing plant biogenic structures in the levee deposits of the Buildex succession (adapted from Buatois et al., 1998).

Evidence of Tidal Influence within the Tonganoxie Sandstone Succession at the Buildex Quarry

The lowermost 5 m of the Tonganoxie Sandstone Member are very well exposed at the Buildex Quarry (Figure 24, 25). Briefly, this succession consists of gray siltstone and mudstone deposits with only about 10% of very fine quartz sand. The siltstones are vertically stacked, and the whole section is bounded above and below by thin coal and paleosol units (Figure 26). The Tonganoxie Sandstone exposure at this particular locality has two very important characteristics: the remarkable lateral continuity of the siltstone beds and the evident systematic vertical variations in stratum thicknesses. In fact, it is at the Buildex Quarry where the Tonganoxie Member exhibits features that are strikingly similar to those of upper-estuary tidal-flat settings of modern macrotidal systems. These features include high aggradation rates, physical and biogenic sedimentary structures, lack of bioturbation, and evidence of frequent emergences. They all suggest that tides have played a role in the deposition of this part of the Tonganoxie sequence. Investigating this tidal role is the theme of this section.

Facies of the Tonganoxie Succession at Buildex Quarry

The sedimentary facies of the Tonganoxie Sandstone at the Buildex Quarry are grouped into two facies: planar-bedded-and-laminated facies (PBL) and channel-and-levee facies (CL) (Lanier et al., 1993) (Figure 26). Based on vertical and systematic variations in bed thickness and based on physical sedimentary structures, the two main facies are further divided into subdivisions. The PBL facies is divided into A1, A2, and A3 units, and the CL facies is subdivided into B1 and B2 units (Figure 26) (Table 3). This sort of classification is useful and important for our research in order to locate the exact stratigraphic position of any evidence of tidal effects and to relate any stratigraphic relationships. However, detailed description of each facies and unit is beyond the scope of this thesis and for a summary of these facies see Table 3.

Planar-Bedded-and-Laminated Facies (PBL)

This facies consists entirely of siltstone strata with total thickness of 2.8 m. Individual laminae and beds of the PBL facies range in thickness from as little as 0.05 cm to as much as 12.5 cm (Lanier et al., 1993), being thicker within Unit A2 and thinner in both

A1 and A3 Units (Figure 26). Generally, these vertically accreted beds are laterally extensive, parallel laminated, and normally graded with some local convolutions. All siltstone beds within this facies show systematic vertical changes in their thicknesses where individual strata thicken then gradually start to thin in an upward direction, creating very evident symmetric cycles that seem to comprise the whole section of the PBL facies (Figure 26, 27A).



Figure 24. General view of the quarry exposure showing two walls or faces. Note the steepness of one of the walls that limits the access to the wall and makes it harder for a close observation.

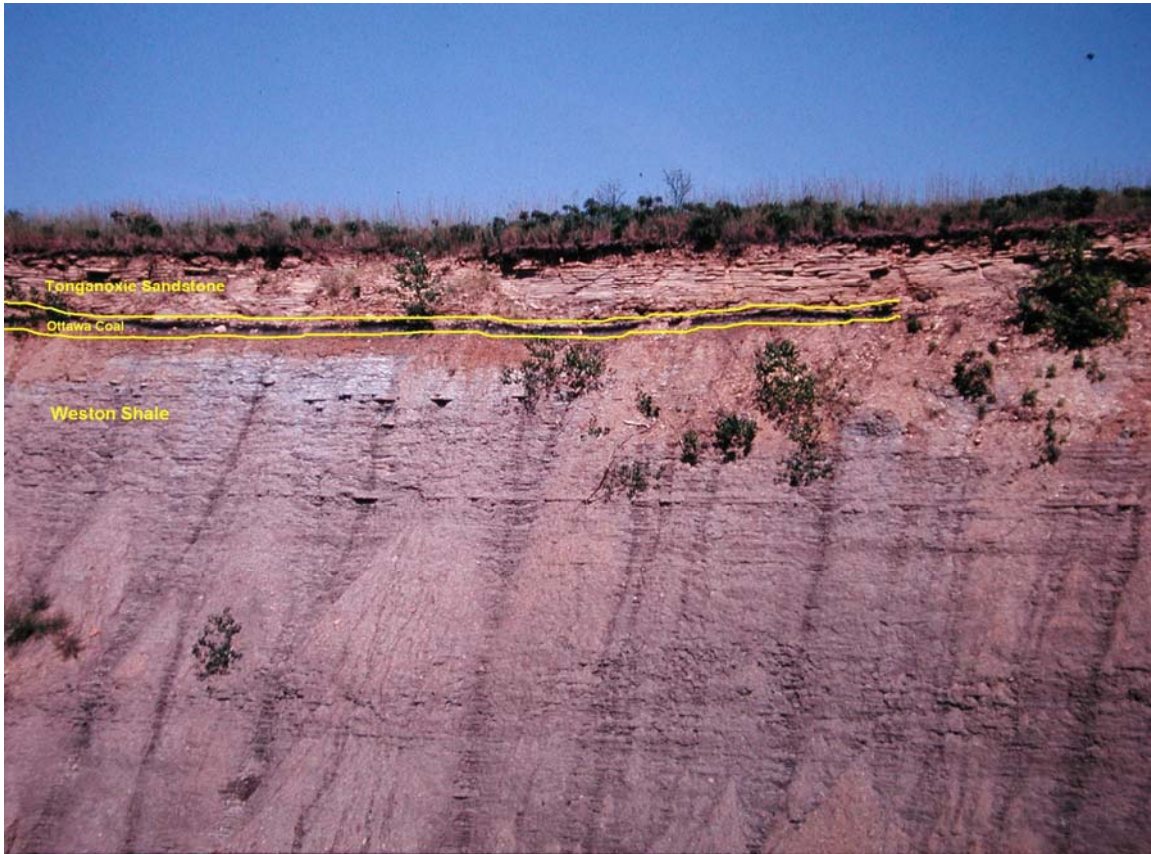


Figure 25. View of the Tonganoxie succession at Buildex Quarry. The photo also shows the Weston Shale and the Ottawa Coal. The contacts between these three units are traceable for a quite long distance. Some important features that can be seen in this picture include the vertically accreted siltstones of the Tonganoxie Member, the thin coals and paleosols that bound the Tonganoxie Sandstone, and the upright plant fossils.

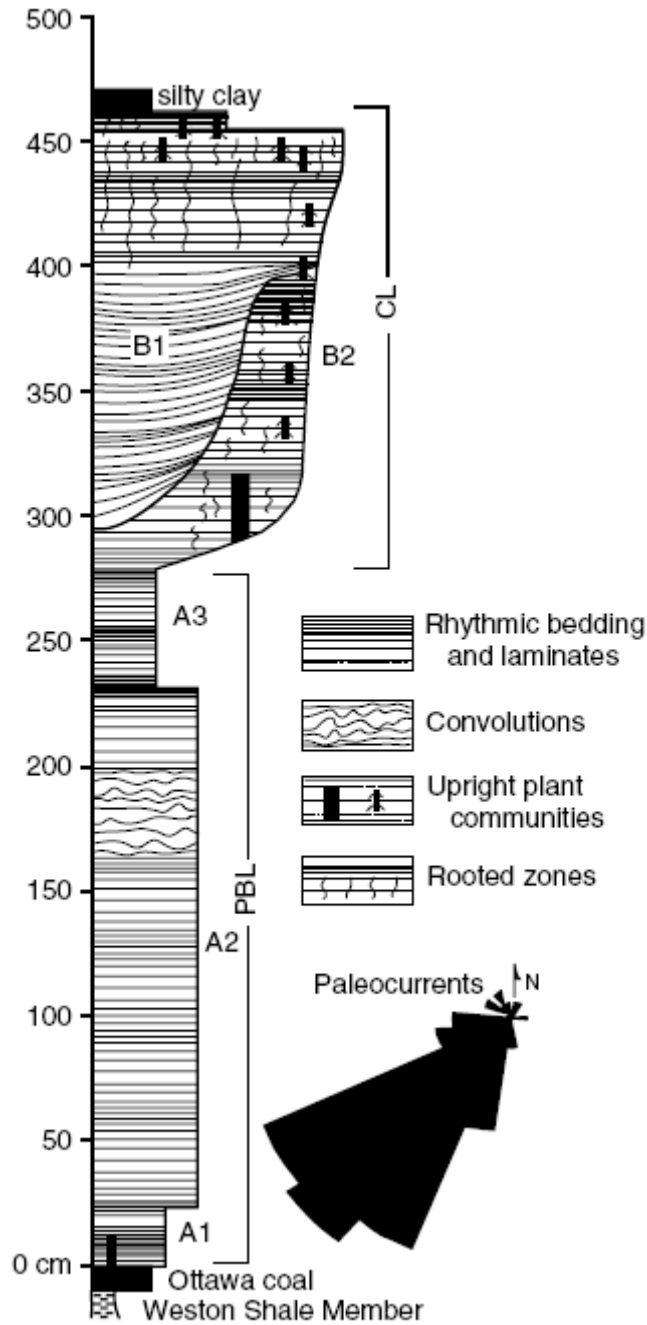


Figure 26. Stratigraphic section showing the complete succession of the Tonganoxie at Buildex Quarry. The succession is divided into two facies: the PBL facies and the CL facies. In turn, these facies are further divided into subunits. Note the rhythmic nature of bedding throughout the whole succession, although it is thicker and more evident within Unit A2. Note also the convoluted unit about 1.5-2 m above the succession base (from Buatois et al., 1998).

Table 3. Description of the sedimentary facies of the Tonganoxie Sandstone succession exposed at the Buildex Quarry (from Buatois et al., 1998).

Facies	Unit	Description
CL	B2	Planar-stratified siltstones locally truncated by the channelized surface. Normal grading, poorly-developed cross-lamination. Drip marks associated with upright plants. Plant leaves and roots. Total thickness: 1.8 m.
CL	B1	Channelized siltstone body, 1 m thick and 10–12 m wide. Strata thin and pinched out laterally towards the erosive bounding surface and culminate upward into planar-stratified beds and a horizontal upper bounding surface. Climbing ripples, parallel-lamination, clay drapes, linguoid ripples, cross-lamination. Drag marks, wrinkle marks, rill marks, runnel marks, runoff washouts, foam marks, raindrop impressions. Trace fossils. Root structures.
PBL	A3	Sharp-based siltstone beds. Normal grading, parallel lamination, climbing ripples, starved ripples. Tool marks, falling-water marks, raindrop impressions, surface drainage or seepage rill marks, wrinkle marks. Trace fossils. Plant leaves and logs. Beds 0.1–1.8 cm thick. Total thickness: 50 cm.
PBL	A2	Sharp-based siltstone beds. Climbing ripples fully developed. Convolute lamination. Individual strata typically include, from base to top, a normally graded division, a parallel-laminated division, a climbing ripple division, and an upper parallel-laminated division. Tool marks, load casts, raindrop impressions, runnel marks. Trace fossils. Plant leaves. Beds 1.4–12.5 cm thick. Total thickness: 2.2 m.
PBL	A1	Sharp-based siltstone beds. Incipient climbing ripples and syndepositional normal microfaults. Upright plant remains rooted in the Ottawa coal. Beds 0.05–1.38 cm thick. Total thickness: 25 cm.

Unit A1 of the PBL Facies

This 25-cm-thick unit represents the basal unit of the planar-bedded-and-laminated facies, and, therefore it directly overlies the underlying Ottawa Coal (Figure 26, 27A). Thicknesses of strata belonging to Unit A1 vary upward in a cyclical and periodical pattern (Figure 27A, 28A). Consequently, these strata are grouped into several packages of 6-14 laminae each, where thicker packages alternate with thinner ones and vice versa (Figure 27A). This type of cyclic vertical thickening and thinning of bedsets has been reported also from modern macrotidal systems that are highly affected by tidal processes (Figure 27B). The transition between this unit and the overlying unit is gradational.

Unit A2 of the PBL Facies

The systematic thinning and thickening persists within this 2.2 m thick unit. However, siltstone bedsets within Unit A2 are thicker bedded than those of A1 and A3 Units. The most noticeable characteristic of this unit is that most of its bedsets exhibit vertical sedimentary structure sequences known as (VSS) (Figure 29). The VSS of this unit includes the following intervals: (A) a massive to normally graded interval; (B) a planar-laminated interval; (C) a cross-laminated interval; and finally (D) a laminated interval with drapes (Figure 29). According to hydrodynamic studies, these VSS intervals represent shifting and transition from one flow regime to another, say, from upper to lower flow regime under conditions of flow deceleration during the ebb phase of the tidal cycle (Banerjee, 1977). In other words, they indicate that this silt-rich succession was largely deposited in an ebb-dominated tidal system. The development of vertical sedimentary structure sequences suggests an increase in sedimentation rates as well. Unit A2 also contains a laterally extensive, convoluted interval that lies 1.5-2 m above the base of the succession (Figure 26). Feather-like structures are a bit common here, indicating an upward movement of water (Figure 29C). Other physical and biogenic sedimentary structures are also common on the surface of the beds. The physical structures include stick drag marks (Figure 30A), microload structures, raindrop impressions (Figure 30B), and runnel marks (Figure 30C, 31C, 33A). The biogenic structures and ichnofossils include *Plangtichnus*, *Haplotichnus* (Figure 32A), *Treptichnus* (Figure 32B, C), arthropod traces (Figure 30C), fish-fin drag marks (Figure 30C, 31A), tetrapod footprints with tail drag marks (Figure 31B), and plant leaves such as fern, seed-

fern, and cordaites foliage (Lanier 1993; Lanier et al. 1993; Buatois et al. 1998; Archer 2004). What matters to us here the most is that the upward rhythmic variations of siltstone bedsets is very clear with cycles containing twelve to fourteen sedimentation units each (Figure 28B).

Unit A3 of the PBL Facies

The rhythmic bedding continues through this 50 cm thick unit with cycles containing nine to thirteen depositional units each (Figure 26, 28C). Asymmetric, sinuous ripple crests are widespread over bed tops. Within Unit A3, both physical and biogenic sedimentary structures are very similar to those of Unit A2. These structures include stick drag marks, prod marks, drag marks of plant fragments, raindrop impressions, standing-water marks (Figure 31C), seepage rill marks, and runzel marks. Tracefossils include arthropod traces, fish-fin drag marks, tetrapod trackways with tail drag marks, as well as *Plangtichnus*, *Haplotichnus*, and *Treptichnus* (Lanier et al. 1993, Buatois et al., 1998).

Channel-and-Levee Facies (CL)

This facies is divided into two subunits: B1 and B2 (Figure 26) (Table 3). However, in terms of physical sedimentary structures and ichnofossils, the two units contain almost the same structures with some minor exceptions. Common structures found in these two units are raindrop impressions, stick drag marks, runzel marks, rill marks, runnel marks, runoff washouts, and foam marks (Figure 32A). In addition, there are ichnofossils such as *Plangtichnus*, *Haplotichnus*, *Treptichnus*, arthropod traces, and fish-fin drag marks, especially within the channel-fill part (B1). The levee sequence (B2) of the CL facies differs slightly in that it contains extensive upright plant fossils with their attached-leaves and roots along with some drip marks. These trees are dominated by calamities (horsetails) and pteridosperms (ferns) (Archer, 2004). The vertical rhythmic variation in strata thicknesses within the channel-and-levee facies, although exists, is not as evident as it is in the planar-bedded-and-laminated facies (Figure 28D). The entire CL succession passes upward into planar-stratified beds, which means the channel deposits eventually merge with the levee facies (Figure 26).

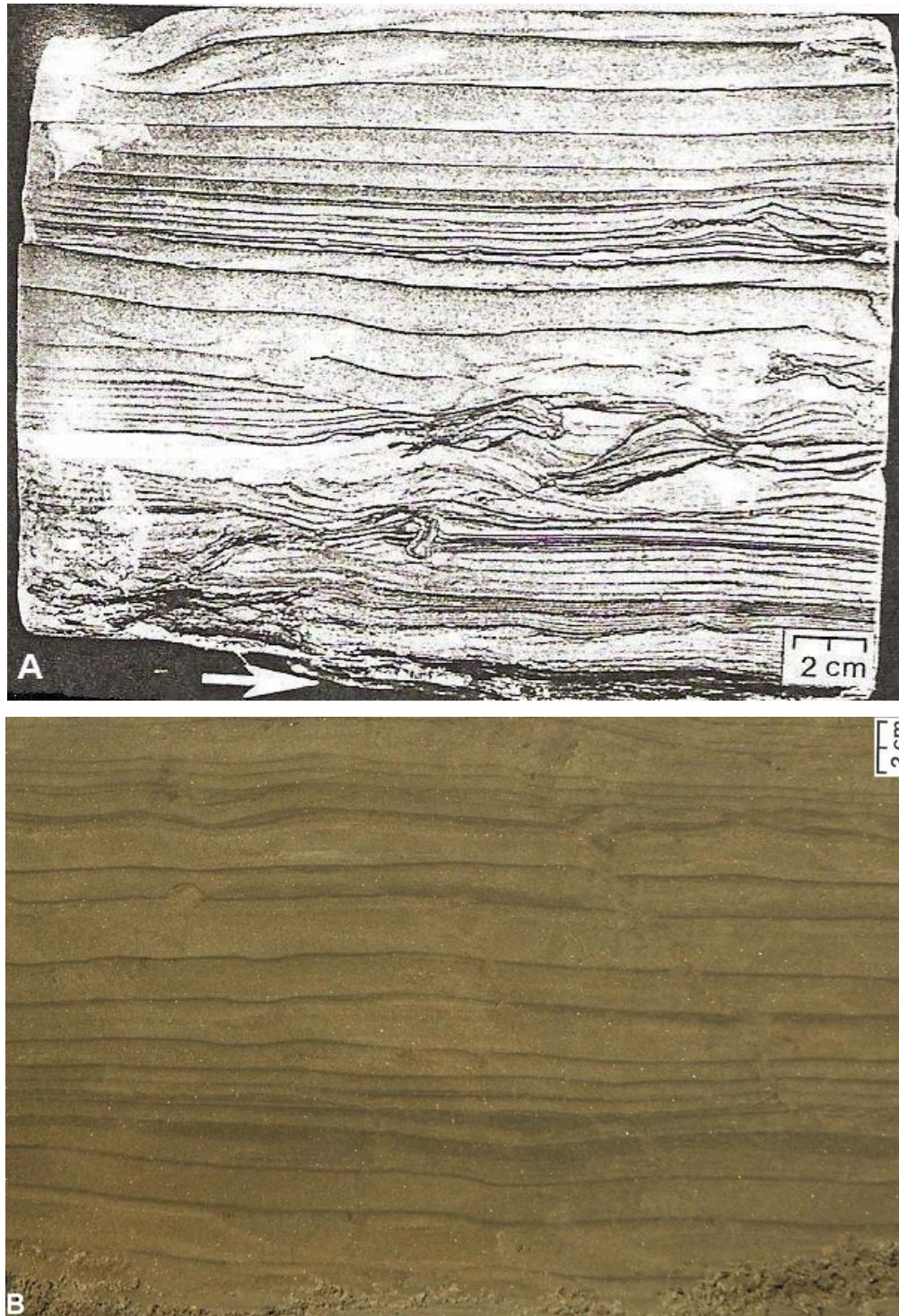


Figure 27. Two figures showing the cyclic thickening and thinning of strata in an upward direction. (A) Slab from Unit A1 of the Tonganoxie succession at the Buildex Quarry. Note the lower arrow pointing toward the underlying Ottawa Coal (from Lanier et al., 1993). (B) Excavation within tidal flat deposits of the Turnagain Arm of Cook Inlet, Alaska. Note how both of these deposits show almost the same style of rhythmic bedding.

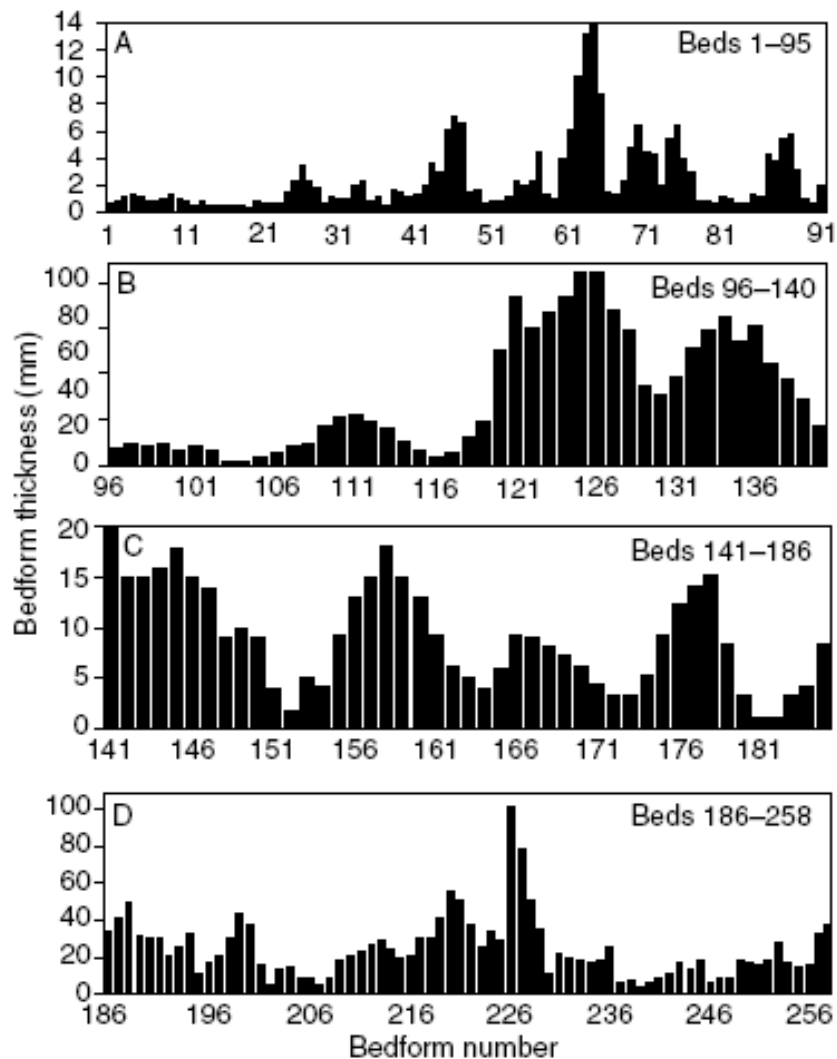


Figure 28. Bar chart showing a clear pattern of cyclicity through the lower part of the Tonganoxie succession at the Buildex Quarry. This rhythmicity is caused by neap-spring tidal cycles. (A) Unit A1, (B) Unit A2, (C) Unit A3, (D) channel-and-levee facies. This chart is based on a study conducted by Lanier et al. (1993) where they plotted the thickness of bedforms vs. the number of bedforms (from Buatois et al., 1998).

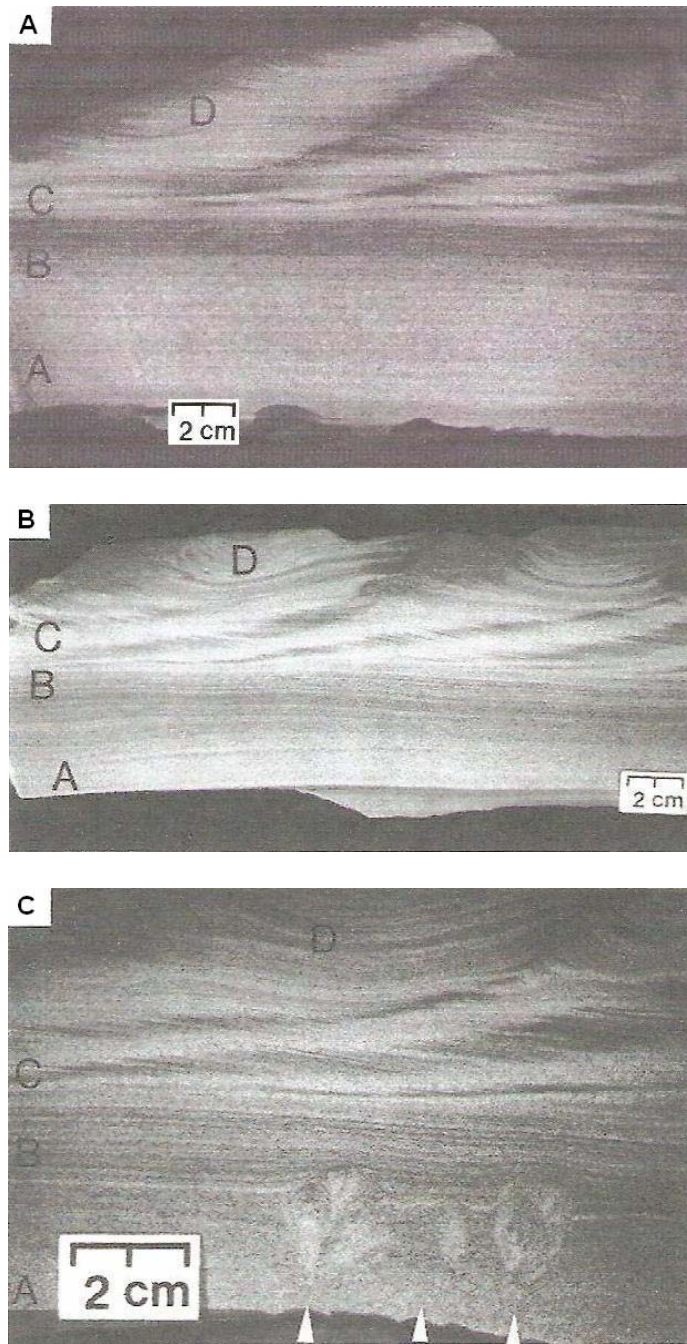


Figure 29. Three figures showing the vertical sedimentary-structure sequences (VSS) within Unit A2. Typically, from bottom up, these intervals are massive to normal graded (A); parallel laminated (B); ripple-cross laminated (C); and draped laminated intervals (D). In this case, these VSS intervals represent shifting and transition from upper to lower flow regime under conditions of flow deceleration during the ebb phase of the tidal cycle. Note the convolution in figure **B**. Note also the fluid movement structures (arrows) in figure **C** and the resulting water-escape structures, indicating rapid sedimentation and high water content during deposition (modified from Lanier et al., 1993).

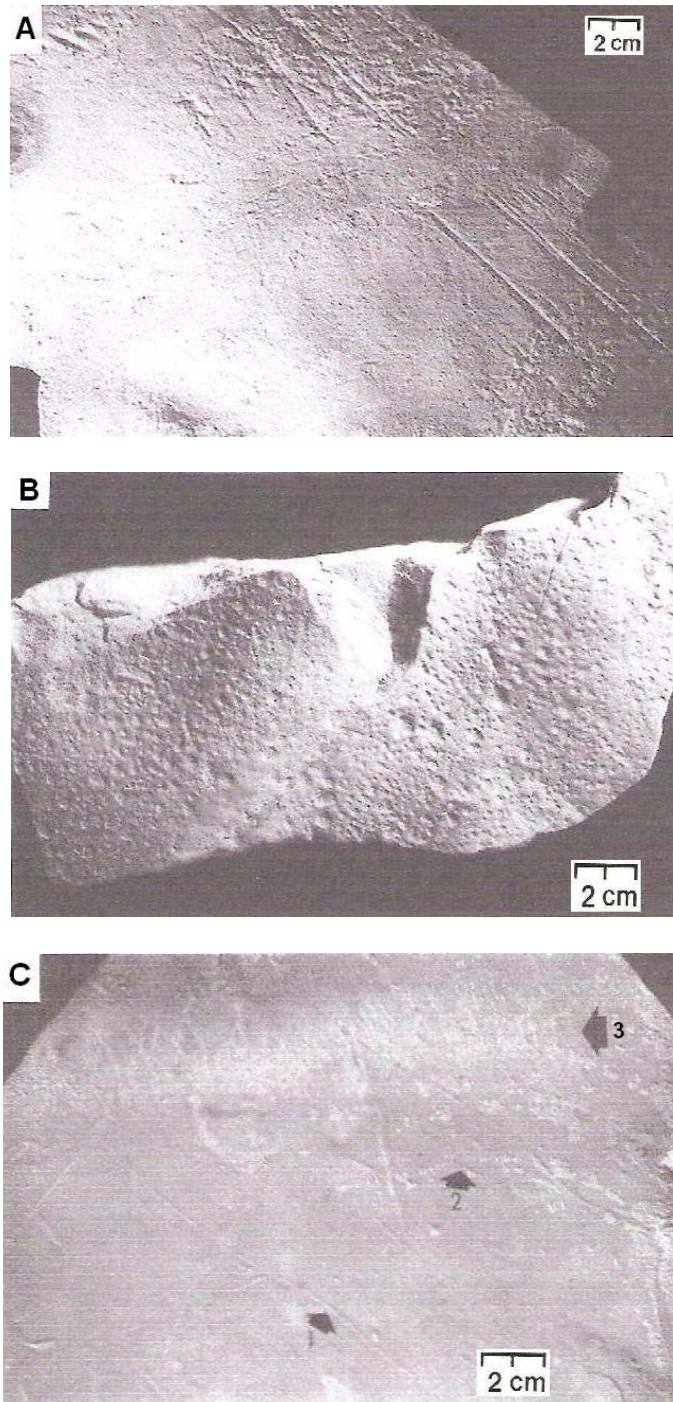


Figure 30. Some sedimentary structures from bedding planes of the Tonganoxie laminated siltstones. **(A)** Drag marks and tiny raindrop impressions on a bed top. **(B)** Raindrop impacts on an upper rippled surface. **(C)** This surface contains more than three sedimentary structures. The main structures are marked by three arrows (1) fish-fin drag marks, (2) arthropod traces, and (3) very small runnels (adapted from Lanier et al., 1993).

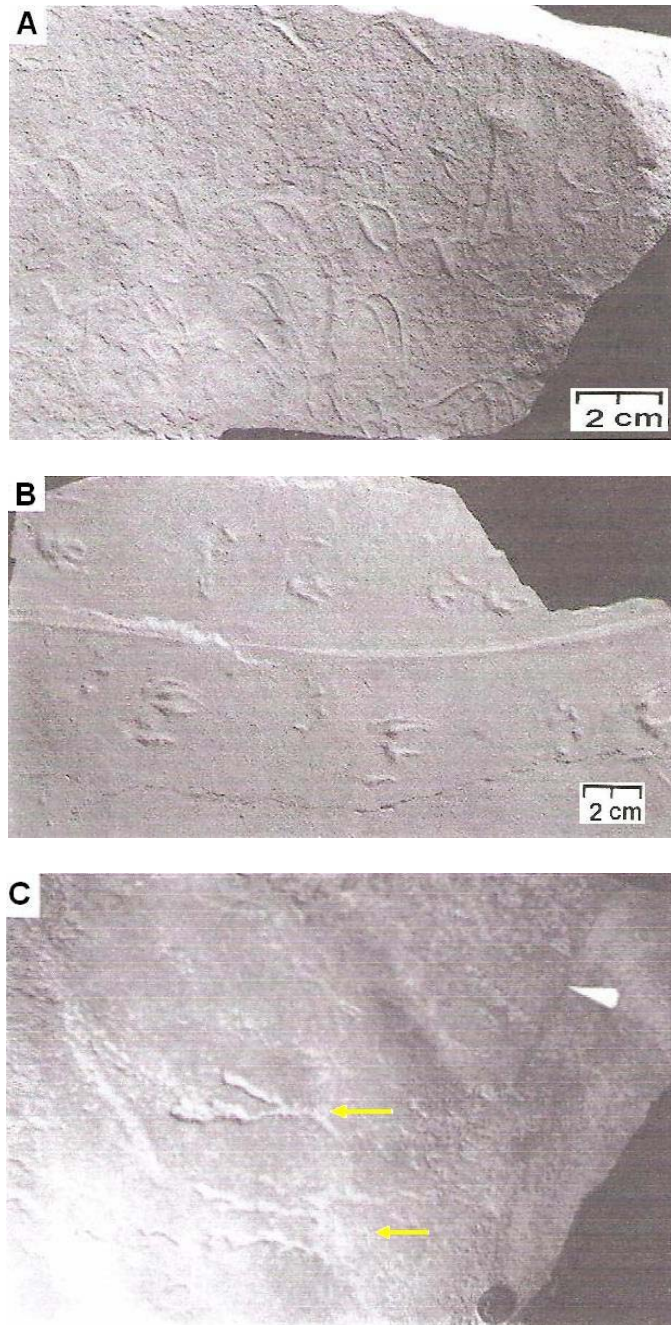


Figure 31. Sedimentary structures and biogenic traces found on bedding planes. (A) Fish-fin drag marks. (B) Tetrapod footprint trackway with tail drag mark (middle line). (C) Few dendritic runnels (yellow arrows) and a standing-water mark (white arrow) (adapted from Lanier et al., 1993).



Figure 32. (A) Foam marks (black arrows) and *Haplotichnus* trace fossils (yellow arrow). (B) *Treptichnus bifurcus* (black arrow) surrounded by runnel marks. (C) *Treptichnus pollardi* (A is modified from Lanier et al., 1993, and B and C are adapted from Buatois et al., 1998).

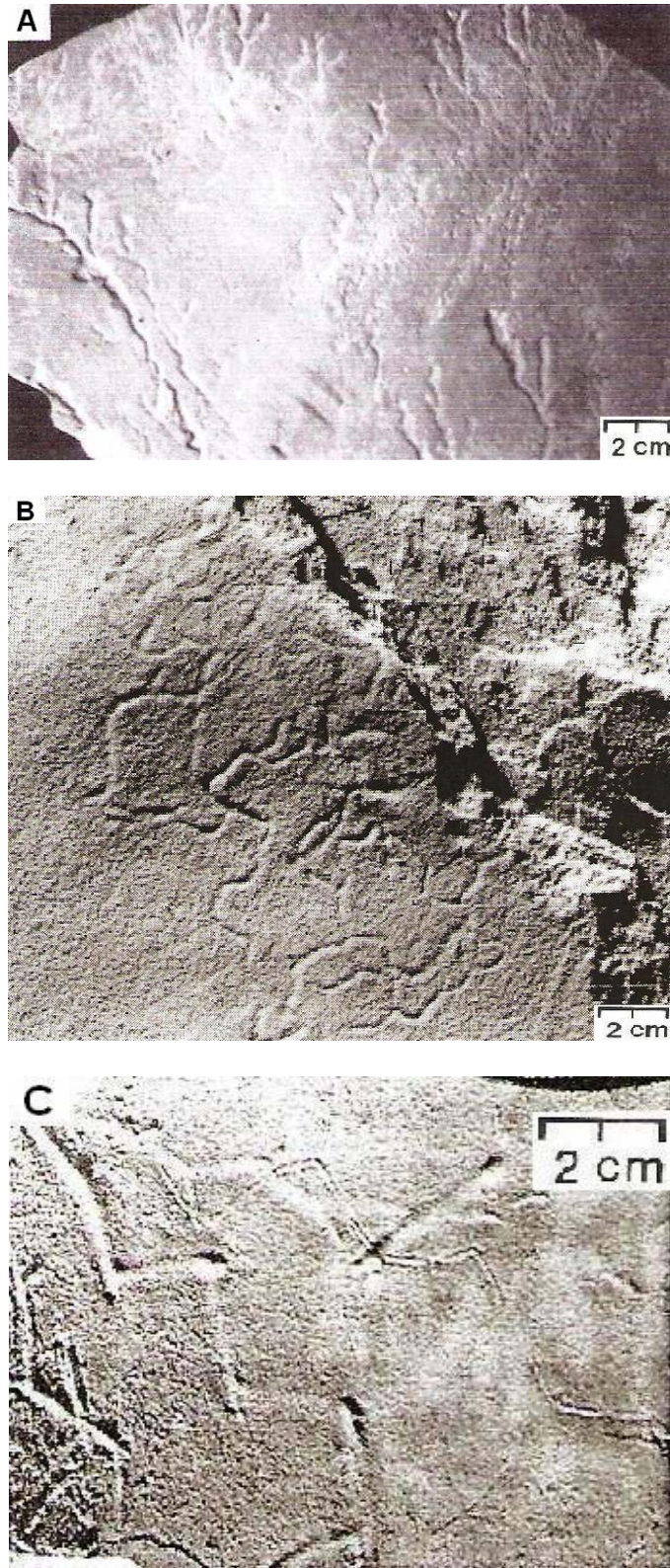


Figure 33. (A) Many dendritic runnel marks taken from Unit A2. (B) Irregular network on a bed surface. (C) Several zigzag burrows (A is adapted from Lanier et al., 1993; B is adapted from Buatois et al., 1998; and C is modified from Archer 2004).

Discussion and Interpretation

There are many aspects and features found within the lower part of the Tonganoxie Member exposure at the Buildex Quarry that are very similar to those usually associated with fluvial overbank/floodplain deposits. Moreover, individual bedsets of the Tonganoxie contain vertical sequences of sedimentary structures that are apparently very similar to the VSS of turbidites. Nevertheless, there is strong evidence that tidal processes may have played a significant part in influencing the mechanism of sedimentation during the deposition of the Tonganoxie Member. This evidence is based on three characteristics: the rhythmic vertical variation in bed thickness throughout the succession, the wide variety of physical and biogenic sedimentary structures, and the brief and repetitive nature of subaerial exposures that may have occurred after every single sedimentation event (Lanier et al., 1993). The latter two features are strongly related to each other. The cyclic vertical thickening and thinning of the bedsets is interpreted as being the result of the influence of lunar cycles (Kvale et al., 1989). What happens here is that tidal cycles strongly influence tidal ranges, flow velocities, and, consequently, rates of sediment transport and deposition or vertical aggradation rates (Kvale et al., 1999). These three variables reach their maximum capacity and strength during spring tides, and they become weaker during neap tides. Thus, we can confidently conclude that the systematic thickening and thinning of bed forms found in the lower part of the Tonganoxie represent the rhythmic alternation between neap and spring parts of tidal cycles. In other words, thicker and thinner strata correspond to spring and neap tides, respectively. The fact that the Tonganoxie succession contains a maximum of 14 sedimentation units per neap-spring tidal cycle further supports the interpretation of tidal influence and indicates a diurnal tidal system as well. Lanier et al. (1993) conducted a detailed analysis of cyclic changes in stratum thickness by plotting bed-form thicknesses vs. bed-form numbers (Figure 28). Their results clearly show the impact of tidal processes on the deposition of this part of the Tonganoxie sequence, and, therefore, these deposits are considered as tidal rhythmites.

Regarding the extensive suite of physical and biogenic sedimentary structures, a question might arise of how these structures may indicate any evidence of tides. Well, these structures suggest that subaerial exposures were periodic, brief, and may have

occurred following each sedimentation event. Their periodicity and association with sedimentation events are consistent with neap-spring tidal cycle interpretation. This means that during spring tides, when tidal ranges are so high, flooding occurs and tidal flats, including upper-estuary flats, become flooded and submerged. Deposition of laminae takes place during this interval because of the high capacity of the system to carry sediments. During intervals of low tides, in contrast, tidal flats emerge, and conditions become more suitable for widespread activities of surface and near-surface organisms that produce a variety of biogenic structures such as surface trails and trackways. Conditions during this low tide period are also perfect for the occurrence of physical sedimentary structures (e.g. drag marks, raindrop impressions, and runoff washouts). This scenario occurs prior and shortly after every sedimentation event which clearly explains the existence of these structures on both bed tops and bed soles. The briefness of the subaerial exposures is best explained by the fact that the Tonganoxie Member has been apparently deposited in a predominantly diurnal tidal system and particularly during the ebb-phase of the tidal cycle when the time of turnaround between flood and ebb phases, known as slack water, was too short (Lanier et al., 1993, Archer 2004). The existence of thin clay drapes in the Tonganoxie supports this interpretation of ebb-phase depositional conditions. Interestingly, brief slack-water intervals also have been observed in some modern macrotidal estuarine settings, namely the Cook Inlet of Alaska where slack-water intervals last about 15 minutes or less (Bartsch-Winkler and Ovenshine 1984; Archer, 2004).

Similar silty tidal rhythmites have been documented and described from several Carboniferous-age settings, especially in the eastern USA, such as the laminated mudstones of the Middle Pennsylvanian Brazil Formation and the Hindostan Whetstone within the Mansfield Formation, both of Indiana, USA (Kvale and Archer, 1990; Kvale and Archer, 1991). However, differences do exist between the Tonganoxie and the other tidally influenced Carboniferous-age deposits. In other words, there are not a lot of ancient successions that are perfectly similar to the Tonganoxie, at least not to the degree that permits a close comparison except for some limited examples. Fortunately, there are several modern depositional systems that can be used as analogous to the Tonganoxie exposure at Buildex such as the Bay of Fundy (Nova Scotia, Canada), the Cook Inlet

(Alaska, USA), and the Amazon River mouth area (Brazil), to name a few.

Stratigraphic Sections

Stratigraphic sections have been constructed based on the description of two cores that were taken from different wells. The total thickness of Mechaskey core is about 145 feet. Shales and mudstones dominate this core, and they range in thickness from about 3ft. to as much as 30 ft. (Figure 35). They also vary in lithology from purely massive mudstone and shale units (Figure 36A) to highly micaceous sandy shale. While some units of the Mechaskey are poorly laminated (Figure 36B), other units exhibit very well developed lamination and planar bedding (Figure 37A). This planar lamination has been reported from modern analogs as well, and it indicates the possibility of deposition by high turbid water apparently under flow deceleration conditions (Archer and Johnson, 1997). The most important characteristic found within some of these fine-grained units is the presence of regular variations in thicknesses of successive laminae, creating vertically accreted units (Figure 35, 37B). Such deposits are known as cyclic tidal rhythmites or neap-spring cycles, and their importance comes from the fact that tidal processes in modern depositional environments generate very similar rhythmic bedding patterns. Thus, stratigraphic units containing these rhythmites such as unit 9 and unit 12 of the Mechaskey (Figure 35, 38, 39) are useful not just to prove the existence of tidal influence during deposition but to help in paleogeographic reconstructions and reconstructions of palaeotidal regimes as well (e.g., Archer et al., 1991; Archer and Johnson, 1997; Kvale et al., 1999). This is even more applicable if no truncated cycles exist. Moreover, some units within the Mechaskey core contain interlaminations of mud and very fine sand (Figure 37A, 39), suggesting a rhythmic change in current velocities which is also a characteristic common in tide-dominated settings.

Aelschlaeger core, on the other hand, is composed mostly of well-sorted coarse-grained sediments (Figure 40, 41). Thick sandstone units with grain sizes ranging from fine to very coarse are predominant (Figure 41A, B). Thin conglomerate units are also common, and are the most noticeable features of this described interval (Figure 41C, D). Other sediments include fossiliferous and non-fossiliferous limestone (Figure 42), well-developed paleosol, and coal. Differences between these two fills, which belong to the

Tonganoxie incised-valley network, are due to the relative proximity to highstand coastlines or to the expansion of the compound fill (Kvale and Archer, 2007). In other words, Aelschlaeger coarse-grained sediments seem to represent trunk paleovalley fills, whereas Mechaskey fine-grained deposits look more like tributary paleovalley fills, or fills that usually occupy Segment 2 of Zaitlin et al. (1994) divisions of simple incised-valley fills.

Stratigraphic Section Legend

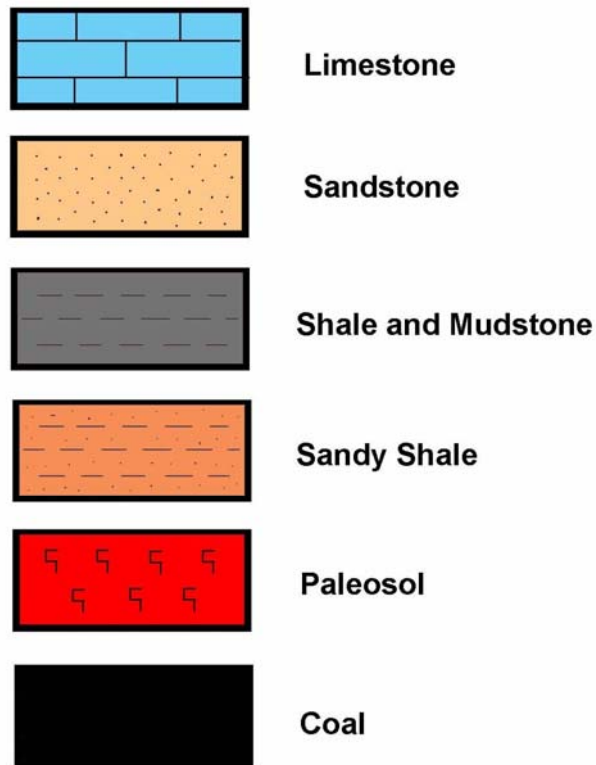


Figure 34. Stratigraphic Section Legend

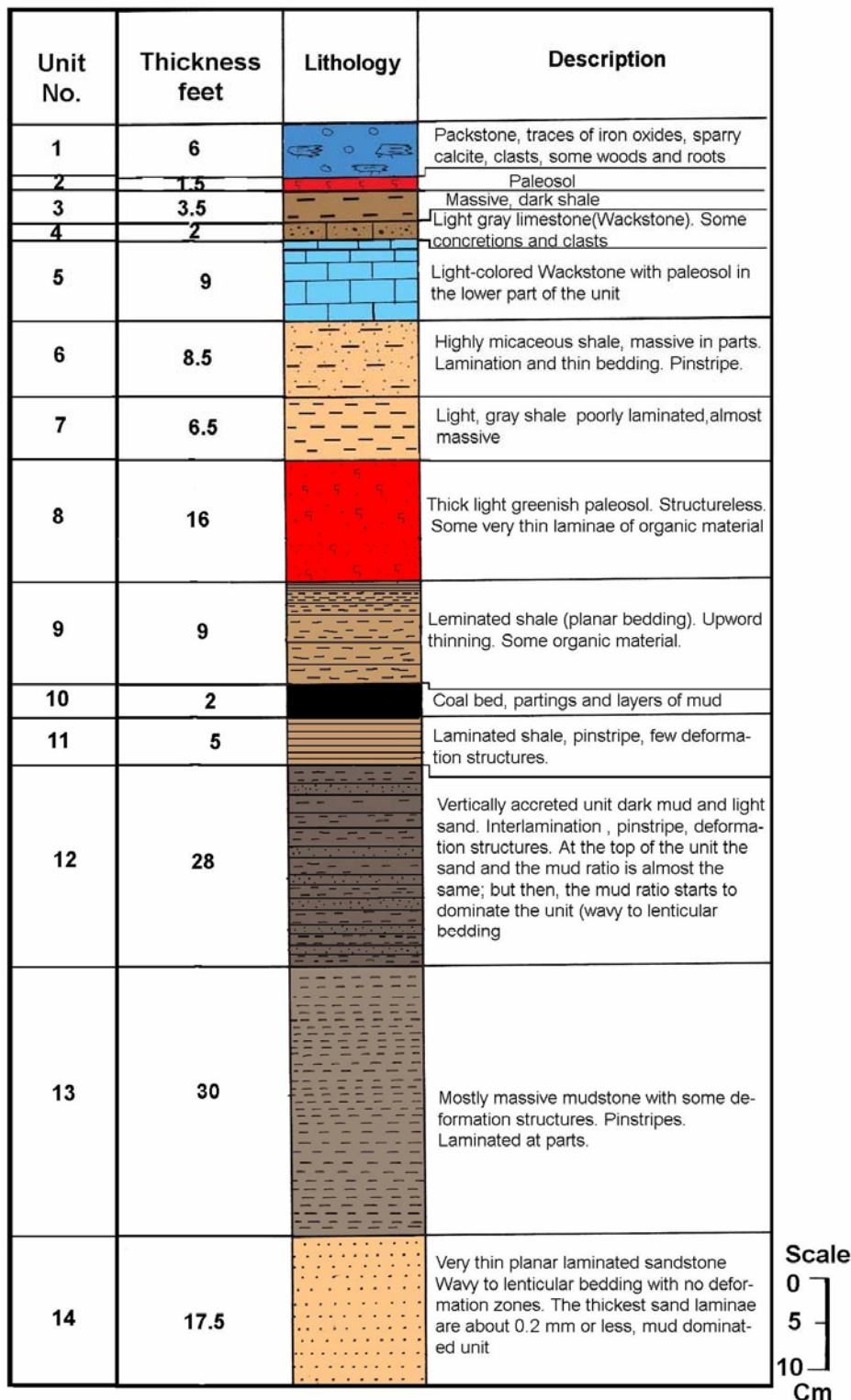


Figure 35. Stratigraphic section of Mechaskey core. Note the dominance of fine-grained sediments throughout the section. Also, note the cyclicity within unit 9 and unit 12. Note that unit 9, which apparently contains regular neap-spring cycles, is positioned directly over the underlying coal unit, just like typical well-developed rhythmites.



Figure 36. Shales and mudstones within Mechaskey core vary in thickness as well as in lithology and development of lamination and planar bedding. Some units are massive (**A**) while others are poorly laminated (**B**). Note the high organic content in unit B.

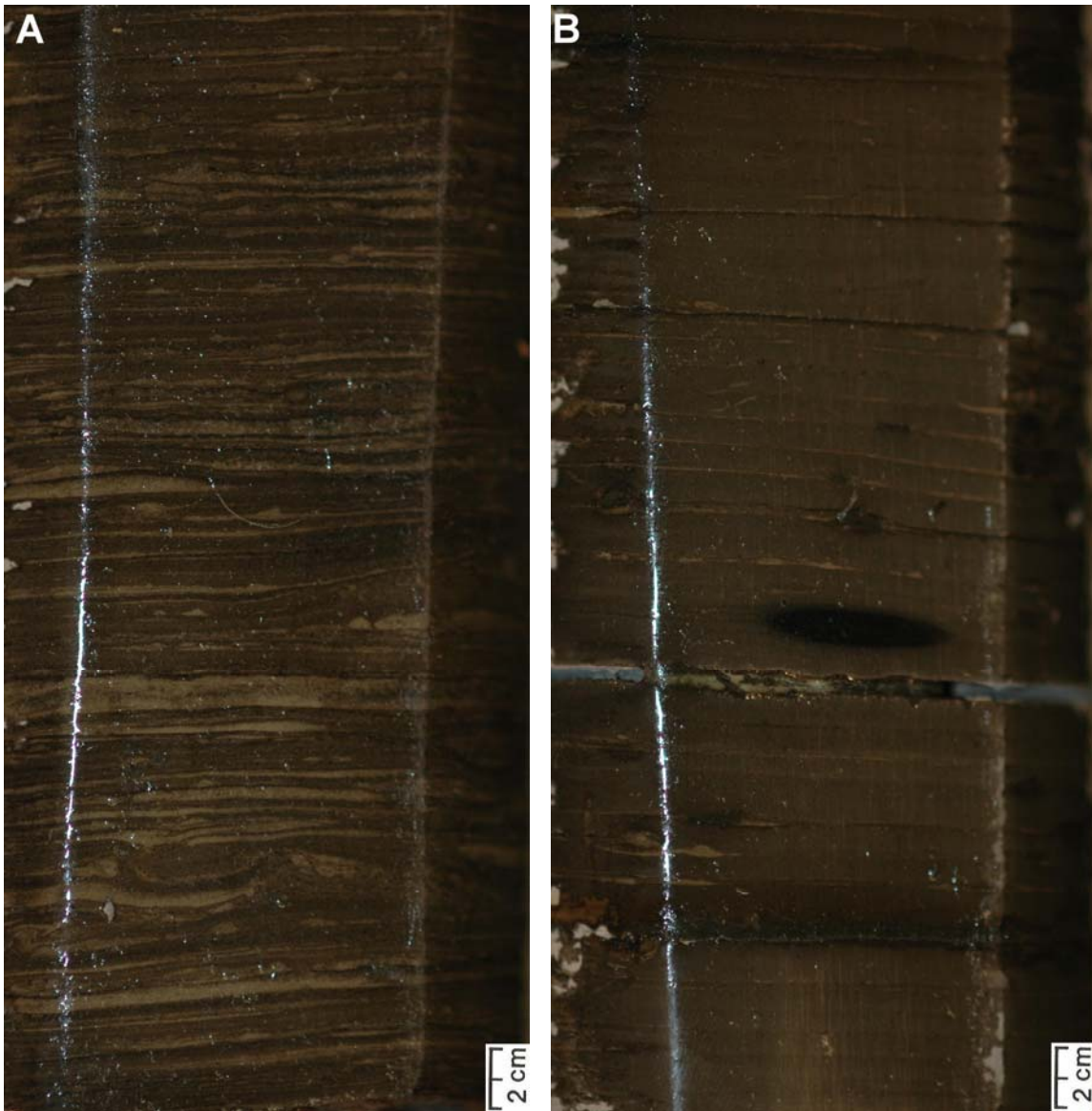


Figure 37. Many fine-grained deposits of Mechaskey contain well-developed planar lamination (A). Note the interlamination of mud and very fine sand in this unit. Cyclic tidal rhythmites or neap-spring cycles with regular variations in thicknesses of successive laminae are well-formed within some short segments of the Mechaskey (B). Note the rhythmic bedding pattern of this unit.

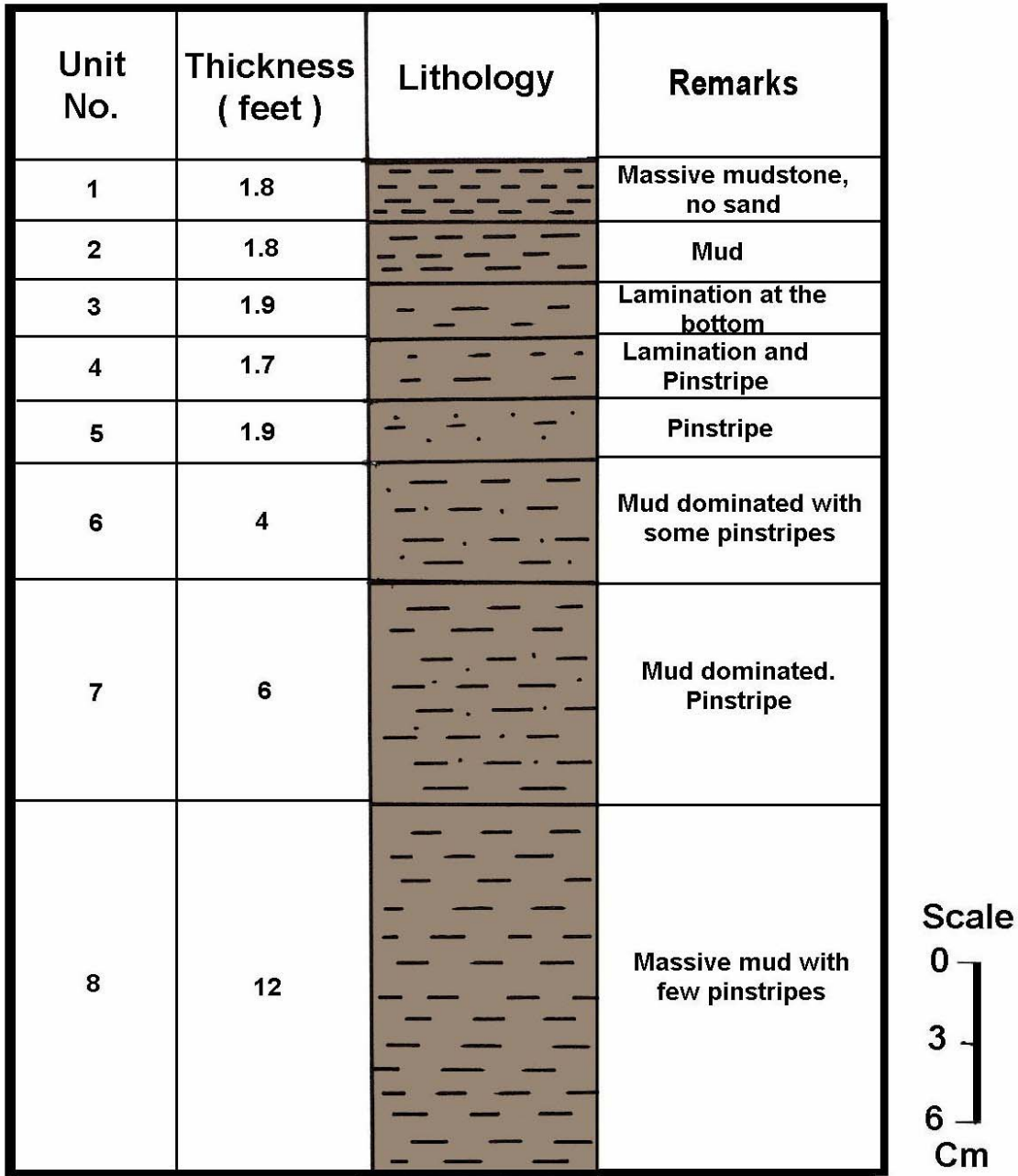


Figure 38. Small section representing unit 9 of Mechaskey core and showing some details. The most noticeable feature in this unit is the rhythmic change in beds and laminae thicknesses, upward thinning in this case. This cyclic bedding pattern has been termed as cyclic tidal rhythmites, and is usually associated with tidally influenced sedimentation taking place within macrotidal estuaries.

Unit No.	Thickne- ss (feet)	Lithology	Sand : Mud (Ratio)
1	2		Mud dominated
2	2		Mud dominated
3	2		Equal
4	2		Mud dominated
5	2		Equal
6	2		Mud dominated
7	2		Mud dominated
8	2		Equal
9	2		Mud dominated
10	2		Mud dominated
11	2		Equal
12	2		Mud dominated
13	2		Mud dominated
14	2		Equal

Scale

0
3
6
Cm

Figure 39. Small section representing unit 12 of Mechaskey core and showing some details. Note the interlamination of mud and very fine sand, which suggests a regular change in current velocities during transportation and deposition within a tide-dominated environment. In addition, note the maximum 14 events within this neap-spring cycle, indicating a dominantly diurnal tidal system.

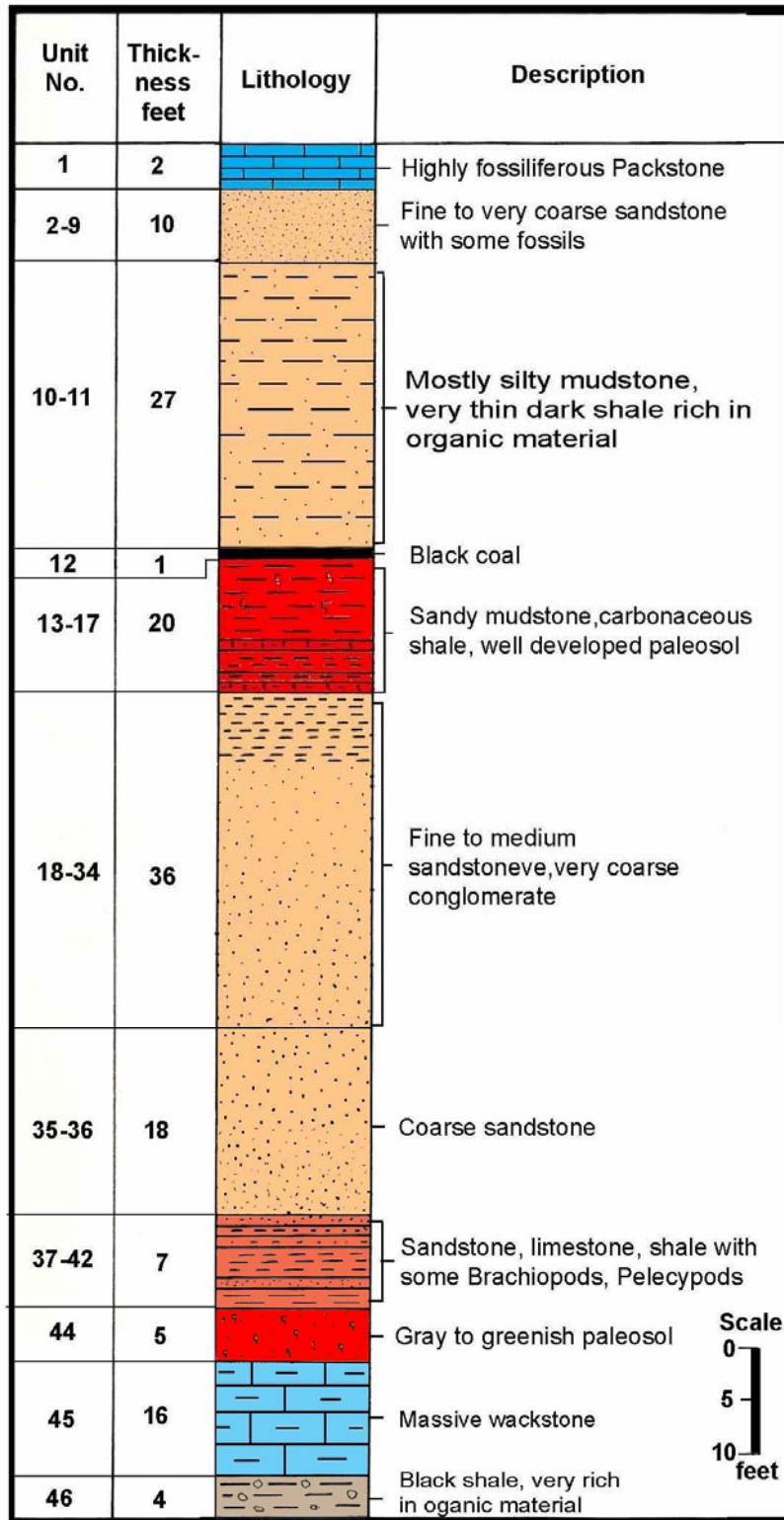


Figure 40. Stratigraphic column constructed based on part of Aelschlaeger core. Note the predominance of coarse-grained deposits. Note also the interlamination of sandstones and shales in unit 37-42. Other deposits include limestone and well-developed paleosol.

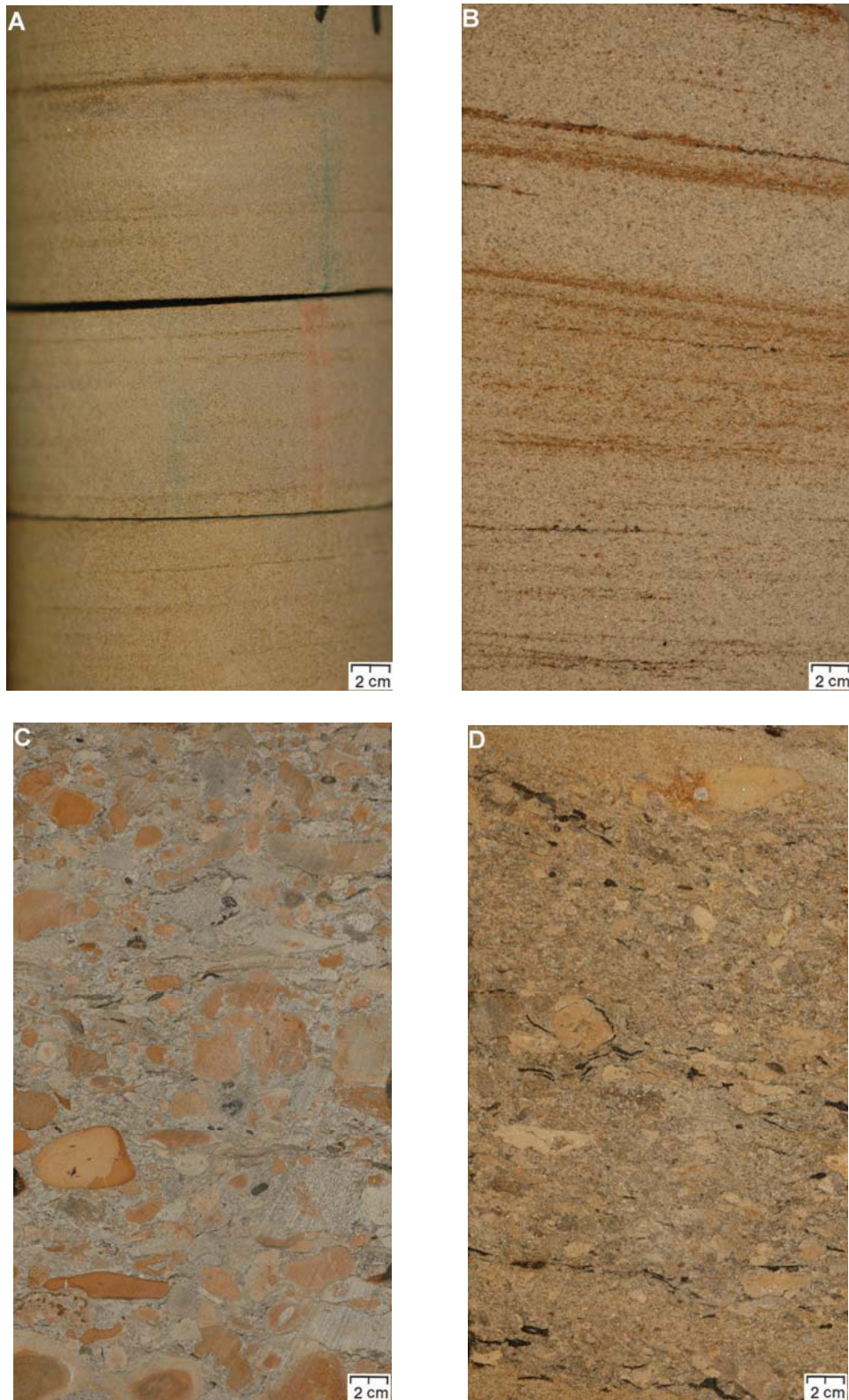


Figure 41. Aelschlaeger core is dominated by clastic coarse-grained sediments. These deposits are mostly sandstones with grain sizes that range from fine (A) to very coarse (B). Note the evident mica particles especially within coarse-grained sandstone. This core as well contains poorly sorted conglomerates (C) (D).

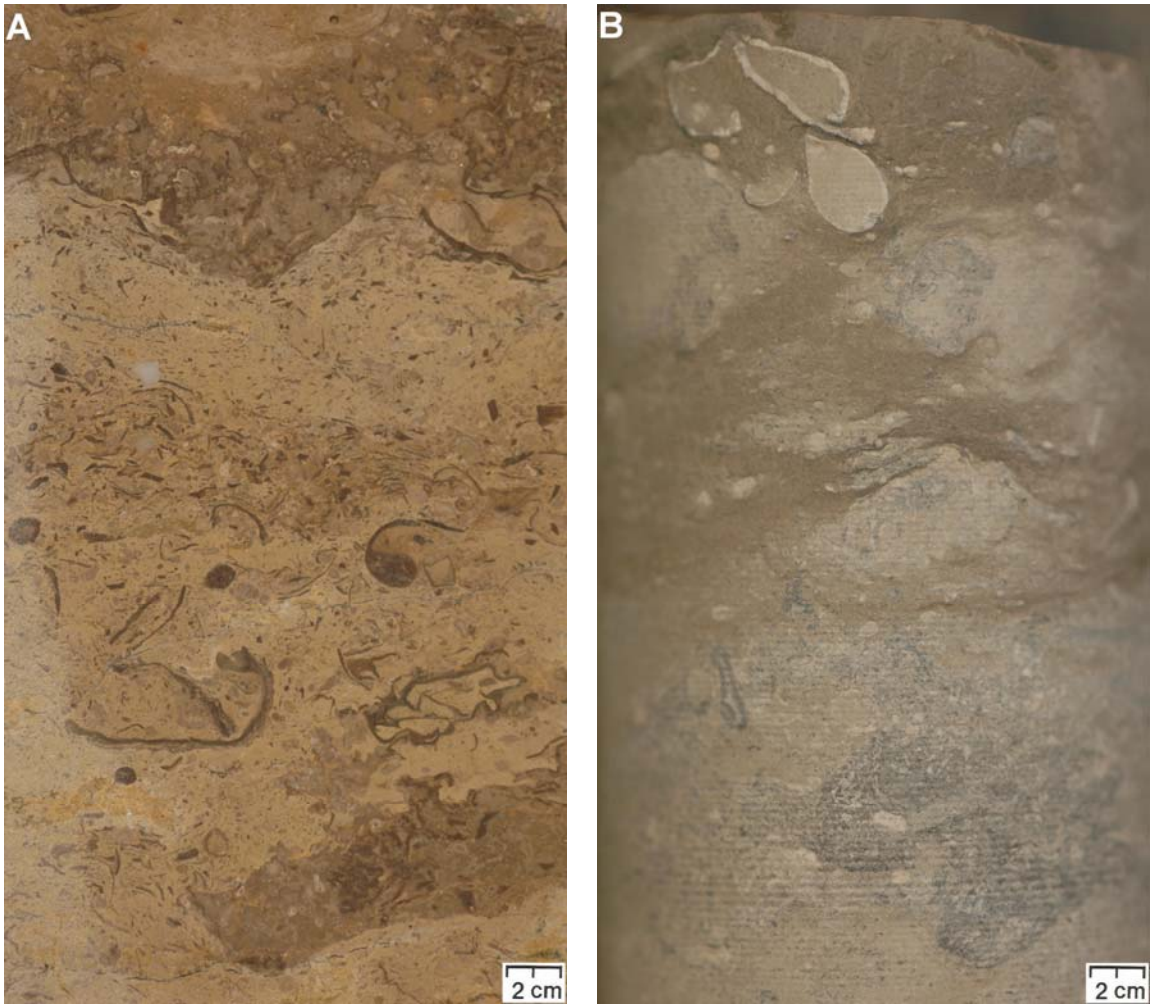


Figure 42. Limestone units within described Aelschlaeger core are rather thick. These limestones are mostly fossiliferous (**A**) (**B**), especially in the uppermost part of the core. Fossils include bivalves and brachiopods. Note the disarticulated brachiopods in unit A (middle) and the articulated brachiopods in unit B (upper left).

The Modern Analog

Location and General Information

The area examined as a modern analog includes data from Cook Inlet in south-central Alaska, USA (Figure 43). Many studies have been conducted on the upper part of Cook Inlet (e.g., Carlson, 1970; Sharma and Burrell, 1970; Bartsch-Winkler, 1982, 1988; Bartsch-Winkler and Ovenshine, 1984; Archer, 2004; Greb and Archer, 2007). However, the study conducted by Bartsch-Winkler and Ovenshine (1984) is considered the first detailed analysis of Cook Inlet intertidal zone sediments. Compared to other modern macrotidal settings, this area has the highest latitude of 61° N. Lat. (Figure 43, 44) (Archer, 2004; Oey et al., 2007). In general, it is an area with complex, embayed coastlines bordered by mountains, roofed with glaciers, with extensive marshes and bluffs. This area has some large embayments, and the Cook Inlet is one of the largest embayments in that region. Its width is about 37-83 km, and the Inlet extends more than 300 km from the Gulf of Alaska in the south to the city of Anchorage in the northeast where it splits into two shallower extensions or arms (Oey et al., 2007; Bartsch-Winkler and Ovenshine, 1984).

The two extremities of Cook Inlet are the Knik Arm, located north of Anchorage, and the Turnagain Arm, situated southeast of the city of Anchorage (Figure 43). These two arms are supplied with glacial meltwater delivered by relatively small rivers that originate from alpine glaciers. There are no major rivers flowing into the Turnagain Arm (Archer, 2004; Bartsch-Winkler and Ovenshine, 1984). Moreover, the rivers that feed the Turnagain Arm are much smaller than those of the Knik Arm. As a result, the Knik Arm is almost completely filled with fine-grained sediments, and its yearly sediment supply is estimated to be between 13 and 19 million tons. On the other hand, the Turnagain Arm is only partly filled with sediments with yearly sediment supply of about 2.5 million tons (Bartsch-Winkler and Ovenshine, 1984). This partial sediment filling and limited supply does not make the Turnagain Arm area unsuitable for this study. In fact, it is one of many other reasons that promoted this area as the source area for modern analogs because this lower fluvial contribution induces an active tidal sedimentation in the Turnagain Arm. Generally, the highest discharge of rivers takes place during the summer, whereas lower sediment discharge rates occur during the winter and during times of low rainfall.

In addition to glacial rivers, there is another source of sediment supply. This source is the erosion of Pleistocene bluffs that surround the Cook Inlet, especially around its upper part.

In general, the outer portions of Cook Inlet are mostly erosional, whereas the inner segments are of depositional nature. The Cook Inlet is one of the highest tidal range areas in the world with tidal ranges exceeding 9 m (Figure 44) (Archer and Hubbard, 2003). The inlet is also among the most seismically active areas in the world. This is very important in affecting sedimentation patterns of the Cook Inlet because seismically active areas normally have depositional systems that can easily maintain short-term sedimentary signals, which, in turn, could reveal responses to annual-scale climatic shifts. Furthermore, earthquakes, along with volcanic eruptions, could also affect the nearby tidal zones by causing tectonic uplift, subsidence (Figure 45), sediment consolidation, and sporadic deposition of huge quantities of material (Bartsch-Winkler and Ovenshine, 1984). For instance, the aggradation of intertidal sediment in upper Turnagain Arm began because of the subsidence caused by the sediment consolidation and tectonic lowering of the land, which were induced by the Great Alaskan Earthquake of 1964 (Bartsch-Winkler, 1988; Archer, 2004). This subsidence has also affected a considerable area of spruce forests (Figure 45). It should be mentioned that this area is located close to a major suture zone called the Cook Inlet Benioff Zone between the North American and Pacific plates (Stephens et al. 1984), which explains why it is so active seismically and volcanically.

Another merit of choosing the Turnagain Arm of Cook Inlet in Alaska over the other modern macrotidal analogs is that this area has been influenced only slightly by human activities because of the surrounding state parks and U.S. National Forests (Archer, 2004). Much of our working site, for instance, is within Chugach State Park; hence, the area is protected from growing urbanization and development projects. In addition, these state and national parks have granted us an easy access to our data stations. An example of the limited anthropogenic influence is that the fluvio-estuarine transitional zone within the Cook Inlet is almost untouched compared to those transitional zones of the Bay of Fundy (Canada) and Bay of Mont-Saint-Michel (France) which have been heavily diked. However, the urban expansion in these regions could eventually result in remarkable

environmental changes.

Climate and Precipitation Rates

The Turnagain Arm has an unusual climate because of the subarctic latitudes in addition to the maritime effects. Winters are cold, and the average minimum temperatures are usually below zero for about 7 months of the year (Archer, 2004) (Figure 46A). Although changes in temperature are regular in general, there is a striking seasonal temperature variation with a difference between highest and lowest recorded temperatures of about 71° C (Figure 46A). The highest summer temperatures occur during July and August with an average of 18° C (Archer, 2004). It is noteworthy that the daylight is about 21 hours in late June and just about 3 hours in late December. This remarkable day length variation is a result of the high latitudes of the area (Figure 43, 44).

The total precipitation rate varies significantly in Turnagain Arm with the highest being in August and September, but the average is generally below 25 mm/month (Figure 46B). Moving towards the eastern inland limit of the Turnagain Arm, the precipitation increases remarkably (Figure 46B). This noticeable increase in precipitation rates is linked to orographic influences, and it forms an area of temperate rainforests and peatlands along the coastlines of inner parts of the Turnagain Arm (Archer and Greb, in press). Although rainfall is intense, the widespread vegetation interrupts and reduces the sediment flux in the rivers and streams that draw off the areas of rainforests.

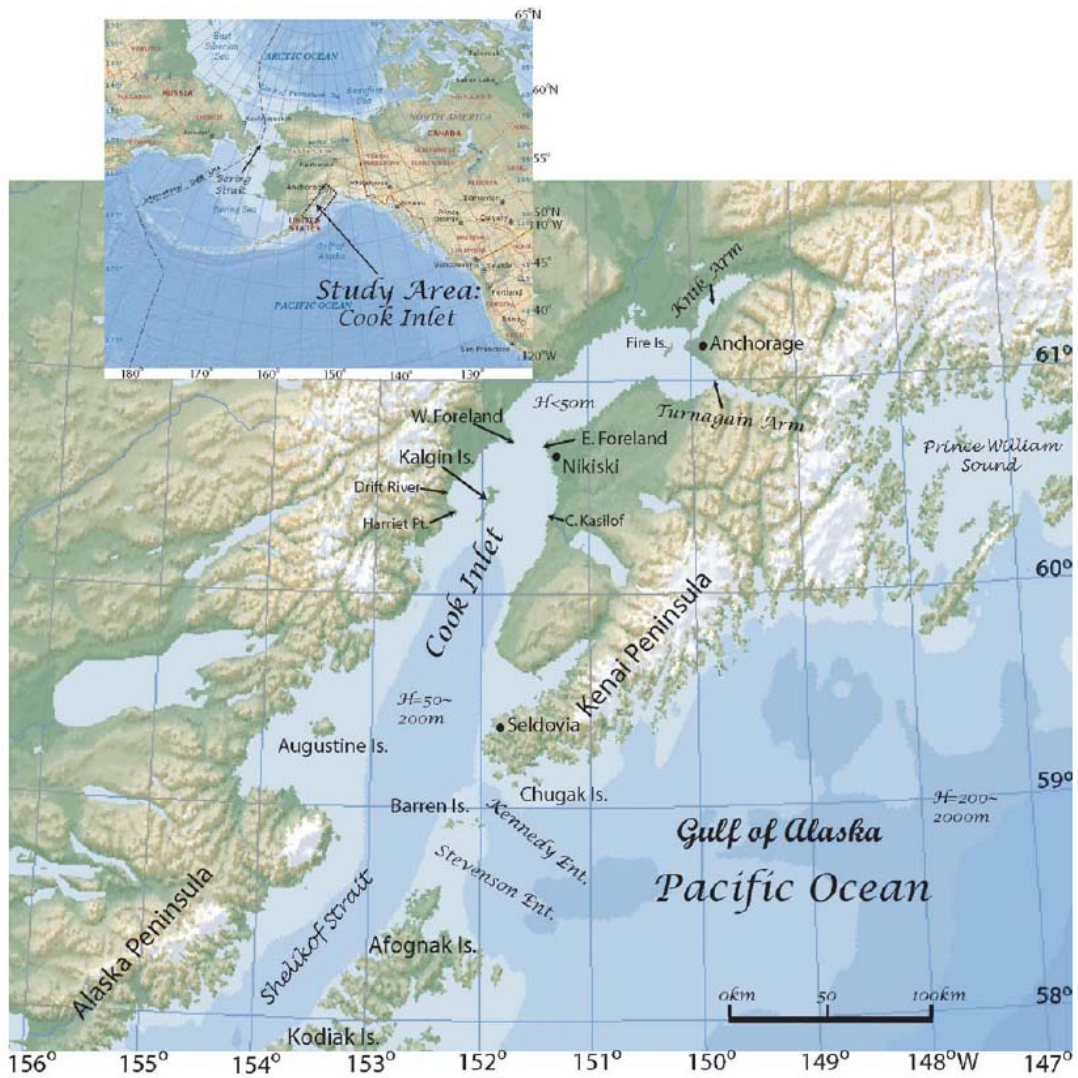


Figure 43. Map showing the location of the Cook Inlet on the south-central coast of Alaska, USA. It also shows the Knik Arm and the Turnagain Arm along with major topographic and geographic features surrounding the area (from Oey et al., 2007).

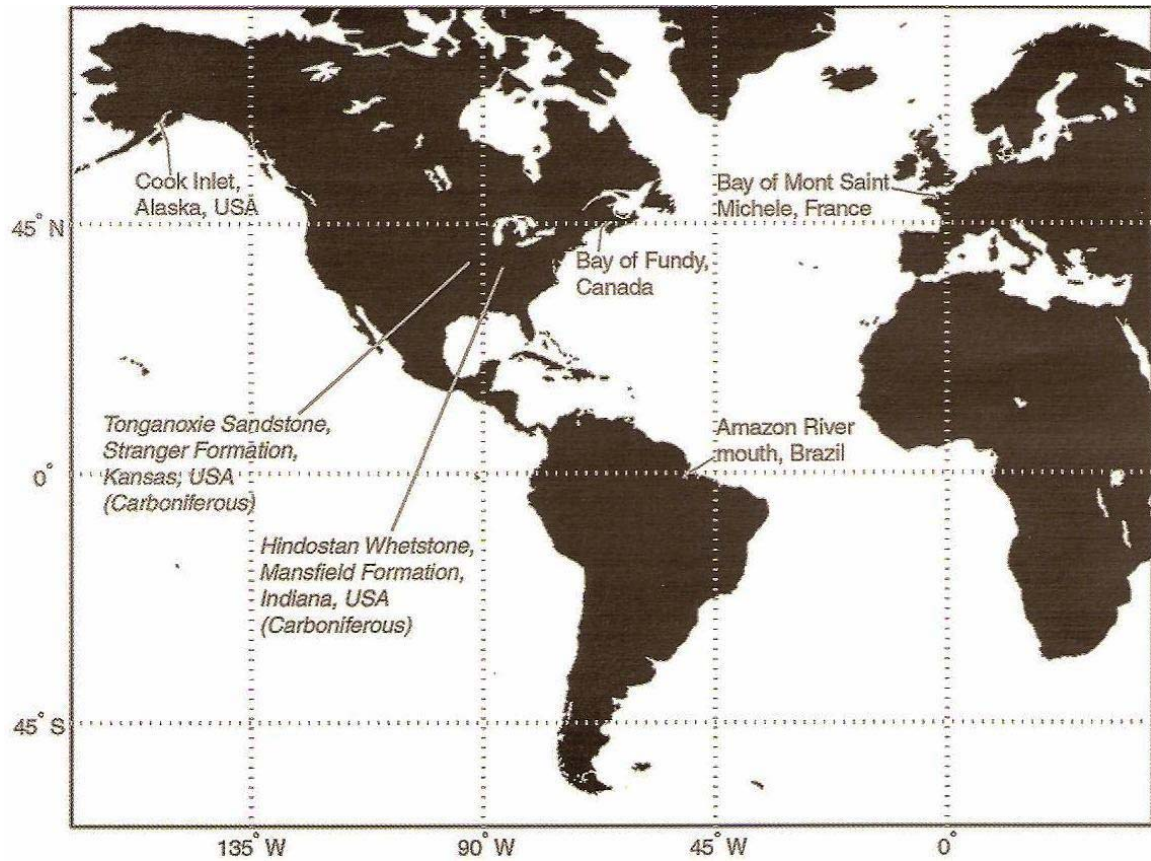


Figure 44. Location of the Cook Inlet along with some other world's highest tide areas such as the Bay of Fundy, the Bay of Mont Saint Michel, and the Amazon River mouth. It also shows two ancient (Carboniferous) macrotidal settings including the Tonganoxie Sandstone of Stranger Formation, Kansas, USA, which is our ancient study area. Note the very high latitude of Cook Inlet compared to the other sites (from Archer, 2004).



Figure 45. Photos showing a huge area of spruce forests affected by the Great Alaskan Earthquake of 1964. This earthquake caused several meters of subsidence. Consequently, significant parts of spruce forests were dropped down into the upper intertidal zone (A). Note also the resulting uprights and in-place tree stumps (B).

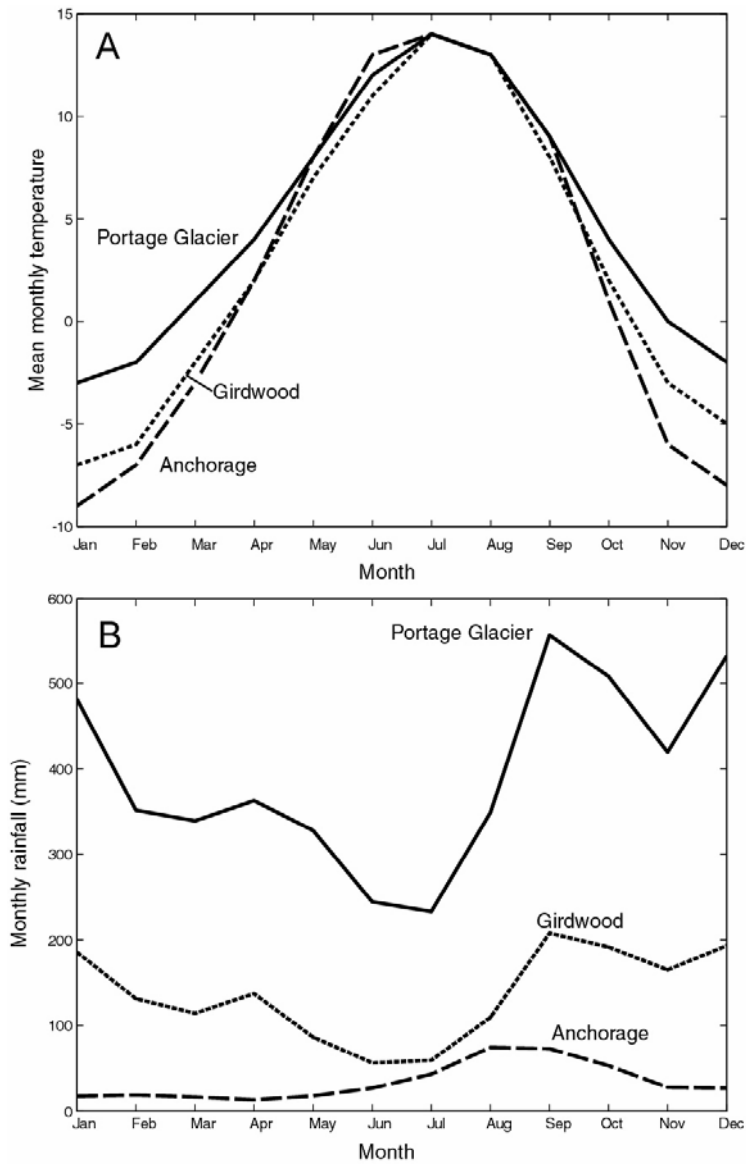


Figure 46. Chart showing (A) mean monthly temperature and (B) monthly rainfall of the Turnagain Arm area. Note the huge variation in the precipitation as we move from Anchorage city toward the eastern inland limit of the Turnagain Arm (from Archer and Greb, in press).

Depositional Zones

The Turnagain Arm of Cook Inlet has an estuarine depositional setting that is very similar to some other typical macrotidal estuaries such as the Bay of Fundy (Nova Scotia, Canada) and the Bay of Mont Saint Michel (France). However, there are some differences caused by its high relief of bounding topography, glacial and tectonic history, and the climate of the estuary (Archer and Greb, 1995). This southeast-trending, funnel-shaped estuary is about 75 km long and from 3 to 23 km wide, being widest at the mouth close to Fire Island and narrowest at the estuary head towards the east (Bartsch-Winkler and Ovenshine, 1984) (Figure 43, 47). Turnagain Arm can be described as an ancient fjord that has been accumulating deposits for more than 14000 years, and it is still an area of contemporary deposition (Bartsch-Winkler et al. 1983).

There are six distinct depositional zones within Turnagain Arm (Figure 47B). These zones are: (Zone 0) an outer zone located at the point between the arm and the main inlet; (Zone 1) linear sandbars and large tidal channels; (Zone 2) silt and sand flats with narrowing tidal channels; (Zone 3) fluvio-tidal point bars in the fluvio-estuarine transition; (Zone 4) braided to meandering fluvial channels with floodplains, and (Zone 5) glacio-lacustrine systems. Before describing each of these depositional zones in some detail, it is important to briefly talk about the depositional elements that created this type of zonation such as salinity, tides, and fluvial and glacial components. As mentioned above, the erosional and depositional settings within Cook Inlet have many similarities in common with other hypertidal systems that are affected by very high tidal ranges. One of these similarities is that all these macrotidal systems have very similar subdivisions of the depositional area. The subdivisions are: (1) bayward; (2) sand flats of mid-estuary; and (3) fluvio-tidal point bars (Figure 47A). However, the difference between the Turnagain Arm and the other estuaries is that while the outer four zones (0, 1, 2, and 3) are found in almost all hypertidal systems, zone 4 and zone 5 are unique to Turnagain Arm. The abundance of side drainages that enter into the Turnagain Arm is yet another major difference.

Zone 0

Zone 0 covers the seaward end of the Turnagain Arm and huge areas of the southern portion of Cook Inlet, and it is generally characterized by aggressively receding coastal

sea cliffs. In this zone, there is a shortage of long-term deposition. Nevertheless, it has depositional facies that consists of broad mud and sand flats in addition to gravelly beaches. Such facies regularly encompass large dropstones carried by floating icebergs. The mud in Zone 0 is thinly layered, and it normally overlies the sands and the gravels. However, the mud flats within this zone are highly bioturbated and thixotropic (Archer and Greb, in press).

Zone 1

This zone is known as the zone of maximum tidal range and is positioned landward from the outer estuary (Archer and Hubbard, 2003). It starts at the eastern end of the Chickaloon Bay where two faults cross the arm. The point where zone 1 begins is characterized by two things. First, the estuary quickly narrows because of the faults. Second, the seaward sand flats end in the estuary funnel and tidal channel processes start to control most of the estuary (Archer and Greb, in press). Due to lateral limitation of the estuary, the tidal flow here is linear. Zone 1 has also large, non-attached sand bars that are by and large oriented parallel to the axis of the Inlet (Figure 47B).

Zone 2

Zone 2 can be recognized when laterally broad flats replace the elongate nonshore-attached bars of Zone 1 (Figure 47B). This transition between Zone 1 and Zone 2 takes place at Bird Point. At that locality, the bedrock rim expands out into the estuary, causing a bedrock blockage in the estuary funnel. As a result, the central tidal channel bifurcates into two minor channels. The tidal flats in this zone are very extensive laterally, and they cover most of the inner parts of the Turnagain Arm (Figure 48, 49). These flats consist mostly of medium-to coarse silt and fine-grained sand. Tidal bores have a big impact on the suspended-sediment concentration in Zone 2 because very high levels of turbidity occur during their passage (Figure 51). This turbidity zone is generated by erosion in the lower intertidal zone (Figure 51A), which accounts for the widespread pitted and scoured flats within lower intertidal areas.

Rates of vertical accretion can be exceptionally high in this zone because of bore-induced turbidity (Archer and Greb, in press). The good thing about these high sedimentation rates is that they could mirror the diurnal disparity of the tidal system via the alternation of thicker and thinner beds and layers. In addition, very high rates of

sedimentation significantly reduce long-term habitation in tidal flats. Hence, the degree of bioturbation can be greatly minimized, which provides an excellent potential for preservation of biogenic and physical sedimentary structures, especially surficial trackways (Archer, 2004). Although excessive bioturbation does not have enough time to developed within such active depositional conditions, dewatering features associated with rapid sedimentation are common.

Zone 3

The transitional area between Zone 2 and Zone 3 (Figure 47, 48) exhibits steady change from laterally widespread tidal flats to more laterally limited fluvio-estuarine systems. One of the most important features within Zone 3 is the fluvio-tidal point bars, which are dominated by graded laminae and thin beds. The beds in this zone show alternating thinning and thickening neap-spring tidal cycles that can be traced for long distances, especially within cutbank exposures (Figure 50A) (Archer and Greb, in press). These tidal cycles are also known as tidal rhythmites, cyclic rhythmites, or small-scale tidal bundles (Kvale et al., 1999), and some workers refer to them as heterolithic rhythmites or heterolithic bedding especially if there is an obvious contrast between grain sizes (Ehlers and Chan, 1999). Typical tidal rhythmites appear as vertically stacked cyclic alternations of silt/sand-rich and mud-drape laminae (Figure 50B). The importance of this lamination is that the deposition of individual laminae is probably the result of single tidal events or flood tides. Thus, laminae thicknesses probably reflects tidal heights and flow velocities that exist during neap-spring tidal cycles. The sedimentary facies of this zone are very comparable to some Carboniferous-age siltstone facies such as the planar-stratified siltstone assemblage of the Tonganoxie Sandstone at Buildex Quarry, which exhibits similar systematic thickening and thinning throughout its vertical sequence, as we have seen earlier. Just like Zone 2, widespread bioturbation is not common here, and there are similar types of surficial features such as trails and trackways.

Zone 4

While the transition from Zone 2 to Zone 3 is gradual, the conversion from Zone 3 to Zone 4 is incredibly abrupt especially in terms of sediment type (Figure 48). At the transitional area, there are three rivers flowing into the arm (Figure 48). River systems in zone 4 are either braided or highly sinuous. Usually, these streams reside in abandoned

glacial valleys, and they are dominated by coarse fluvial gravels that are composed of metasedimentary rocks such as gray mudstone, siltstone, argillite, and some greywacke (Archer and Greb, in press). It should be mentioned that major glacial meltwater rivers are light-colored due to the high amounts of suspended glacial silt; thus, they are sometimes called Whitewater Rivers. On the other hand, minor and small rivers that drain areas of moderate rainforests are called Clearwater Streams because they contain clearer water.

Zone 5

Zone 5 includes the inland limits of the fluvial drainage basins. It is dominated by glacio-lacustrine systems (Archer and Greb, in press) (Figure 47, 48).

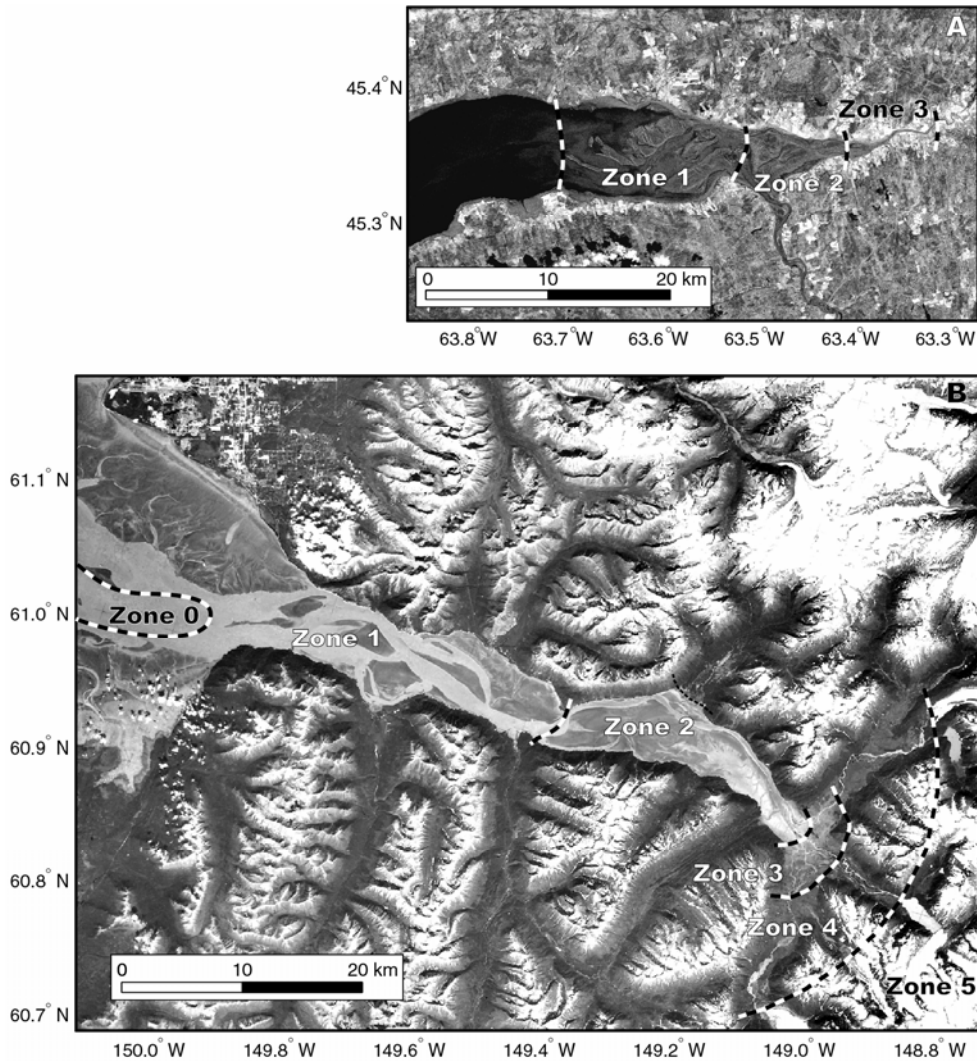


Figure 47. Aerial photos of the Turnagain Arm showing: (A) six distinct depositional zones of Turnagain Arm from the outer zone (Zone 0) to the glacio-lacustrine system zone (Zone 5), or the inland limits of the fluvial drainage basins. (B) three subdivisions of the depositional area that are commonly recognized within macrotidal systems (from Archer and Greb, in press).

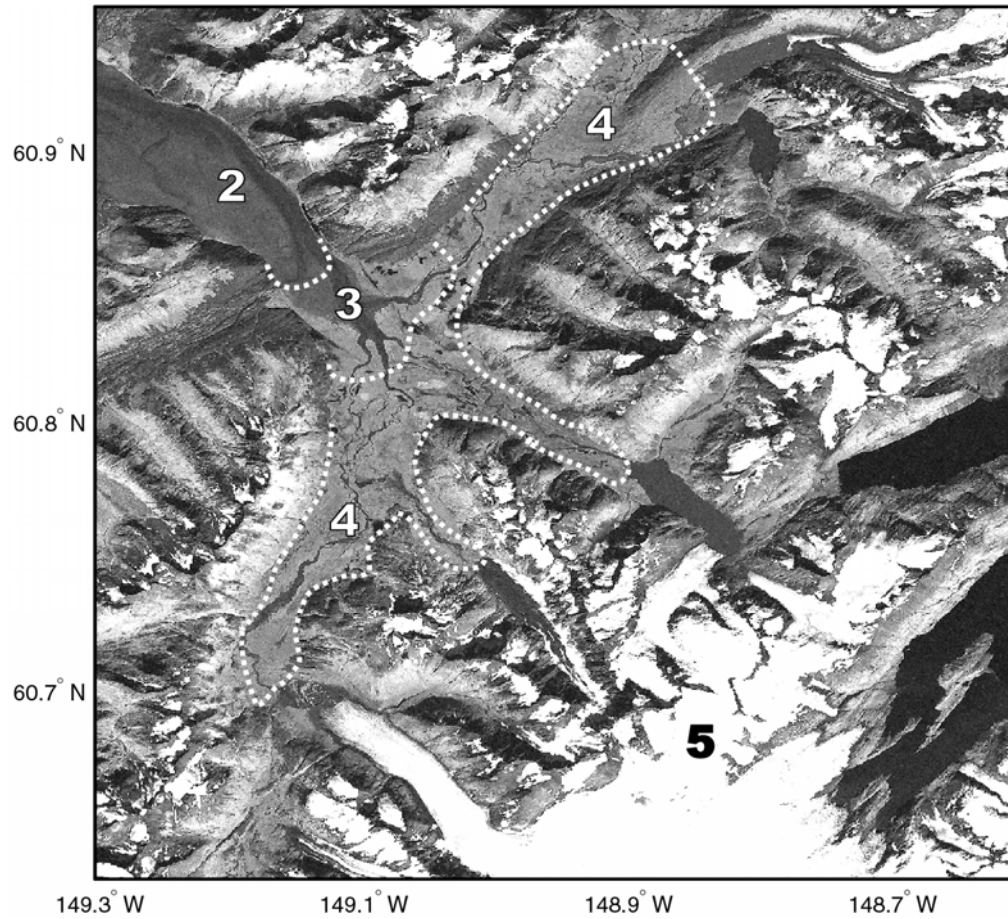


Figure 48. Photo showing some transitional zones within the depositional zonation of the Turnagain Arm, Cook Inlet, Alaska, USA. Note the gradual transition between zone 2 and zone 3 and the abrupt transition between zone 3 and zone 4 (from Archer and Greb, in press).



Figure 49. A view of a laterally extensive tidal mudflat at Bird Point in the Turnagain Arm, Cook Inlet, Alaska. Note the partly glacier-covered mountains in background and the huge, laterally extensive flat in the foreground. Also, note the widespread ripples on the surface of the flat (Mansour for scale).

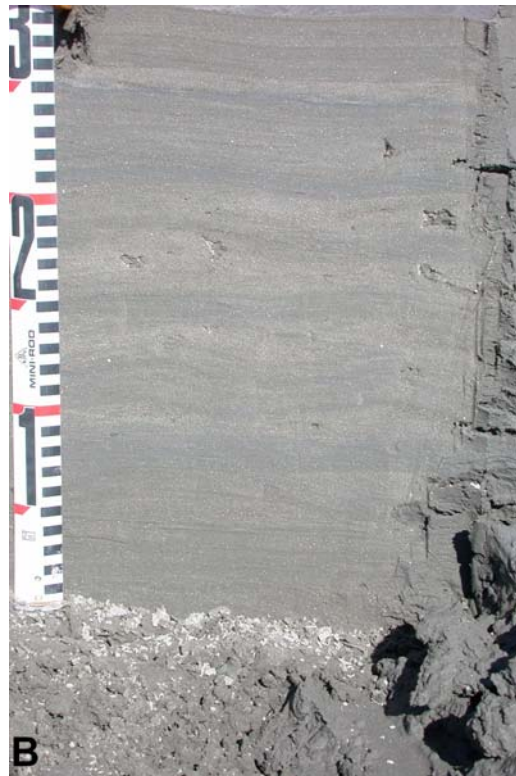


Figure 50. Tidal rhythmites are very important features within bed units of zone 3. (A) cutbank exposure of soft sediment deformation and rhythmites that can be traced for long distances. (B) An excavation showing vertically stacked cyclic alternations of silt/sand-rich and mud-drape laminae, or tidal rhythmites.

Tidal Influence within the Turnagain Arm

There are several modern settings that are strongly comparable to the depositional environment of the Tonganoxie Sandstone. These modern systems mimic the Tonganoxie in terms of the presence of tidal rhythmites, high depositional and vertical aggradation rates, distinctive biogenic and physical sedimentary structures, and evidence of periodic and recurrent emergences. They can be analogs for the Tonganoxie in terms of geometry as well. For instance, some of these environments are typical funnel-shaped estuaries, similar to the Tonganoxie paleovalley. Out of these modern analogs, Turnagain Arm of Cook Inlet of Alaska was selected, which is very similar to the Tonganoxie even with respect to prevailing hydrodynamic conditions and sedimentation controls. All these modern analogs, however, have something in common. This mutual aspect is that they all exist in macrotidal systems occupying the upper-estuary tidal-flat environments. Particularly, they exist at locations where fluvial and estuarine systems intermingle to form what is known as fluvial-estuarine transitional zone. In addition, they all contain pervasive tidal signatures and estuarine modes of sedimentation. The aim of this section is to describe, investigate, and then interpret all the characteristics that we have directly observed in the Turnagain Arm. These features will include high sedimentation rates, rhythmic bedding, biogenic and physical structures, and mechanism of sedimentation, among others.

Tidal System of the Cook Inlet and Turnagain Arm

Although all depositional environments are considered as the ultimate destination of sediment, each of these environments acts in such a unique way. In order to understand the uniqueness of a depositional environment, however, it is necessary to comprehend the mechanism of deposition within that specific environment. Therefore, this involves an examination of the tidal system of the Cook Inlet with special focus on Turnagain Arm's tides and currents.

Like some other modern estuaries, the Turnagain Arm experiences the occurrence of tidal bores (Figure 51). These tidal bores occur twice daily and tend to proceed and mark the onset of almost every incoming flood tide at the lower intertidal limit of Turnagain Arm and throughout all of its tidal channels. Cook Inlet bores are normally 1 m in height,

but they sometimes can reach heights of up to 2 m (Archer 2004). There are some factors on which the height of tidal bores depends. These include tide height, prevailing wind and ice conditions, and location and morphology of tidal channels (Bartsch-Winkler, 1982). The tidal waves, or bores, move at relatively high speeds of more than 4 m/sec; hence, they generate tidal currents that range from 2 m/sec at the mouth of Cook Inlet to about 3-4 m/sec within the Turnagain Arm, according to measurements conducted by Alaska Department of Highways (1968). Tidal bores are of considerable importance for deposition within the Cook Inlet and its arms, to the degree that some workers believe that there might be a genetic association between tidal bores and the deposition of cyclic rhythmites (Archer 2004). Sediments in Turnagain Arm are transported and deposited by suspension, and previous studies have shown that suspended sediment values are very high after the passage of tidal bores. Current flows are so strong that high levels of turbidity are generated (Figure 51A). It should be mentioned that tidal bores also take place during the winter in this area despite the formation of ice covers.

Tidal currents reach their maximum velocities prior to flooding events during flood tides and at midcycle during ebb tides (Bartsch-Winkler and Ovenshine 1984). However, these current velocities are governed by the height and range of high and low tides and, to some degree, by location. Vigorous currents along with freshwater input and Coriolis effects create turbulence that characterizes all the stages of the tidal cycle (Figure 51B). This turbulence is proportional to tidal range; for instance, it is stronger on the east side of Cook Inlet where tidal ranges are about 0.7 m greater than those of the west side (Bartsch-Winkler and Ovenshine 1984). In general, tides of Cook Inlet are mixed-semidiurnal with diurnal tides varying in range from 4.2 m at the mouth of the inlet to 9 m at the city of Anchorage. The overall system is dominated by flood tides that bring sediments into Turnagain Arm from areas located outside of the watershed of Turnagain Arm rivers. The domination of flood tides is confirmed by laboratory analyses and mineralogical studies of Turnagain Arm sediments (Bartsch-Winkler et al., 1983).



Figure 51. Photos showing the occurrence of tidal bores, which occur twice daily and mark the onset of every incoming flood tide. Note how tidal bores erode the lower intertidal flats to generate high levels of turbidity (A). Also, note the turbulence created by vigorous currents (B). This turbulence characterizes all the stages of the tidal cycle.

Biogenic and Physical Sedimentary Structures in Turnagain Arm

To better understand the biogenic structures and to make an accurate interpretation of many of the physical sedimentary structures of any depositional environment, we need to have a prior knowledge about the organisms that lived, or are living, in that particular environment. In Turnagain Arm and in Cook Inlet in general, there is an obvious lack of infaunal activities. This lack of infauna can be attributed to the shortage of fine organic material on which filter-feeding organisms depend for their survival and to the inadequacy of solar energy caused by high suspended-sediment loads. It is also attributed to the high rates of sedimentation that reduce long-term habitation in tidal flats. When we look more closely, however, we find that the major players here are high current velocities and the overall dynamic nature of this environment, which also influence textural patterns in Turnagain Arm.

The most notable organisms in Cook Inlet and Turnagain Arm areas are anadromous fish, marine mammals, hooligan, some species of salmon, Beluga whales and porpoise (Bartsch-Winkler and Ovenshine, 1984), and one or two species of bivalves. This lack of infaunal organisms in the intertidal zone of Turnagain Arm has minimized the effect of bioturbation. Hence, the existence of unaltered sedimentary structures is very noticeable. More importantly, this reminds us of the lack of infaunal animal activities within the lower part of the Tonganoxie Sandstone at the Buildex Quarry, as discussed earlier. This could imply that conditions dominating the Turnagain Arm today might have dominated the depositional environment of the Tonganoxie Sandstone Member, or at least part of it.

The most evident and widespread sedimentary structures in Turnagain Arm intertidal flats are surface ripple marks (Figure 52). However, extremely large-scale dunes do not usually form in the intertidal zone because these intertidals are mainly composed of fine-grained sediment, which does not permit the formation of such huge dunes (Reineck and Singh, 1973). Ripples here vary in shape and in size based on their position within the intertidal zone and on water depth under which they form (Figure 52). Four categories of ripples can be recognized as we move from seaward limit of intertidal sediment near estuary mouth to topographically higher regions towards the head of the estuary (Bartsch-Winkler and Ovenshine, 1984). Megaripples are the largest with average wavelengths of 4.7 m and average amplitudes of 0.7 m. These ripples develop at the lowest limit of tidal

flats under deepest water conditions, and they contain the coarsest deposits compared to the other types of ripples. As water depths become a bit shallower, straight-to-sinuus-crested ripples (Figure 52A) start to form on the megaripples. Lunate and linguoid ripples form as a result of modification and obliteration of the straight-crested and sinuous ripples as water depths become less than about 0.25 m at higher portions of the intertidal zone. Wind-wave ripples are usually found superimposed on the lunate and linguoid ripples as well as on the straight-crested ripples. While the megaripples may possibly show flood-tide orientations at some locations, the other types of ripples indicate directions of ebb-tide flows (Figure 52B, C). Rill marks, which are shallow erosional features, along with subaerial erosion commonly modify and alter the shape of those ripple marks.

In addition to surface ripple marks, there are other features found on the sediment surface. It must be mentioned, however, that most of these features are low-relief structures (Archer, 2004). One of the most widespread features in the upper intertidal mudflats of Turnagain Arm are burrows especially zigzag-shaped burrows (Figure 53A). These very shallow burrows are identical to those found, and previously described, within the Tonganoxie Sandstone of Kansas. Fish-fin drag marks are another widespread features found on the surfaces of Turnagain Arm sediments (Figure 53B, C). Like burrows, fish-fin drags have been extensively documented from several Carboniferous rhythmites. Tetrapod trackways and other animal footprints, especially those produced by birds and by mammals such as bears and moose are also common across upper mudflats of Turnagain Arm (Archer, 2004) (Figure 54). When we compare these modern trackways with Carboniferous ones, we must be extra cautious because although they both may indicate the prevalence of similar physical sedimentology such as extensive thixotropic mudflats and periodic subaerial exposures, they do not necessarily refer to the same trackway-producing animals. This is due to the hundreds of millions of years that separate these two periods, allowing evolution and extinction to play a role.



Figure 52. Photos showing different types of ripples. (A) Straight-crested ripples in fluvial sand. (B) Complex ripples that are ebb directed. (C) A bar covered with widespread, ebb-directed ripples.



Figure 53. Several features from upper intertidal mudflats. **(A)** Zigzag burrow. **(B)** Fish-fin drag marks. **(C)** A typical fish-fin drag marks. Note the parallel two marks made by the frontal fins and the other sinusoidal marks made by the dorsal fins.



Figure 54. Tetrapod trackways and footprints produced by different animals. **(A)** Bird tracks. **(B)** Bear footprint. **(C)** Moose tracks. Note that trackways of birds and mammals are the most common types in Turnagain Arm.

Upright trees are among the features that have been reported from both the basal Tonganoxie Sandstone Member and the Turnagain Arm. They usually exist in Turnagain Arm as dead upright spruce trees encased in upper intertidal rhythmites (Figure 55A). In addition, they are most often underlain by and associated with peat layers (Figure 55B). This scenario is comparable to that of the Tonganoxie Sandstone Member of Kansas where pteridosperms are encased within laminated siltstones (Lanier et al., 1993; Archer, 2004). The major difference is that in the Carboniferous case the uprights are associated with coal strata instead of peat accumulations that characterize modern macrotidal settings. Ice-rafted blocks resulting from ice deposition have been also documented (Figure 55C), but they have not been investigated in detail (Bartsch-Winkler and Ovenshine, 1984).

Other biogenic and physical sedimentary structures encountered in the intertidal flats of Turnagain Arm that are very similar to those of the Tonganoxie Sandstone include: *Arenicola* type bioturbation and burrows (Figure 56A, B), wrinkle marks (Figure 56C), foam marks (Figure 57A), raindrop imprints (Figure 57B), and drip marks (Figure 57C). We have also seen mud volcanoes (Figure 58A) and drag marks produced by dead insects and fallen leaves (Figure 58B, C). In addition, the flats contain the following structures: *Plangtichnus* type burrows and traces (Figure 59A), *Treptichnus* like traces (Figure 59B), arthropod trails and tracks (Figure 59C), Swirly biogenic features (Figure 60A), looping biogenic features (Figure 60B), and dewatering and degassing caverns (Figure 60C).



Figure 55. Upright trees in Turnagain Arm exist as dead upright spruce trees encased in upper intertidal mudflats (A). Many of these spruces are underlain by thick peat layers (B). Note the ice-rafted blocks resulting from ice deposition (C).



Figure 56. Arenicola type bioturbation and burrows (A) (B). Wrinkle marks (C). The high preservation potential that the Turnagain Arm enjoys helps in preserving such fragile and delicate structures.



Figure 57. Some physical sedimentary structures on tidal flat sediment surfaces. **(A)** Foam marks. **(B)** Raindrop imprints. **(C)** Drip marks from an overhanging brush. Compare the size of the raindrop imprints and that of the drip marks.



Figure 58. Spectacular mud volcanoes are well preserved in Turnagain Arm flats (A). Drag marks such as those produced by leaves (B) and by dead bugs (C) are also found undisturbed.



Figure 59. Superficial burrows and traces within the Turnagain Arm and the Tonganoxie are strikingly similar. (A) *Plangtichnus* type burrows and traces. (B) *Treptichnus* like traces. (C) Arthropod tracks.



Figure 60. Intertidal rhythmites also contain structures such as (A) Swirly biogenic features, (B) Looping biogenic features, and (C) dewatering and degassing caverns at Bird Creek.

Internal Facies within Turnagain Arm Sediments

Internal structures of any sedimentary body are highly sensitive to the flow system that was operating during their formation. Therefore, any changes within a single flow regime or shifting from one flow regime to another flow system such as from upper to lower flow regime, and vice versa, are reflected and preserved by internal sedimentary structures of the sedimentary body affected by these regimes. Flow conditions such as current velocities, flow deceleration during ebb phase of the tidal cycle, and flow acceleration during flood phases all influence the internal sedimentary facies formed under such conditions. As a result, we have seen earlier that the lower part of the Tonganoxie succession at Buildex Quarry contains some characteristic intervals of vertical structure sequences (VSS), especially within its thickest siltstone bedsets of Unit A2. The aim of this section is to compare these vertical sedimentary structure sequences of the Tonganoxie Sandstone with similar internal structures reported from the Turnagain Arm.

The four VSS intervals that have been documented within some of the Tonganoxie bedsets are: (A) a massive to normally graded interval; (B) a planar-laminated interval; (C) a cross-laminated interval; and finally (D) a laminated interval with drapes (see Figure 29) (Lanier et al., 1993). Interestingly, in a study conducted by Bartsch-Winkler and Ovenshine (1984), radiographs of X-rayed box cores taken from Turnagain Arm sandbars have revealed similar four transitional facies of sedimentary assemblages (Figure 61, 62). In general, these internal facies are characterized by combinations of planar laminae and ripple-cross laminae. The bedding here is thin with an average thickness of about 2.4 cm (Bartsch-Winkler and Ovenshine, 1984).

Facies A consists of uniform planar and parallel laminae. It is evenly laminated to such an extent that discrete strata are almost unidentifiable (Figure 61A). Sediments within facies A range in size from fine to medium sand. On top of this facies, cross-laminations generated by ripple marks do sometimes exist (Figure 61A). Facies A is the product of maximum flow velocities of upper plane-bed regime. In other words, it was formed under extremely high energy conditions. Facies B, on the other hand, is composed of both planar and ripple-cross laminae that reflect an alternation between high-flow and intermediate- to low-flow conditions, respectively (Figure 61B). Sediments here are

mostly very fine sands with modest percentages of silts. There is an upward decrease in mean grain size and in flow energy due primarily to decreasing water depths. This upward-fining pattern is characteristic of intertidal environments. Facies C is similar to facies B except that in facies C, cross-laminations predominate (Figure 62A). In addition, sediment of facies C is finer and ranges from very fine sand to very coarse silt with higher organic content in form of plant rootlets (Bartsch-Winkler and Ovenshine, 1984). It is obvious that during the deposition of this facies, flow velocities were lower compared to those of facies A and B. Facies D is similar to facies A, being both parallel laminated (Figure 61A, 62B). However, facies D is composed totally of silt-size deposits with extremely high amounts of plant debris. In fact, some layers within facies D are entirely made up of plant remains (Figure 62B). Facies D represents deposition within upper intertidal zones during the last stage of high tide where flow velocities are very low, just before high-tide still stand.

Discussion and Interpretation

Although hydrologic studies indicate that flood currents are predominant in Turnagain Arm, directional-current surface structures such as ripples along with internal structures of sandbars are mostly ebb-oriented. The sequence of internal facies found within Turnagain Arm can be explained as a result of a single daily tidal cycle. Parallel and horizontal laminations (facies A) represent high-flow regime that normally takes place during early flood stages and midstages of flood and ebb flow events. This planar bedding resulting from high-flow regimes is characteristic of low and middle intertidal flat sediments. Combinations of cross bedding and parallel lamination (facies B and C) represent deposition under high to intermediate or even low flow conditions taking place during intermediate stages of flood and ebb flows. This pattern of facies usually characterizes midlevel intertidal flats. Parallel, but otherwise finer-grained, laminations reflect deposition under the lowest flow velocities occurring during the late stages of daily tidal cycles. These laminations are found within upper intertidal mudflat deposits (Ovenshine et al., 1976). So far, we have seen that the Turnagain Arm exhibits characteristics that are typical of intertidal environments except for its lack of infauna. In addition, most of its characteristics are indicative of high tidal ranges and high current

velocities.

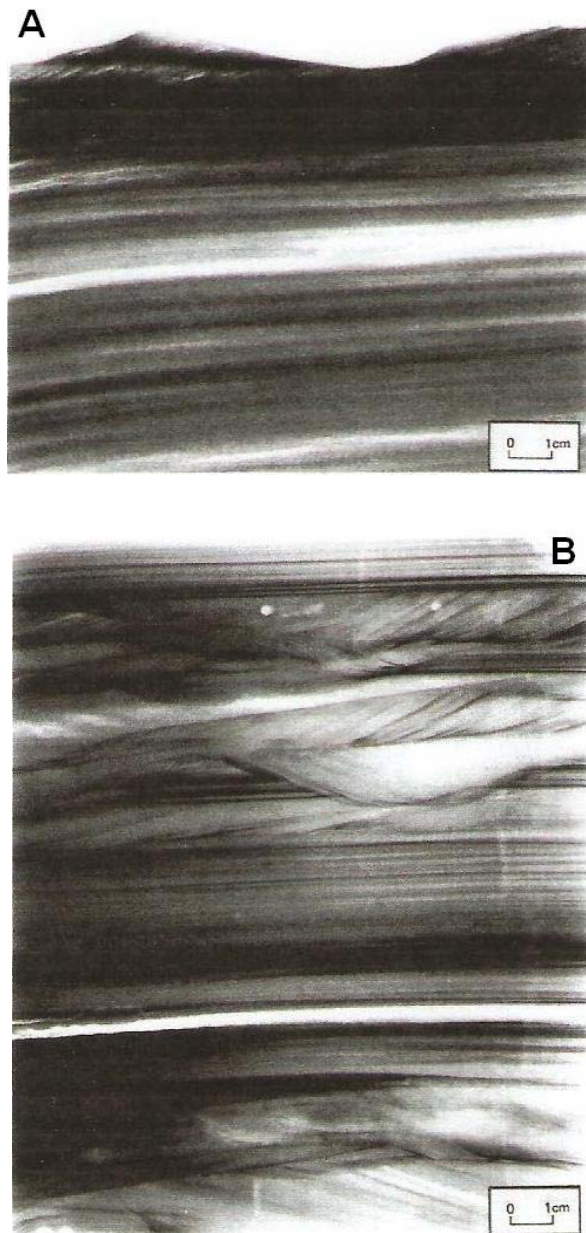


Figure 61. Images of X-rayed box cores showing: **(A)** Planar laminations within facies A. Note the lunate-linguoid ripple marks on the top. Note also the high degree of uniformity. **(B)** A combination of high-flow parallel lamination and intermediate-flow cross bedding within facies B. Note the almost equal percentages of parallel- and cross-laminations and compare it to that of facies C (modified from Bartsch-Winkler and Owenshine, 1984).



Figure 62. Images of X-rayed cores showing: **(A)** Facies C dominated by cross-lamination with plant remains and some air voids. Note the upward transition to a more parallel-laminated facies. **(B)** Laminar bedding within facies D with high percentages of voids and rootlets. Note that, unlike facies A, discrete laminae can be easily identified here (modified from Bartsch-Winkler and Ovenshine, 1984).

Observations of Cyclic Tidal Rhythmites

Perhaps the most obvious evidence of the existence of tidal influence within a particular depositional environment is the occurrence of what are now famously known as cyclic tidal rhythmites (Figure 63). The key factor here is the relationship between thicknesses of individual laminae and tidal ranges and between tidal heights and current speeds. Tidal-current velocities are dependent on the height and range (amplification) of high and low tides or neap-spring tidal cycles (Bartsch-Winkler and Ovenshine, 1984). High tidal ranges are usually associated with swiftly flowing currents and high tidal-current velocities. Depositional environments experiencing extreme tidal ranges, more than 4m, are considered as macrotidal environments (Archer and Hubbard, 2003). The dynamic nature of such sedimentary environments increases the capacity of currents for transporting and depositing relatively high amounts of sediments. Thus, higher tidal ranges generate thicker sedimentation units than those generated by lower tidal ranges, representing sedimentation during spring and neap tides, respectively (Figure 63). This implies that tidal-current speeds are directly proportional to rates of sediment accumulation (Archer, 1995). As a result, and based on the mentioned relationships, the relative volume of sedimentation of a single tidal cycle can be predictable. The other key factor in the formation of vertically accreted tidal rhythmites is that high and low tides occur in a rhythmic or cyclic way, which accounts for the development of vertical, or even lateral (Mazumder and Arima, 2005), progressive thinning and thickening within individual laminae bedsets (Figure 63, 64, 65).

There are several challenges arise when dealing with cyclic tidal rhythmites. The first challenge is the fact that there are some processes that are not astronomically induced, such as lacustrine varves, but they still can produce physical sedimentary structures that apparently mimic those rhythmites generated by tidal processes (Kvale et al., 1999). In other words, rhythmic bedding can be generated away from any tidal influence on deposition. Moreover, working in reality, we must take into account as well the complications caused by the act of waves and storms (Figure 63B) as well as river-discharge seasonality (Archer, 1995). Therefore, very careful identification of the potential producing forces for tidal rhythmite deposits is required. This means that we must be sure about the progressive thickening and thinning within vertically stacked

packages of laminae being a result of changing current speeds associated with lunar orbital cycles and not a function of some other processes that have nothing to do with changing lunar cycles.

The other challenging issue related to rhythmite investigations is the evaluation of completeness of ancient tidal rhythmite records. Most techniques involved in tidal rhythmite studies require complete and continuous neap-spring tidal cycles (Kvale et al., 1999). Many tidal rhythmite records, however, are not always perfectly complete in the real world, and they often show evidence of truncation of neap-spring cycles. This is very common within tidal rhythmites that were formed in uppermost intertidal zones of tide-dominated estuaries (Archer and Johnson, 1997). The absence of continuously preserved neap-spring tidal records imposes some difficulties. This is very true especially if we take into account that these rhythmites are recently being used to extract palaeoastrophysical information such as estimating lunar retreat rates and other ancient lunar orbital dynamics such as variations in Earth-Moon distance over the past geologic time (see Archer and Johnson, 1997; Kvale et al., 1999). In such cases, complete and long rhythmite records are essential for performing highly accurate analyses. However, some creative methods have been proposed and used to compensate for the lack of complete tidal records. The modeling of the development of cyclic tidal rhythmites by using predicted tidal-height data is just an example of these new techniques, which are very helpful when dealing with modern rhythmites (Archer and Johnson, 1997). It should be noted that this process of evaluating tidal rhythmite records includes investigations of potential subaerial exposures that may have occurred within intertidal settings and any possible subsequent effects. It should also be emphasized that despite their incompleteness, tidal deposits could still hold important information that, in turn, can be used in many different useful ways.

There are still some controversial issues even with regard to the most appropriate tidal theory that should be used when interpreting the origin of cyclic tidal rhythmites (e.g. equilibrium tidal theory vs. dynamic tidal theory), not to mention the difficulties that come up when determining whether the neap-spring cycles in question are synodically or tropically driven (Kvale, 2006). Ambiguities and confusion related to tidal terminology are yet another story. However, discussing all these issues is beyond the scope of this

thesis.

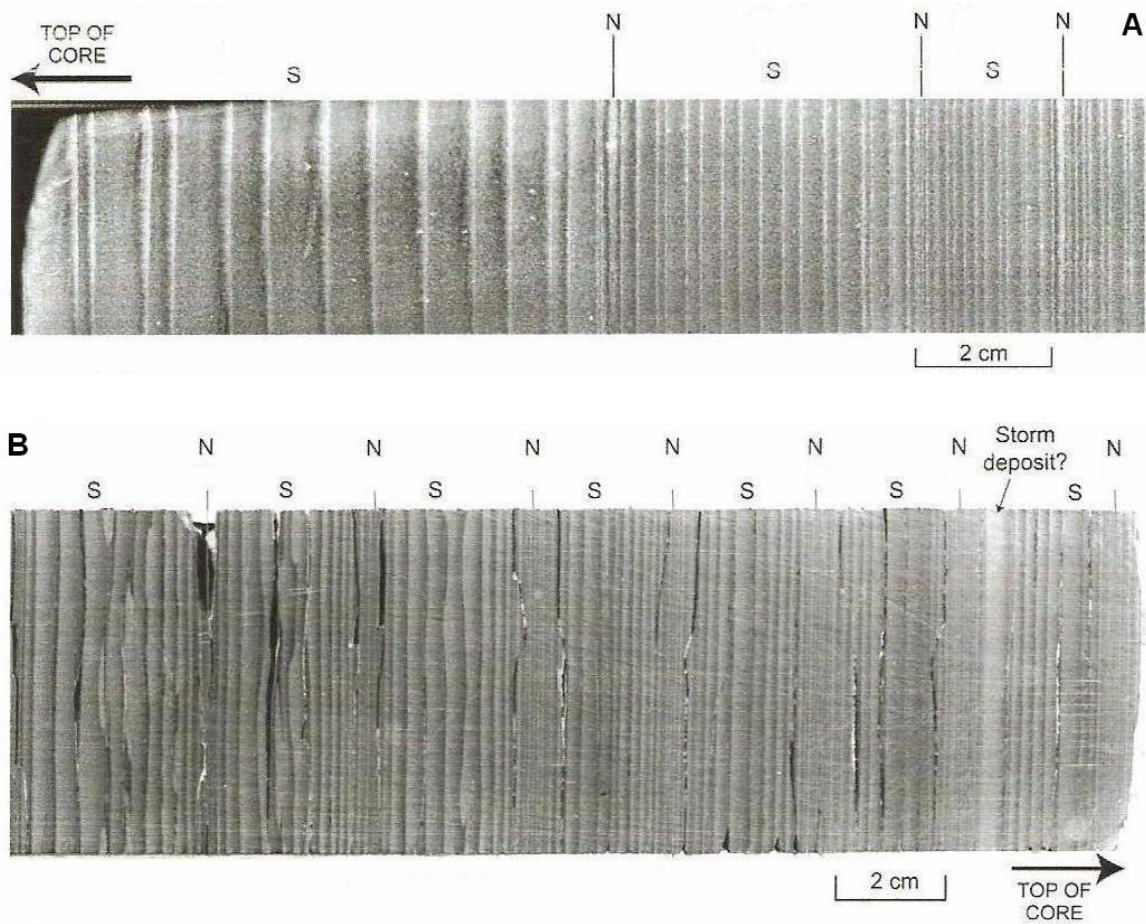


Figure 63. Tidal deposits showing small-scale cyclic tidal rhythmites and consisting of vertically stacked laminae with systematic changes in thickness. These variations in laminae thicknesses represent neap (N) and spring (S) tidal cycles. Note that laminae deposited during spring tides are thicker than those deposited during neap tides. These are Upper Carboniferous, ancient, rhythmites. **(A)** From Mansfield Formation and **(B)** From Brazil Formation of Indiana, USA. Also, note the probable storm deposit in **(B)**, which highlights the complications that may exist because of the action of waves and storms. Modified from Kvale (2006).

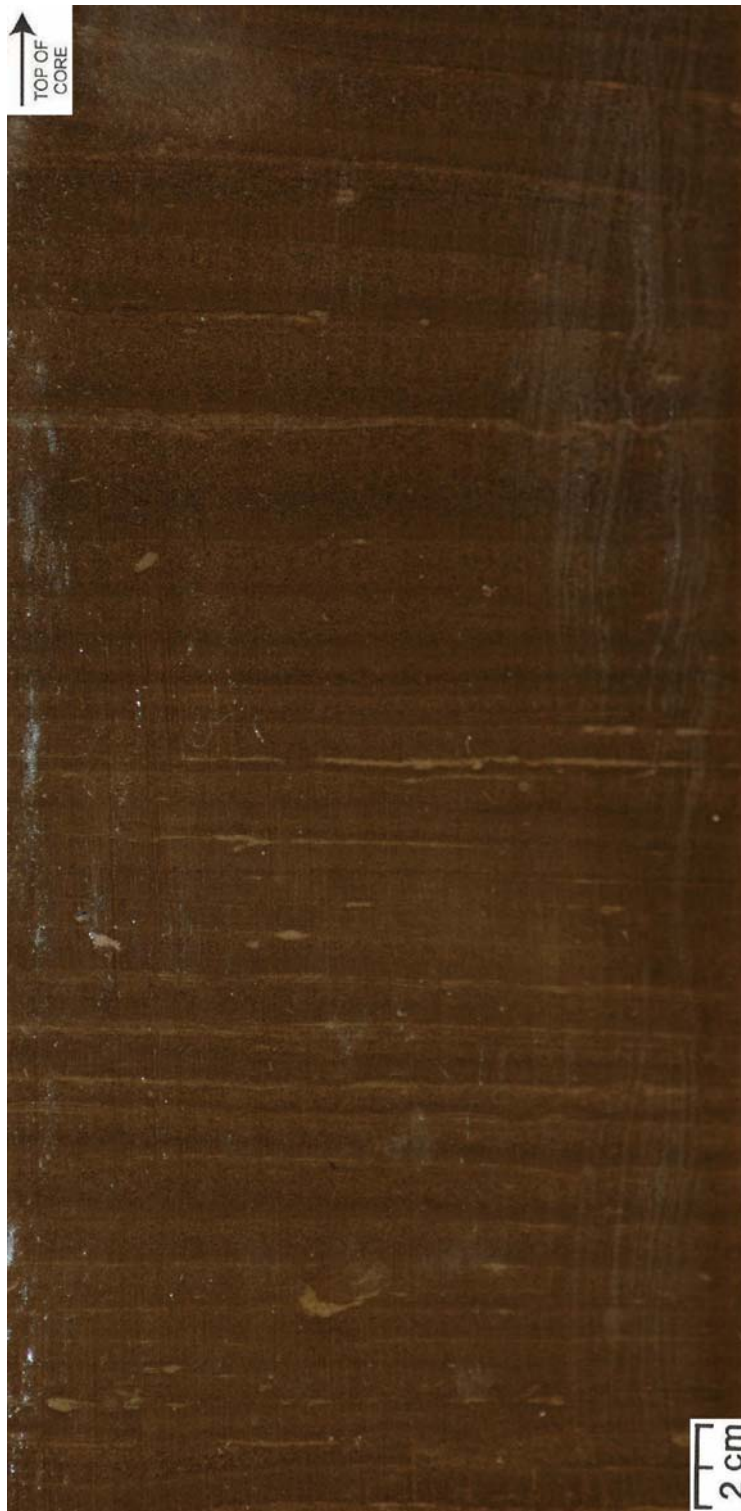


Figure 64. Photograph of a segment of Tonganoxie Sandstone core (Mechaskey). This part exhibits what is believed to be tidal cyclicity. Cycles here consist of normally graded, flat-laminated siltstone interbedded with thin claystone laminae. Note the upward thickening and thinning.

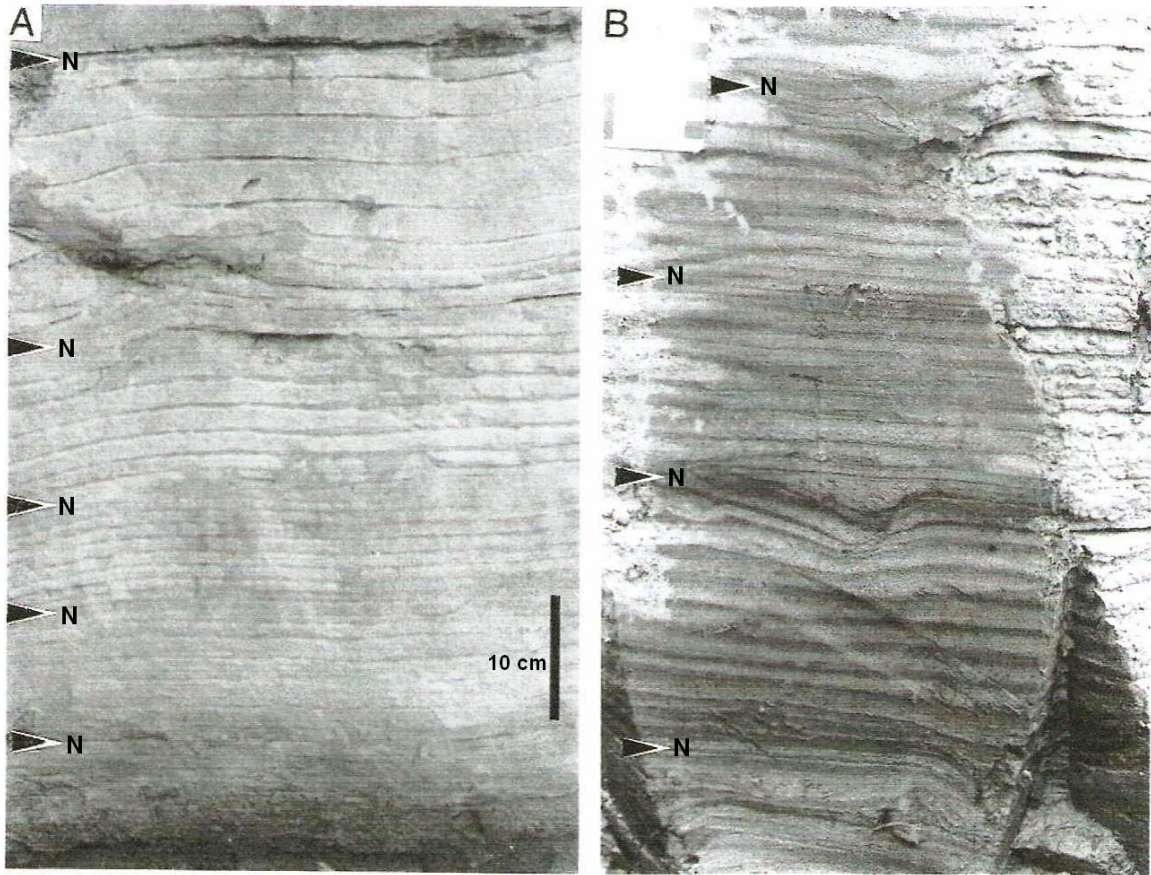


Figure 65. Many attempts have been made to compare cyclic tidal rhythmites formed in modern macrotidal settings with ancient counterparts. This photograph shows two outcrops that contain strikingly similar rhythmites. The rhythmites here are flat-laminated with obvious variations in laminae thicknesses. **(A)** From the Carboniferous Tonganoxie Sandstone, Kansas, USA; and **(B)** From the Bay of Mont Saint Michel, France. Black arrows point to sets of laminae that were deposited during neap periods “N” of the tidal cycle, which consists of neap and spring parts. Modified from Lanier et al. (1993).

The aim of this section is to first define cyclic tidal rhythmites in general and then present those rhythmites that we have observed and documented within both the Pennsylvanian Tonganoxie Sandstone Member of Kansas (Figure 64) and the Turnagain Arm of Alaska (modern setting) (Figure 66, 67, 68).

Many definitions have been proposed for cyclic tidal rhythmites. Although these definitions are generally consistent, the terminology being used in tidal literature is can be confusing (Archer, 1995; Archer and Johnson, 1997; Kvale, 2006). Simply, cyclic tidal rhythmites are small tidal bundles that exhibit regular and systematic changes in thicknesses of successive laminae or thin beds (Figure 63). It is believed that these thickness variations represent and reflect astronomically induced tidal events such as neap and spring tides (Figure 63, 65). Therefore, it comes as no surprise to note that many workers refer to such sedimentary structures as neap-spring cycles. These cycles usually consist of several sets of clay-draped ripples that are vertically stacked together (Figure 66), and hence the whole bedding in this case can be described as being flaser, wavy, or lenticular (Archer, 1995; Kvale et al., 1999). They may also consist of normally graded, flat-laminated siltstone interbedded with thin claystone beds and laminae (Figure 67, 68). Normally, rhythmites that belong to the first type are known as heterolithic rhythmites, whereas rhythmites that fall within the second category are referred to as silty cyclic rhythmites (Archer et al., 1994; Archer, 1995; Archer and Johnson, 1997). During the course of this study, we have encountered both the heterolithic and the silty rhythmite types. The focus herein, however, is on the latter form.

Studies of cyclic tidal rhythmites are of three types that include observing modern rhythmites, investigating rhythmites of ancient settings, and, accordingly, building theoretical models for palaeoastronomical and sedimentological implications (Archer and Johnson, 1997). In general, tidal rhythmites are more common in muddy, tide-dominated settings. These cyclic rhythmites are usually found right above a thin, locally formed coal seam, and are themselves overlain by another coal layer or, at least, organic-rich zone that is heavily rooted (Lanier et al., 1993; Archer and Johnson, 1997). In addition, tidally generated rhythmites contain distinctive physical and biogenic sedimentary structures that are suggestive of deposition within intertidal environments and could give clues about the exact position within the tidal frame, as discussed earlier.

Silty rhythmites, in which we are more interested, have been documented and described from several Upper Carboniferous-age settings such as Mansfield Formation and Brazil Formation of Indiana (Figure 63) and the Stranger Formation of Kansas (Figure 65A) (Kvale et al., 1989; Kvale and Archer, 1991; Lanier et al., 1993; Archer et al., 1994). In fact, some sort of tidal cyclicity was observed during examination of Tonganoxie Sandstone cores (Figure 64). Modern macrotidal settings also contain very similar silty rhythmites that can be used as analogs for the Carboniferous ones (Figure 65). The most studied modern sites, with regard to cyclic tidal rhythmites, are Cook Inlet of Alaska, USA; Bay of Fundy, Nova Scotia, Canada; Bay of Mont Saint Michel, northwestern France (Figure 65B); and the mouth of the Amazon River, Brazil (see Archer, 2004; Bartsch-Winkler and Ovenshine, 1984; Bartsch-Winkler, 1988; Dalrymple et al., 1991; Tessier et al., 1995). The Turnagain Arm of Cook Inlet does contain regular and spectacular cyclic tidal rhythmites. Some of these rhythmites were directly observed during fieldwork in August of 2006, and they were evident to such an extent that neap-spring tidal cycles, known as tidal periodicities, can be easily distinguished within a series of successive, vertically stacked sets of laminae (Figure 66, 67, 68). Both thin and thick rhythmites have been reported from Turnagain Arm. Thick rhythmites usually show thick-thin pairing called couplets (Figure 68B), indicating a well-developed diurnal inequality (Archer, 2004). Moreover, such couplets are characteristic of intertidal deposits. However, modern cyclic rhythmites, especially right after deposition, consist of wet and thixotropic sediments. Therefore, excavation within these deposits must be done with extra caution. As a result, it is not easy to analyze long records for the sake of extracting encoded tidal events (Archer, 2004; Archer and Johnson, 1997).

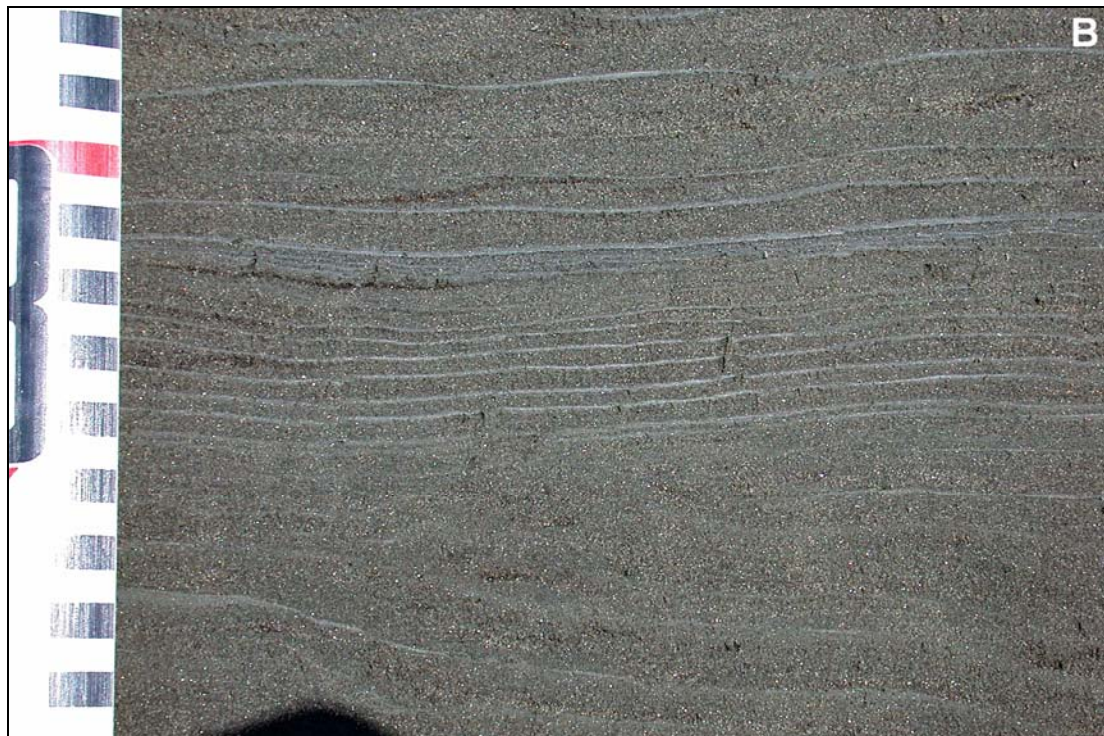


Figure 66. Two excavations within upper intertidal flats of Turnagain Arm. **(A)** Relatively thick rhythmites from 20 Mile Creek. Note the stacked, mud-draped ripples (center). **(B)** Thin neap-spring cycles overlain by thick rhythmites and consisting of clay-draped laminae.



Figure 67. Excavations within upper intertidal deposits of Turnagain Arm, particularly from Glacier Creek. **(A)** Neap-spring cycles formed within mud-dominated rhythmites. **(B)** Neap-spring cycles consisting of flat-laminated, silty laminae (light) interbedded with thin clayey laminae (dark). Tidal rhythmites within Turnagain Arm are clearly defined and single neap-spring cycles can be easily observed and numbered, as in (B). Note the existence of soft sediment deformation especially within unit 3 and 5 of (B).



Figure 68. (A) Thin rhythmites. (B) Thick rhythmites exhibiting thick-thin pairing known as couplets. Such couplets usually indicate a well-developed diurnal inequality (Archer 2004), and are characteristic of deposition within intertidal environments.

Soft-Sediment Deformation Structures

Soft-sediment deformation structures are sedimentary features that form during or immediately after the deposition of sediment, before the process of consolidation begins. They range in intensity of deformation from slightly disturbed strata to heavily contorted, broken, and shifted laminae and beds, and in scale, range from microscopic to megascopic forms. Because deformation here is contemporaneous with deposition, some workers, especially in earlier literature, refer to sedimentary features produced by this deformation as penecontemporaneous deformation structures, and herein we call them soft-sediment deformation structures. These structures have been documented in many sedimentary sequences, but they tend to exist within depositional environments that are dominated by coarse silt to fine sand deposits (Mills, 1983; Reineck and Singh, 1973). This tendency is due to the high depositional rate within such environments and to the low permeability and low shear strength of the grains that fall within this grain-size category. This does not exclude, however, the fact that soft-sediment deformation does affect deposits of almost all grain sizes. These controlling parameters and sediment hydrodynamics have been observed within the Turnagain Arm of Cook Inlet, where accumulation rates are high, and suspended sediments are composed of up to 40% of very fine sand and an average of 35% of medium silt (Archer 2004, Bartsch-Winkler and Ovenshine, 1984).

Four main processes are usually involved in the generation and development of soft-sediment structures. These mechanisms are: (1) liquefaction or fluidization; (2) shear stress; (3) slope failure and slumping; and (4) reverse density gradation or unequal loading (Mills, 1983). Therefore, although soft-sediment deformation features are simply defined as being the result of the disruption of unconsolidated sedimentary layers, they are, in fact, the products of complex combinations of these four processes. Soft-sediment deformation features are considered as important diagnostic tools. They have been used to determine depositional processes and environments, paleoslope and paleocurrent orientations, seismic activities, and extreme and chaotic depositional events such as periodic floods or storms. However, this diagnostic importance of these deformation structures has been questioned, reevaluated, and even minimized recently. This is because mechanisms and hydraulic conditions accountable for the development of soft-sediment

structures may exist in a wide variety of depositional environments. In other words, different types soft-sediment features can be produced by a single mechanism, and a specific deformation structure can be generated by different mechanisms or a combination of two or more deformational processes. For instance, liquefaction and fluidization processes are involved in the development of several structures such as dish and pillars, sheet structures, sand volcanoes, and sedimentary dikes and sills. On the other hand, dish and pillar structures may be formed by mechanisms other than liquefaction or fluidization (Mills, 1983). Therefore, any direct environmental interpretations based solely on the apparent relationship between some soft-sediment features and specific lithologic sequences could be misleading unless other available information is taken into consideration. Nevertheless, it has been proven that certain deformational processes are associated with certain depositional conditions. Reverse density deformation, for example, tend to occur in environments dominated by weakly compacted muds resulting from rapid sedimentation rates. Thus, representative structures of processes of deformation can be useful in analyzing hydrodynamic conditions, in determining paleocurrent orientations, and in making interpretations about paleoseismic and chaotic events (Mills, 1983). What increases this diagnostic value is the fact that soft-sediment deformation structures are of local nature. This means they are usually restricted to a single sedimentary unit within undeformed units (Reineck and Singh, 1973).

The aim of this section is to present and discuss some of the soft-sediment deformation structures that we have observed during the investigation of the Tonganoxie Sandstone core and Turnagain Arm deposits. This could be a very helpful approach because although deformation features are not decisive indicators of particular depositional settings, they do suggest specific deformational processes that, in turn, could give us a clue about the hydraulic and sedimentological conditions that may have prevailed during the time of deposition. Our ultimate goal, therefore, is to provide supportive evidence that the depositional environment of the Tonganoxie Sandstone Member of northeastern Kansas is very similar, in many respects, to that of the Turnagain Arm of Alaska.

The most noticeable deformation structures seen within the examined Tonganoxie Sandstone core are load structures (Figure 69), slump and slump-like structures (Figure 70), and distorted bedding (Figure 71). Load structures form when there are unequal

loading and liquefaction, resulting from the deposition of a sand layer over a water-saturated or hydroplastic mud stratum. In this situation, a vertical adjustment takes place at the sand-mud boundary causing the sand to sink down in the underlying liquefied mud (Figure 69B). They are also formed by differential deposition as a response to the piling up of sinking ripples (Reineck and Singh, 1973). The ripples in this scenario are known as load-casted ripples (Figure 69A). Additional factors that may contribute to their formation include viscosity and cohesion of sediment particles (Mills, 1983). Load structures have been reported from flysch deposits, glacial sediments, channels of intertidal mudflats, and shallow-water environments. Most importantly, these structures have been associated with depositional environments characterized by rapid mud accumulation that is occasionally interrupted by rapid deposition of medium-grained sands (Reineck and Singh, 1973; Potter and Pettijohn, 1977). Note that sand deposition here implies that rapid influx of dense sediments may have occurred periodically. Such influx is usually initiated by quiet, normal depositional events such as shifting of tidal channel sands or by periodic or chaotic events such as floods or storms, respectively.

Slump structures are features that form as a result of down-slope movements of semi-consolidated sediment layers under the influence of gravitational forces (Potter and Pettijohn, 1977) (Figure 70). The definition clearly implies that liquefaction and slope failure are the most important mechanisms responsible for slumping; however, other factors may play a role such as sedimentation rates, type of sediment deposited, and instability caused by overloading (Mills, 1983). The result of slumping processes ranges from simple distortion of the original lamination and bedding with only partial or no displacement at all (Figure 70) to a chaotic mixture of different sorts of deposits. Slump structures have been reported from slope deposits, flysch deposits, continental margins, and inclined point bars within intertidal flats (Reineck and Singh, 1973). Because they usually retain at least some traces of down-slope movements, slump structures are highly useful in determining paleocurrent and paleoslope directions (Figure 70). What matters for us here about these features, however, is their association with rapid sedimentation rates.

Many types of contorted bedding fall within the category of slump structures (Figure 71). The contortion is produced by slump movements of already deposited yet

unconsolidated sediments. As an evidence of their origin under the influence of gravity, contorted beds and laminae, especially within muddy deposits, are sometimes affected by small-scale gravity faults (Figure 71A). Liquefaction, shear stress, and reverse density loading or overloading are all critical for the development of contorted bedding. It has been proven that these deformational processes are somehow associated with environments undergoing high rates of sedimentation (Greb and Archer, 2007; Archer, 2004). This could provide real insights into the conditions of deposition of the Tonganoxie Sandstone sequence. Again, extra caution should be taken when using soft-sediment deformation structures as diagnostic tools for any environmental reconstructions.

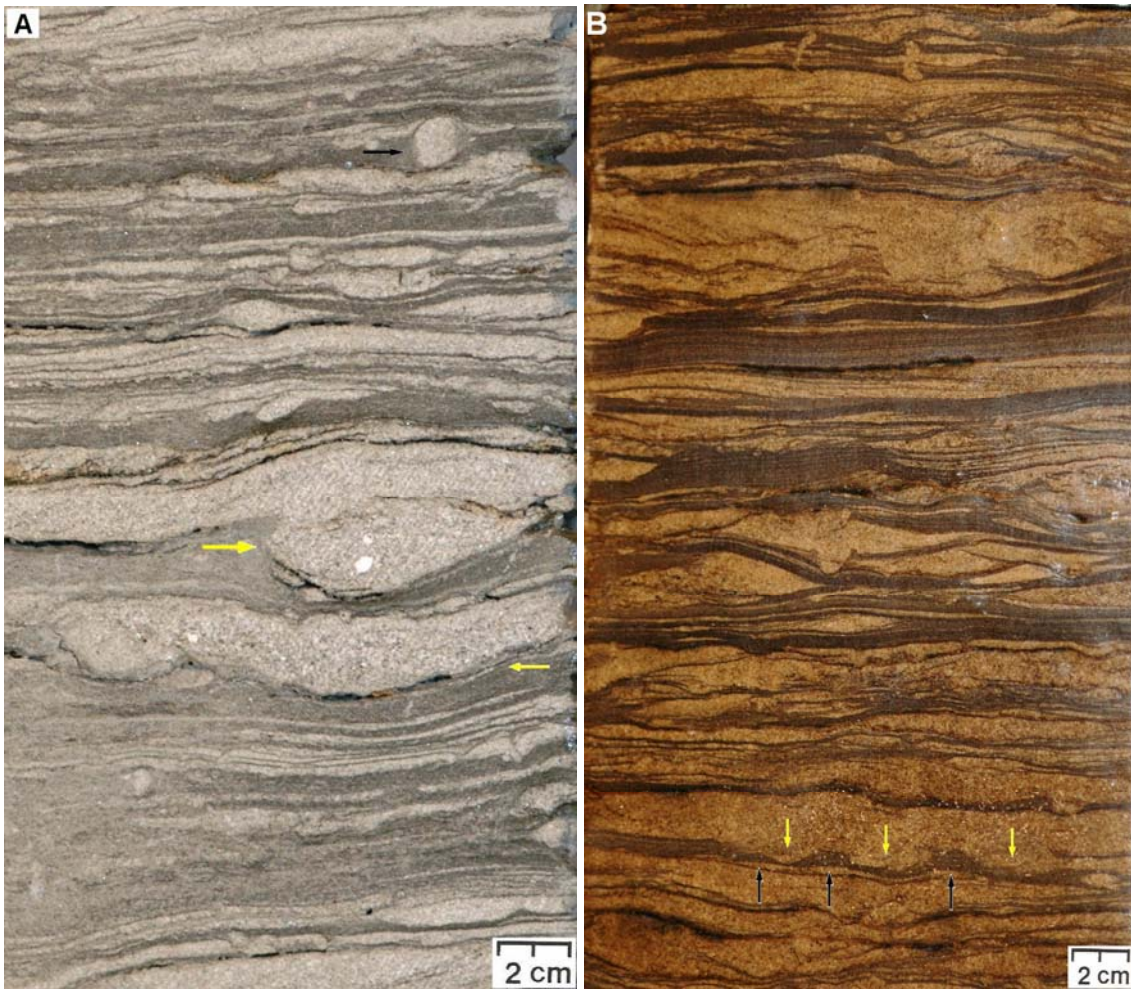


Figure 69. Photos of the Tonganoxie Sandstone core showing different types of load structures. **(A)** Load structures resulting from the deposition of sand layers over mud layers. Note how the sand sank down into the mud (yellow arrows). It also shows what appears to be the first stage of the development of “load-casted ripples.” **(B)** Load structures produced by unequal loading. The yellow and black arrows here clearly show the vertical adjustment at the sand-mud interface.

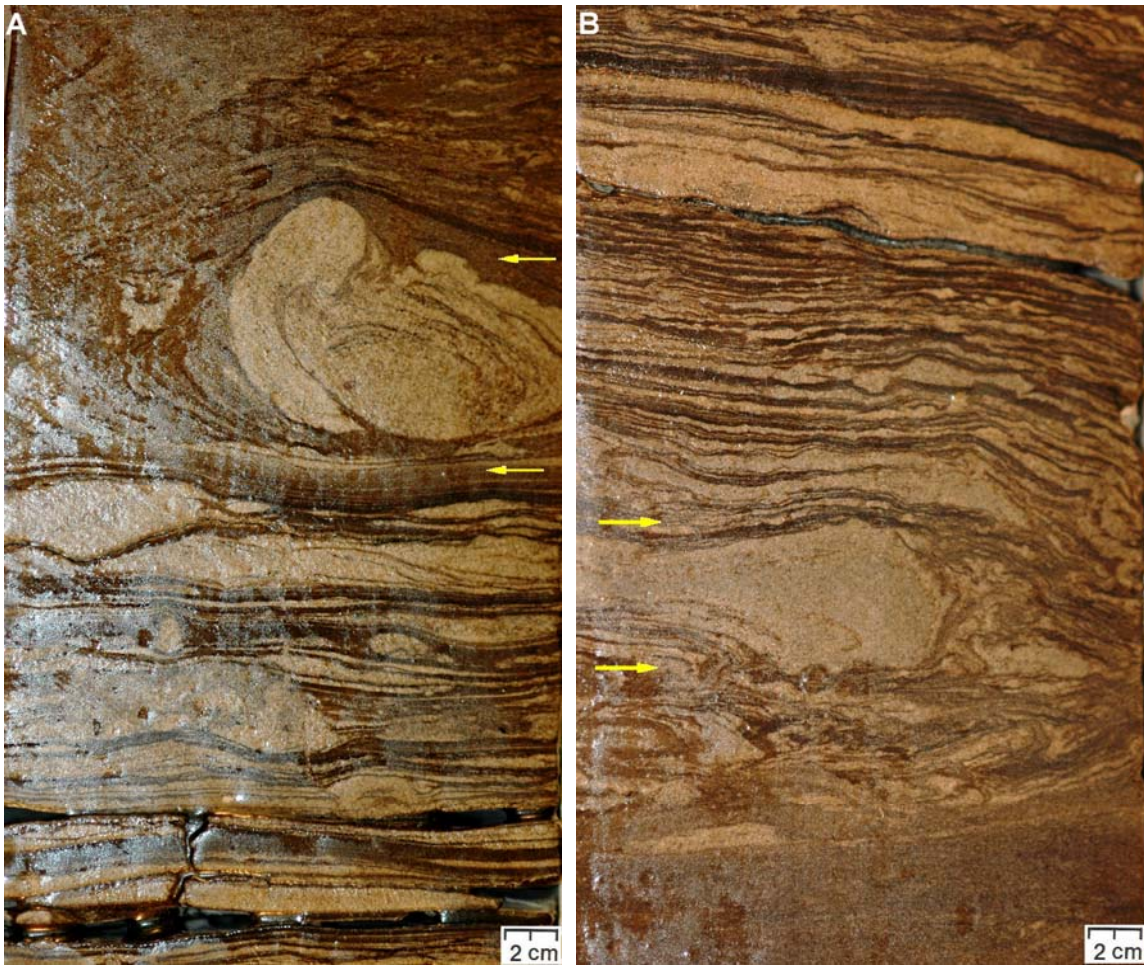


Figure 70. Two photos of the Tonganoxie Sandstone core showing slump structures. **(A)** A slump structure produced by the slumping of a sand mass (upper right). The sand mass is embedded in a muddy matrix. **(B)** A slump structure seen within sand-mud interbedded facies. Note that slumping here has created irregular contortion within surrounding layers. Yellow arrows in both photos indicate the potential down-slope movements of the sediments. In B, the movement is consistent with inclination orientation of the overlying laminae and beds (upper).

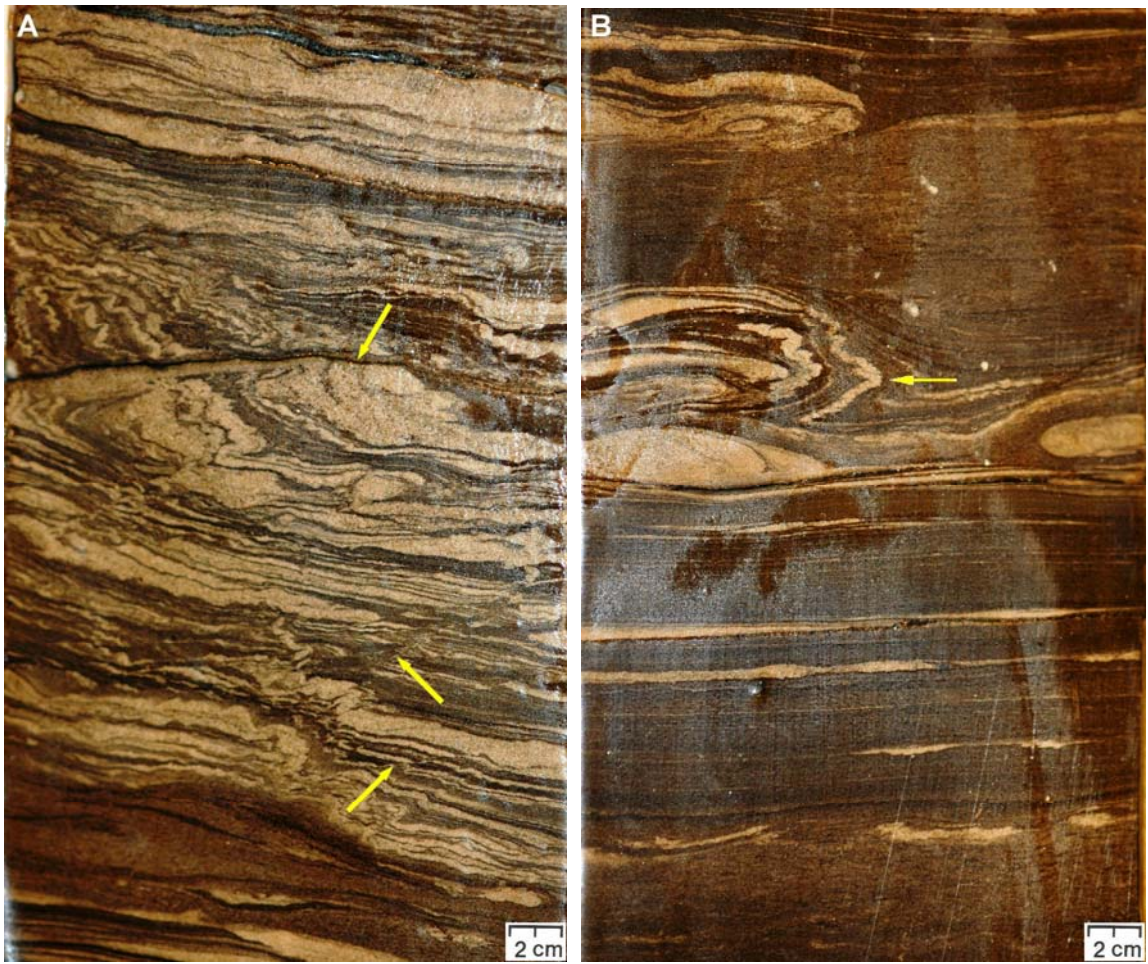


Figure 71. Two segments of the Tonganoxie Sandstone core showing different types of distorted bedding. **(A)** Extremely contorted interbedded unit restricted vertically by undeformed units. Note the existence of some small-scale gravity faults (yellow arrows). **(B)** Slightly contorted laminae (yellow arrow) with some sort of folding.

Widespread soft-sediment deformation structures were observed within upper intertidal flats of Turnagain Arm of Alaska during fieldwork in the summer of 2006. These structures are very similar to those found in some Carboniferous facies of USA (Archer, 2004). The most notable features being convolute bedding (Figure 72, 73), load structures (Figure 74), flame structures (Figure 75), contorted bedding with dish structures (Figure 76), and ball-and-pillow structures (Figure 77).

Convolute bedding is an intensive and continuous folding of originally parallel layers within a well-recognized sedimentation unit. The convoluted zone is usually overlain and underlain by undeformed and flat-laminated zones, making sharp parallel contacts (Figure 72, 73). These parallel surface can be attributed to waning current flows or to a sudden and abrupt shift from lower flow-regime conditions, represented by contorted laminae, to upper flow-regime conditions, represented by parallel surfaces and laminae (Mills, 1983). In a view perpendicular to the bedding plane, convolute laminae can be described as a series of broad troughs alternating with pointed crests (Figure 72B, 73A). The origin of convolute bedding has been attributed to many processes, but differential liquefaction is believed to be the major player. In fact, liquefaction is a very important process for the development of convolute bedding especially in tidal environments. For example, during periods of low tide, the surface of fine-grained non-cohesive deposits is subaerially exposed; hence, sediments start to compact due to expulsion of pore water leading eventually to local liquefaction and convolution (Mills, 1983). However, the liquefaction itself is usually triggered by other factors such as overloading and seismic shocks. Because Turnagain Arm is located within a seismically active area and has prolonged periods of freezing temperatures (Archer, 2004), these two factors are considered here as liquefaction inducers. Some workers have attributed convolute bedding to vigorous current activities and ripple deformation. This assumption is also suitable for Turnagain Arm's convolute bedding because shear stress can be exerted on sediment surfaces there during the passage of about 2 m-high tidal bores (Greb and Archer, 2007). This bed shear deforms low-shear strength deposits such as unconsolidated and liquefied sediments. Other workers believe that it has something to do with slumping processes. Slumping does make a lot of sense especially if we take into account the fact that convolute bedding is very common within steeper slopes of

intertidal bars.

Load structures are expected within Turnagain Arm deposits wherever there is an unequal or differential loading, causing the sand to sink down into finer-grained deposits (Figure 74). Sometimes, this differential loading along with liquefaction induces the underlying fine deposits, usually mud, to move up into the overlying coarse-grained unit (Figure 74A). Features produced by such vertical adjustment are known as flame structures especially if the upward-directed mud intrusions take the shape of pointed tongues (Figure 75). Distorted bedding is also common within upper intertidal deposits of Turnagain Arm (Figure 73B, 76). Although we have talked about it previously, we should mention here that in the case of Turnagain Arm, this distortion could be the result of slumping caused by melting of ice masses entrapped in the sediments (Archer, 2004; Reineck and Singh, 1973). Contorted bedding here is usually confined between parallel and flat-laminated facies (Figure 76), indicating a fluctuating flow regime during deposition.

Dish structures are not uncommon within Turnagain Arm rhythmites. Small dish structures were found associated with contorted bedding (Figure 76A). Dish structures are thin lens-shaped to flat semi-permeable laminae. They genetically belong to water-escape structures, and are related to rapid deposition (Mills, 1983). Liquefaction and fluidization are the most important processes for their origin. Some spectacular ball-and-pillow structures have been also observed within Turnagain Arm rhythmites (Figure 77). Ball-and-pillow structures usually form when a sand layer, overlaying a mud layer, is shocked, say, by seismic activities. In such circumstances, the sand layer starts to break up into smaller pillow-, saucer-, or kidney-shaped pieces (Figure 77B). These individual sand masses sink down into the underlying mud deposits. These structures are either partly connected with each other or completely disconnected and surrounded by a muddy matrix (Figure 77A). Mechanisms involved in the formation of ball-and-pillow structures include reverse density gradation along with cohesion and viscosity of sedimentary particles (Mills, 1983). Ball-and-pillow structures are not reliable indicators of any specific depositional environments, but they do indicate rapid deposition rates taking place during their formation (Reineck and Singh, 1973). Note that many workers have experimentally produced similar deformation features.



Figure 72. Photos showing convolute bedding in cutbanks within Turnagain Arm. **(A)** Eroded convolute laminae with a very distinct flat surface on the top of the unit. **(B)** Convolute bedding with complicated folding of the laminae. Note the lateral continuity of the convoluted interval.



Figure 73. Convolute bedding within Turnagain Arm rhythmites, Alaska, USA. **(A)** Convolution confined to a single bed within undeformed beds. Note the characteristic alternation between the sharp crests and broad troughs. **(B)** Distorted convolute bedding with only two distinguishable troughs. The unit is overlain by flat-laminated unit (rhythmite). Note the sharp contact between the two intervals. The marker is about 12 cm.

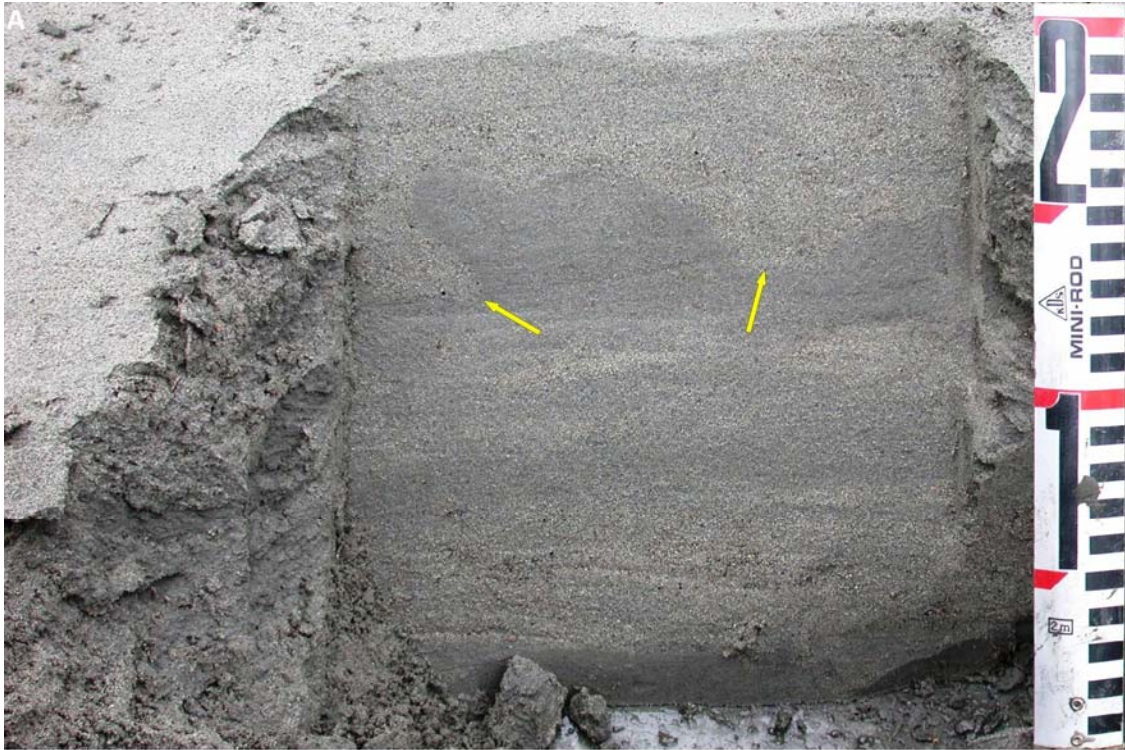


Figure 74. Load structures caused by unequal loading of sands over finer-grained deposits. **(A)** Load structures with rounded knobby bodies (yellow arrows) produced by the sinking of the sand into the underlying sediments. **(B)** Load structures produced by overloading, where the sand sank down in the form of lobes. Note how the underlying layers are distorted and bent downward under the lobes (lower center).



Figure 75. Load structures in uppermost intertidal flats. **(A)** Load structures along with some ball and flame structures (upper left). **(B)** A single, large flame structure (center) within just one-day accumulation. Note how the flame is pointed and tongue-shaped.

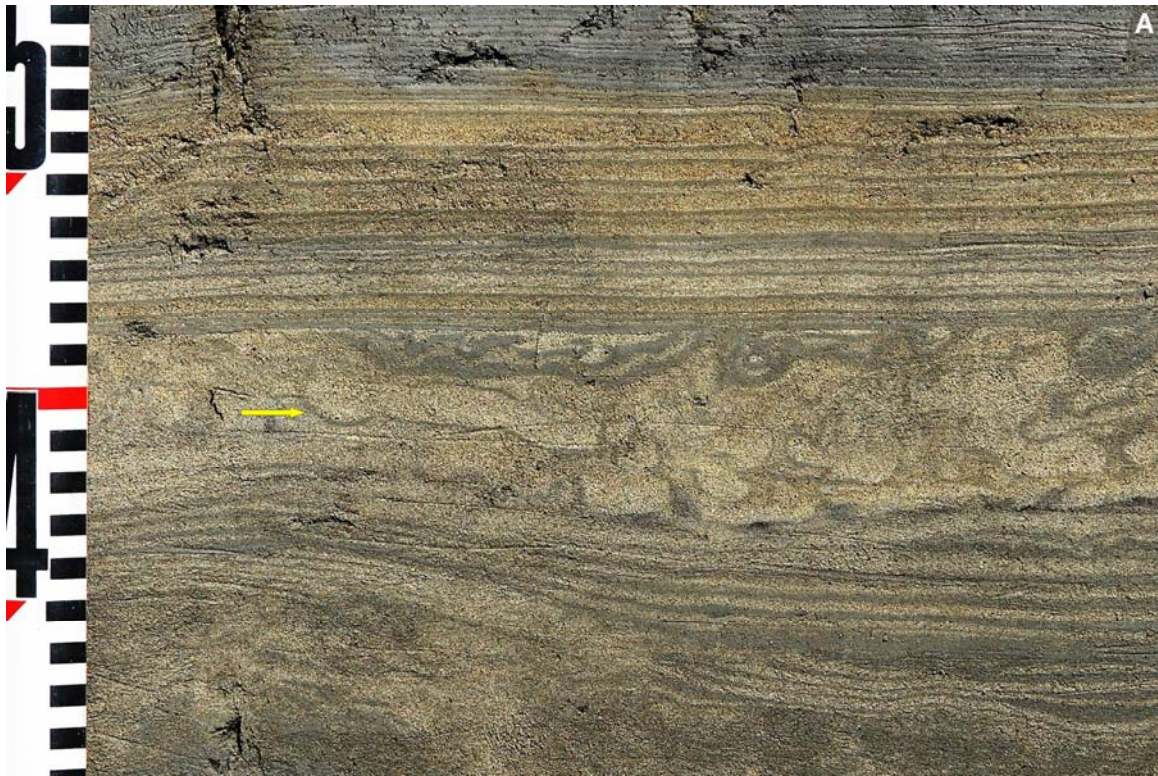


Figure 76. Contorted bedding within Turnagain Arm rhythmites. **(A)** Intensively contorted laminae with some small-scale dish structures (yellow arrow). **(B)** Distorted laminae (center). Note how contorted bedding is sharply underlain and overlain by untouched, flat-laminated deposits.

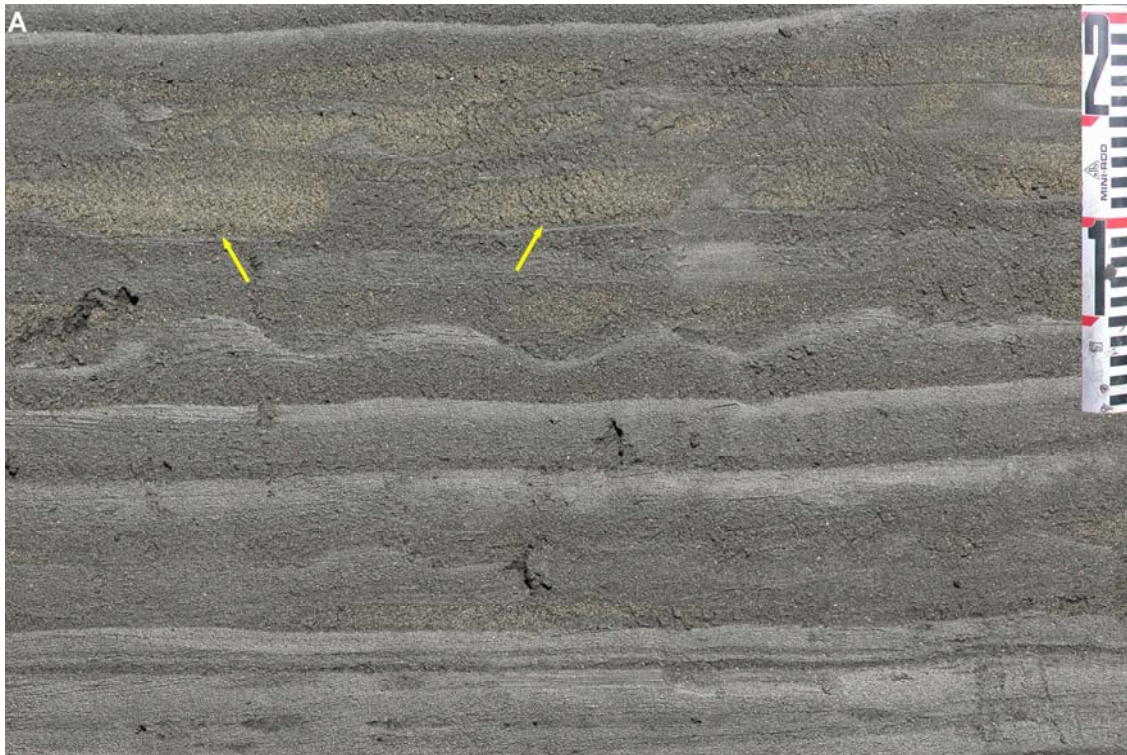


Figure 77. Ball-and-pillow structures. **(A)** Sand balls or masses (yellow arrows) apparently separated from the overlying sand layer. **(B)** Pillow-shaped sand body (center) floating in a muddy matrix. Note that the pillow is encased in some curved laminae, indicating the involvement of the underlying mud layers in the deformation.

Conclusions

The Tonganoxie paleovalley is a funnel-shaped erosional feature that was incised during the late Missourian sea level fall and then filled with sediments during an early Virgilian transgressive event. It contains a fining-upward succession of conglomerate, sandstone, and mudstone, exhibiting a transition from fluvial to estuarine to marine conditions, with marine influence increasing upward. Such incised valley fills (IVF) are very important as petroleum exploration targets. It is estimated that 15% of all oil-producing reservoirs and 28% of all gas-producing reservoirs in the state of Kansas are of IVF type, and nearly 50% of lately discovered oil reservoirs and 70% of gas bearing reservoirs are within incised valley fill deposits as well.

The Tonganoxie Sandstone Member (Stranger Formation, Douglas Group) (Upper Pennsylvanian) of northeastern Kansas is part of the Tonganoxie sequence, and it mostly consists of fluvial and estuarine sandstone and mudstone facies. These siliciclastic deposits are grouped into several facies assemblages. The planar-stratified siltstone assemblage, exposed at Buildex quarry in Franklin County, Kansas, contains the most prominent evidence for a strong tidal influence on the deposition of the Tonganoxie sequence. Precisely, it suggests deposition on tidal flats near or at the fluvial-estuarine transition zone situated within a huge macrotidal estuarine paleovalley. Very similar facies have been observed in Turnagain Arm of Cook Inlet, Alaska, USA. The two settings have a lot in common especially with regard to the existence of cyclic tidal rhythmites, high sedimentation rates and lack of bioturbation, characteristic biogenic and physical sedimentary structures, and some unique hydrodynamic conditions.

Cyclic tidal rhythmites are small tidal bundles that exhibit regular and systematic changes in thicknesses of successive laminae or thin beds. These thickness variations represent and reflect astronomically induced tidal evens such as neap and spring tides; thus, they are sometimes referred to as neap-spring cycles. These cycles consist of several sets of clay-draped ripples that are vertically stacked together, creating flaser, wavy, or lenticular bedding styles (heterolithic rhythmites). They may also consist of normally graded, flat-laminated siltstone interbedded with thin claystone beds or laminae (silty cyclic rhythmites). Tidal rhythmites are common in muddy, tide-dominated settings that are characterized by extreme tidal ranges and high sedimentation rates, and are dynamic

in nature. During this research, similar cyclic tidal rhythmites within some segments of the Tonganoxie Sandstone core, especially within Mechaskey part, and within uppermost intertidal flats of Turnagain Arm have been documented.

The basal Tonganoxie Sandstone Member and the intertidal flats of Turnagain Arm have almost identical assemblages of biogenic and physical sedimentary structures. These features include upright trees, ripple marks, *Arenicola* type bioturbation and burrows, wrinkle marks, foam marks, raindrop imprints, drip marks, mud volcanoes, and drag marks. They also include burrows and traces of *Plangtichnus* type, *Treptichnus*-like traces, arthropod trails and tracks, swirly biogenic features, looping biogenic features, and dewatering and degassing caverns. The high preservation potential of these structures and their occurrence on bed tops and soles suggest that high sedimentation rates, lack of bioturbation activities, and brief and periodic subaerial exposures are characteristics shared by both depositional settings.

Previous detailed studies have revealed that thick siltstone bedsets within the basal Tonganoxie Member exhibit vertical sedimentary structure sequences (VSS). These sequences consist of the following intervals: (A) a massive to normally graded interval; (B) a planar-laminated interval; (C) a cross-laminated interval; and (D) a laminated interval with drapes. Other studies have shown that sandbar deposits of Turnagain Arm contain similar four transitional facies of sedimentary assemblages. In general, they are characterized by combinations of planar laminae and ripple-cross laminae. The development of such vertical structure sequences suggests that hydrodynamic conditions of both settings are generally characterized by high tidal ranges, high current velocities, high sedimentation rates, and fluctuating flow regimes. This research has provided supportive evidence to back up these hydrodynamic interpretations by observing, analyzing, and interpreting some soft-sediment deformation structures within some intertidal flats of Turnagain Arm. In short, this was done by relating some soft-sediment deformation structures to certain deformational processes and then to certain preferable depositional conditions.

References Cited

- Archer, A.W., in press, Controls on Carboniferous Incised-valley Systems in Kansas.
- Archer, A.W., Kvale, E.P. and Johnson, H.R., 1991. Analysis of modern equatorial tidal periodicities as a test of information encoded in ancient tidal rhythmites. In: D.G. Smith, G.E. Reinson, B.A. Zaitlin and R.A. Rahmani (Editors), *Clastic Tidal Sedimentology*. Can. Soc. Pet. Geol. Mem., 16: 189-196.
- Archer, A. W., H. R. Feldman, E. P. Kvale, and W. P. Lanier, 1994a, Comparison of drier- to wetter-interval estuarine roof facies in the Eastern and Western Interior coal basins, USA: *Palaeogeography, Palaeoclimatology, Palaeoecology*, v. 106, p. 171–185.
- Archer, A. W., Lanier, W. P., and Feldman, H. R., 1994b, Stratigraphy and depositional history within incised-paleovalley fills and related facies, Douglas Group (Missourian/Virgilian; Upper Carboniferous) of Kansas, U.S.A.; in, *Incised valley systems—Origin and sedimentary sequences*, R. Boyd, B. A. Zaitlin, and R. Dalrymple, eds.: *Society of Economic Paleontologists and Mineralogists Special Publication*, v. 51, p. 175–190.
- Archer, A.W., 1995. Modeling of cyclic tidal rhythmites based on a range of diurnal to semidiurnal tidal-station data. *Marine Geology*, 123, 1-10.
- Archer, A.W., and Feldman, H.R., 1995, Incised Valleys and Estuarine Facies of the Douglas Group (Virgilian): Implications for similar Pennsylvanian Sequences in the U.S. Mid-Continent, in Hyne, N., eds., *Sequence Stratigraphy of the Mid-Continent*, Tulsa Geologic Society, p. 119-145.
- Archer, A.W., and Greb, S.F., 1995, An Amazon-Scale Drainage System in the Early Pennsylvanian of Central North America. *Journal of Geology*, v. 103, p. 611-628.
- Archer, A.W., and Greb, S.F., Depositional Zonation and Hypertidal Sedimentation within Turnagain Arm, Cook Inlet, Alaska, USA, Kansas: Kansas State University, Manuscript in preparation.
- Archer, A.W. and Johnson, T.W., 1997. Modeling of cyclic tidal rhythmites (Carboniferous of Indiana and Kansas, Precambrian of Utah, USA) as a basis for reconstruction of intertidal positioning and palaeotidal regimes. *Sedimentology*, 44, 991-1010.
- Archer, A.W., 2004, Recurring Assemblages of Biogenic and Physical Sedimentary Structures in Modern and Ancient Extreme Macrotidal Estuaries: *Coastal Research* v. 43, p. 4-22.

Archer, A.W. and Hubbard, M.S., 2003. Highest tides of the world, in Chan, M.A. and Archer, A. W., eds., Extreme depositional environments: mega end members in geologic time: Geological Society of America Special Paper, v.370, p. 151-173.

Archer, A.W. and Kvale, E.P., 1993. Origin of gray-shale lithofacies (clastic wedges) in U.S. midcontinental coal measures (Pennsylvanian): an alternative explanation. In: Cobb, J.C, Cecil, C.B (Eds.), Modern and ancient coal-forming environments. Geological Society of America Special Paper, v. 286, pp. 181-192.

Ball, S. M., 1964, Stratigraphy of the Douglas Group (Pennsylvanian, Virgilian) in the northern Midcontinent Region: Ph.D. thesis, University of Kansas, Lawrence, Kansas, 335 p.

Bandel, K., 1967, Isopod and limulid marks and trails in Tonganoxie Sandstone (Upper Pennsylvanian) of Kansas: The University of Kansas, Paleontological Contributions, v. 19, p. 1-10.

Banerjee, I., 1977, Experimental study on the effect of deceleration on the vertical sequence of sedimentary structures in silty sediments: *Journal of Sedimentary Petrology*, v. 47, p. 771-783.

Bartsch-Winker, S. and Ovenshine, A.T., 1984. Macrotidal subarctic environments of Turnagain and Knik Arms, Upper Cook Inlet, Alaska: sedimentology of the intertidal zone. *Journal of Sedimentary Petrology*, 54, 1221-1238.

Bartsch-Winkler, S., 1988. Cycle of earthquake-induced aggradation and related tidal channel shifting, upper Turnagain Arm, Alaska, USA. *Sedimentology*, 35, 621-628.

Bartsch-Winkler, S., Ovenshine, A.T., and Kachadoorian, R., 1983, Holocene history of the estuarine area surrounding Portage, Alaska as recorded in a 93-m core: *Canadian Jour. Earth Sciences* v. 20, p. 802-820.

Bartsch-Winkler, S., 1982, Physiography, texture, and bedforms in Knik Arm, Upper Cook Inlet, Alaska, during June and July 1980: U.S. Geological Survey Open-File Report 82-464, 6p.

Bass, N.W., 1936, Origin of the shoestring sands of Greenwood and Butler counties, Kansas: Kansas Geological Survey, Bulletin, no. 23, 135 pages.

Benyon, B. M., and Pemberton, S. G., 1992, Ichnological signature of a brackish water deposit—An example from the Lower Cretaceous Grand Rapids Formation, Cold Lake oil sands area, Alberta; in, Applications of ichnology to petroleum exploration—A core workshop, S. G. Pemberton, ed.: Society of Economic Paleontologists and Mineralogists, Core Workshop 17, p. 199-221.

Blum, M.D., and T.E. Törnqvist, 2000, Fluvial responses to climate and sea-level change: a review and look forward: *Sedimentology*, v. 47, p. 2-48.

Bowen, D. W., P. Weimer, and A. J. Scott, 1993, The relative success of siliciclastic sequence stratigraphic concepts in exploration: examples from incised valley fill and turbidite system reservoirs, in P. Weimer and H. Posamentier, eds., *Siliciclastic sequence stratigraphy: AAPG Memoir 58*, p. 15–42.

Bower, R.R., 1961, Dispersal centers of sandstones in the Douglas Group (Pennsylvanian) of Kansas: M.S. thesis, Department of Geology, University of Kansas, Lawrence, KS, 19 pages.

Bowsher, A. L., and J. M. Jewett, 1943, Coal resources of the Douglas Group in east-central Kansas: Geological Survey of Kansas, Bulletin 46, 94 p.

Buatois, L.A.; Mangano, G.; Maples, C.G.; and Lanier, W.P., 1998, Allostratigraphic and sedimentologic applications of trace fossils to the study of incised estuarine valleys; an example from the Virgilian Tonganoxie Sandstone Member of eastern Kansas, pp. [1]-27, In Brosius, L., (ed.); *Current research in earth sciences, 1998*. Kansas Geological Survey, Bulletin, no. 241, pt. 1, p. 1-27

Buatois, L.A.; Mangano, M.G.; Maples, C.G.; and Lanier, W.P., 1997, The paradox of nonmarine ichnofaunas in the tidal rhythmities; integrating sedimentologic and ichnologic data from the Late Carboniferous of eastern Kansas, USA. *Palaios*, vol. 12, no. 5, pp. 467-481.

Carlson, R.F., 1970, The nature of tidal hydraulics in Cook Inlet: *The Northern Engineer*, v. 2, p. 4-7.

Cecil, C. B., 1990, Paleoclimatic controls on stratigraphic repetition of chemical and siliciclastic rocks: *Geology*, v. 18, p. 533–536.

Coveney, R. M., JR., Watney, W. L., and Maples, C.G., 1991, Contrasting depositional models of Pennsylvanian black shales discerned from molybdenum abundances: *Geology*, v. 19, p. 147-150.

Dalrymple, R.W., R.J. Knight B.A. Zaitlin, and G.M. Middleton, 1990, Dynamics and facies model of a macrotidal sand-bar complex, Cobequid Bay-Salmon River Estuary (Bay of Fundy): *Sedimentology*, v. 37, p. 577-612.

Dalrymple, R.W.; Makino, Y., and Zaitlin, B.A., 1991. Temporal and spatial patterns in rhythmities deposition on mud flats in the macrotidal Cobequid Bay- Salmon River estuary, Bay of Fundy, Canada. *In*: Smith, D.G.; Reinson, G.E.; Zaitlin, B.A., and Rahmani, R.A. (eds.), *Clastic Tidal Sedimentology, Memoir Canadian Society of Petroleum Geology*, 16, 137-160.

Dalrymple, R.W., B.A. Zaitlin, and R. Boyd, 1992, Estuarine facies models: Conceptual basis and stratigraphic implications: *Journal of Sedimentary Petrology*, v. 62, p. 1130-1146.

Dalrymple, R.W., Boyd, R. and Zaitlin, B. A. (Eds) (1994). History of research, types and internal organization of incised-valley systems: Introduction to the Volume. In: *Incised-Valley Systems: Origin and Sedimentary Sequences* (Ed. By R. W. Dalrymple, R. Boyd and B. A. Zaitlin), *Spec. Publ. Soc. Econ. Paleont. Miner*, 51, 3-10.

Ehlers, T.A. and Chan, M.A., 1999. Tidal sedimentation and estuarine deposition of the Proterozoic Big Cottonwood Formation, Utah. *Journal of Sedimentary Research*, v. 69, No. 6, p. 1169-1180.

Feldman, H. R., Gibling, M. R., Archer, A. W., Wightman, W. G., and Lanier, W. P., 1995, Stratigraphic architecture of the Tonganoxie paleovalley fill (lower Virgilian) in northeastern Kansas: American Association of Petroleum Geologists, Bulletin 79, p. 1,019–1,043.

Gerlach, P., 2000, Oil and gas production from incised valley fill reservoirs in Kansas: Kansas Geological Survey. February 16, 2000.

Gibling M.R. and Wightman, W.G., 1994, Palaeovalleys and protozoan assemblages in a Late Carboniferous cyclothems, Sydney Basin, Nova Scotia: *Sedimentology*, v. 41, p. 699-719.

Greb, S.F., and Archer, A.W., 2007, Soft-sediment deformation produced by tides in a hypertidal estuary in a meizoseismic area, Turnagain Arm, Alaska: *Geology*, v. 35, p. 435-438.

Heckel, P.H., 1977, Origin of phosphatic black shale facies in Pennsylvanian cyclothems of mid-continent North America: *AAPG Bulletin*, v. 61, p. 1045–1068.

Heckel, P.H., 1983, Diagenetic model for carbonate rocks in Midcontinent Pennsylvanian eustatic cyclothems: *Journal of Sedimentary Petrology*, v. 53, p. 733-759.

Heckel, P.H., 1986, Sea-level curve for Pennsylvanian eustatic marine transgressive-regressive depositional cycles along the Midcontinent outcrop belt, North America: *Geology*, v. 14, p. 330-334.

Kvale, E.P. and Archer, A.W., 2007. Paleovalley fills: Trunk vs. tributary. *AAPG Bulletin*, v. 91, No. 6, p. 809-821.

Kvale, E. P., 2006, The origin of neap-spring tidal cycles: *Marine Geology*, v. 235, p. 5-18.

Kvale, E.P.; Johnson, H.W.; Sonett, C. P.; Archer, A.W.; and Zawistoski, A., 1999. Calculating lunar retreat rates using tidal rhythmites. *Journal of Sedimentary Research*, v. 69, No. 6, p. 1154-1168.

Kvale, E.P.; Archer, A.W., and Johnson, H., 1989. Daily, monthly, and yearly tidal cycles within laminated siltstones: Mansfield Formation (Pennsylvanian) of Indiana. *Geology*, 17, 365-368.

Kvale, E.P. and Archer, A.W., 1990. Tidal deposits associated with low-sulfur coals, Brazil Fm. (Lower Pennsylvanian), Indiana. *Journal of Sedimentary Petrology*, v.60, p. 563-574.

Kvale, E.P. and Archer, A.W., 1991. Characteristics of two Pennsylvanian-age semidiurnal tidal deposits in the Illinois Basin, U.S.A. *In*: Smith, D.G., Reinson, G.E.; Zaitlin, B.A., and Rahmani, R.A. (eds.), *Clastic Tidal Sedimentology*, Canadian Society of Petroleum Geologists Memoir 16, p. 179-188.

Lanier, W. P., H. R. Feldman, and A. W. Archer, 1993, Tidal sedimentation from a fluvial to estuarine transition, Douglas Group, Missourian-Virgilian, Kansas. *Journal of Sedimentary Petrology*, v. 63, No. 5, p. 860–873.

Lanier, W. P., 1993, Bedform sedimentology of the Lonestar Spillway and Buildex Quarry stops; in, *Incised Paleovalley of the Douglas Group in northeastern Kansas—Field Guide and Related Contributions*, A. W. Archer, H. R. Feldman, and W. P. Lanier, eds.: Kansas Geological Survey, Open-file Report 93-24, p. 4-1 to 4-10.

Lins, T.W., 1950, Origin and environment of the Tonganoxie Sandstone in northeastern Kansas: Kansas Geological Survey, Bulletin, no. 86, pt. 5, pp. 105-140.

MacEachern, J. A., and Pemberton, S. G., 1994, Ichnological aspects of incised valley fill systems from the Viking Formation of the Western Canada Sedimentary Basin, Alberta, Canada; in, *Incised valley systems—Origin and sedimentary sequences*, R. Boyd, B. A. Zaitlin, and R. Dalrymple, eds.: Society of Economic Paleontologists and Mineralogists, Special Publication 51, p. 129–157.

Mazumder, R. and Arima, M., 2005. Tidal rhythmites and their implications. *Earth-Science Reviews*, v. 69, p. 79-95.

Mills, P.C., 1983. Genesis and diagnostic value of soft-sediment deformation structures—a review. *Sedimentary Geology*, v. 35, p. 83-104.

Minor, J.A., 1969, Petrology of the Tonganoxie sandstone (Pennsylvanian), Kansas-Missouri: M.A. thesis, Department of Geology, University of Missouri, Columbia, MO, 98 pages.

- Moore, R. C., 1949, Divisions of the Pennsylvanian System in Kansas: Geological Survey of Kansas, Bulletin 83, 203 p.
- Moore, R.C., 1950, Late Paleozoic cyclic sedimentation in central United States: International Geological Congress, Eighteenth Report, pt. 4. pp. 5-16.
- Mudge, M.R., 1956, Sandstones and channels in Upper Pennsylvanian and Lower Permian in Kansas: American Association of Petroleum Geologists, Bulletin, v. 40, no. 4, pp. 654-678.
- Oey, L.Y.; Ezer, T.; Hu, C.; and Muller-Karger, F.E., 2007. Baroclinic tidal flows and inundation processes in Cook Inlet, Alaska: numerical modeling and satellite observations: *Ocean Dynamics*, v. 57, p. 205–221.
- Ovenshine, A.T.; Bartsch-Winkler, S.; O'Brien, N.R., and Lawson, D.E., 1976, Sedimentation of the high tidal range environment of upper Turnagain Arm, Alaska, in Miller, T.P., ed., Recent and Ancient Sedimentary Environments in Alaska: Anchorage, Alaska Geological Society Symposium Proceedings, p. M1-M26.
- Pemberton, S. G., and Wightman, D. M., 1992, Ichnological characteristics of brackish water deposits; in, Applications of ichnology to petroleum exploration—A core workshop, S. G. Pemberton, ed.: Society of Economic Paleontologists and Mineralogists, Core Workshop 17, p. 141–167.
- Posamentier, H.W. and Vail, P.R. (1988) Eustatic controls on clastic deposition II- Sequence and systems tract models. In: *Sea-Level Changes: an Integrated Approach* (Ed. By C.K. Wilgus, B. S. Hastings, C. G. S. C. Kendall, H. W. Posamentier, C.A. Ross and J. C. Van Wagoner), Spec. Publ. Soc. Econ. Paleont. Miner., 42, 125-154.
- Posamentier, H.W., Jervey, M. T. and Vail, P.R. (1988) Eustatic controls on clastic deposition I- Conceptual frameworks. In: *Sea-Level Changes: an Integrated Approach* (Ed. by C.K. Wilgus, B.S. Hastings, C.G.S.C. Kendall, H.W. Posamentier, C.A. Ross and J.C. Van Wagoner), Spec. Publ. Soc. Econ. Paleont. Miner., 42, 109-124.
- Potter, P.E. and Pettijohn, F.J., 1977. Paleocurrents and Basin Analysis. Springer, New York, N.Y., 425 pp.
- Ranger, M. J., and Pemberton, S. G., 1992, The sedimentology and ichnology of estuarine point bars in the McMurray Formation of the Athabasca Oil Sands Deposit, northeastern Alberta, Canada; in, Applications of ichnology to petroleum exploration—A core workshop, S. G. Pemberton, ed.: Society of Economic Paleontologists and Mineralogists, Core Workshop 17, p. 401–421.
- Reineck, H.E., and Singh, I.B., 1973, Depositional Sedimentary Environments, with reference to terrigenous clastics: New York, Springer-Verlag, 439 p.

Salcedo, G.A., and Carr, T.R., 2003, Regional sequence stratigraphy and depositional environments of Lower Pennsylvanian reservoir sandstones, southwestern Kansas: Kansas Geological Survey, Open-file Report, no. 2003-34.

Schumm, S.A. (1977) *The Fluvial System*. John Wiley, New York.

Schumm, S.A. and Brakenridge, G.R. (1987) River responses. In: *North America and Adjacent Oceans during the Last Deglaciation* (Ed. by W.F. Ruddiman and H. E. Wright), *The Geology of North America*. K-3, pp. 221-240. Geological Society of America.

Sharma, G.D. and Burrell, D.C., 1970, Sedimentary environment and sediments of Cook Inlet, Alaska: AAPG, bulletin, v. 54, p. 647-654.

Stephens, C.G.; Rutherford, R.E.; Polson, A.S., Jr.; Commisso, M.D.; and Archer, A.W., 1999, Conglomerates associated with Pennsylvanian incised valley-fill sequences of eastern Kansas, pp. 136-140, In, Merriam, D.F., (ed.); *Geoscience for the 21st century*, transactions of the 1999 American Association of Petroleum Geologists, Midcontinent Section Meeting. Kansas Geological Survey, Open-file Report, no. 99-28, 224 pages.

Stephens, C.D., Lahr, J.C., and Page, R.A., 1984, Seismicity in southern coastal and southeastern Alaska, October 1981-September 1982, in Reed, K. M., and Bartsch-Winkler, S., eds., *The U.S. Geological Survey in Alaska: Accomplishments during 1982*: U. S. Geol. Survey, Circular 939, p. 65-67.

Tarr, R.S., 1934, Origin of Bartlesville shoestring sands, Greenwood and Butler counties, Kansas [discussion]: AAPG, Bulletin, v. 18, no. 12, pp. 1710-1712.

Tessier, B.; Archer, A.W.; Lanier, W.P., and Feldman, H.R., 1995. Comparison of ancient tidal rhythmites (Carboniferous of Kansas and Indiana, USA) with modern analogues (the Bay of Mont-Saint-Michel, France). *International Association of Sedimentologists (IAS), Special Publication*, 24, 259-271.

Van Wagoner, R. M., R. M. Mitchum, K. M. Campion, and V. D. Rahmanian, 1990, Siliciclastic sequence stratigraphy in well logs, cores, and outcrops: concepts for high-resolution correlation of time and facies: AAPG Methods in Exploration Series 7, 55 p.

Wanless, H.R. and Weller, J.M., 1932, Correlation and extent of Pennsylvanian cyclothems: Geological Society of America, Bulletin, v. 43, no. 4, pp. 1003-1016.

Wells, M.R.; Allison, P. A.; Hampson, G.J.; Piggott, M.D., and Pain, C.C., 2005. Modelling ancient tides: the Upper Carboniferous epi-continental seaway of Northwest Europe. *Sedimentology*, v. 52, p. 715-735.

Wightman, W.G., D.B. Scott, F.M. Medioli, and M.R. Gibling, 1993, Carboniferous march foraminifera from coal-bearing strata at the Sydney basin, Nova Scotia: a new tool for identifying paralic coal-forming environments: *Geology*, v. 21, p. 631-634.

Wood, J.M., J.C. Hopkins, 1989, Reservoir sandstone bodies in estuarine valley fill: Lower Cretaceous Glauconitic Member, Little Bow Field, Alberta, Canada: *AAPG Bulletin*, v. 73, p. 1361-1382.

Zaitlin, B.A., R.W. Dalrymple, and R. Boyd, 1994. The stratigraphic organization of incised-valley systems associated with relative sea-level change, *in* R. Dalrymple, R. Boyd, and B. Zaitlin, eds., *Incised valley systems: Origin and sedimentary sequences*; *SEPM Special Publication 51*, p. 45-60.

APPENDIX A
Accumulation Rates

Location 1: Tidal Bore, flags were put on the 6th and checked on the 7th of August 2006, 1st row.

Flag No.	Accumulation Rate (ft)
1	6"
2	No data
3	7"
4	7"
5	8"
6	8" ½
7	8"
8	7" ½
9	6" ¾
10	6"
11	6" ½
12	6" ¾
13	5"
14	6" ½
15	No data
16	1"
17	1' 2"
18	No data

Location 2: Tidal Bore, flags were put on the 6th and checked on the 7th of August 2006, 2nd row.

Flag No.	Accumulation Rate (ft)
1	No data
2	No data
3	3"
4	6" 5/8
5	6" 5/8
6	6" ¾
7	1' 1" ¾
8	7" 3/8
9	8"
10	7" 5/8
11	7" ½
12	6" 7/8
13	7"
14	8" 3/8
15	8" ½
16	6" 3/8
17	6" 3/8
18	7" 1/8

19	7" 3/8
20	8" 1/8
21	8" 1/2
22	8" 5/8
23	10"
24	9" 7/8
25	8" 1/8
26	No data
27	2" 1/2
28	4" 1/4

Location 3: Bird Point, put on the 6th and checked on the 8th of August 2006.

Flag No.	Accumulation Rate (ft)
1	No data
2	2"
3	2" 5/8
4	2" 1/4
5	3" 1/4
6	1" 3/8
7	1" 5/8
8	1" 1/2
9	1" 1/4
10	1" 1/4
11	5/8"
12	1" 5/8
13	1' 1"
14	1" 1/2
15	1" 1/4

Location 4: Peterson Creek, put on the 6th and checked on the 8th of August 2006.

Flag No.	Accumulation Rate (ft)
1	1" 1/8
2	3/4"
3	3/4"
4	5/8"
5	1/2"
6	5/8"
7	1"
8	7/8"
9	3/8"
10	1/4"
11	1/2"
12	3/8"

Location 5 : Girdwood, put on the 7th and checked on the 9th.

Flag No.	Accumulation Rate (ft)
1	3/4"
2	1/2"
3	No data
4	3/8"
5	1/2"
6	1/2"
7	5/8"
8	5/8"
9	3/8"
10	1/2"
11	3/8"
12	3/8"
13	1/2"

Location 6: Tidal Bore # 1, top set, flags were put on the 10th and checked on the 11th of August 2006.

Flag No.	Accumulation Rate (ft)
1	No data
2	3" 1/4
3	5" 3/4
4	4"
5	2" 1/2
6	No data
7	No data
8	No data
9	No data
10	2" 1/4
11	1" 7/8
12	2" 3/8
13	1" 5/8
14	1" 5/8
15	2" 3/8

Location 7: Portage Creek # 2, flags were put on the 10th and checked on the 13th of August 2006.

Flag No.	Accumulation Rate (ft)
1	1" 1/8
2	1/2"
3	1/8"
4	1/16"
5	1" 3/4
6	2" 7/8
7	4"
8	2" 1/2
9	1" 1/4
10	1" 1/4
11	7/8"
12	1" 1/2
13	1"
14	1" 3/8
15	3/4"
16	1/2"
17	3/8"
18	3/8"
19	1/16"
20	1/8"
21	1/2"
22	1/16"
23	1/8"
24	3/8"
25	1/16"
26	1/4"
27	1/8"
28	1/8"
29	1/4"
30	1/8"
31	1/4"
32	3/8"
33	1/2"

APPENDIX B
Core Description

(1) Mechaskey Core Description

Unit No.	Depth (feet)	Thickness (feet)	Description
1	2-8.02	6.02	Packstone, traces of iron oxides, sparry calcite, clasts, some woods and roots.
2	9.5	1.48	Paleosol
3	12.87	3.37	Massive, dark shale
4	14.48	1.61	Light gray limestone (Wackstone). Some concretions and clasts.
5	15.27	0.79	Light green shale
6	23.05	7.78	Light-colored Wackstone with paleosol in the lower part of the unit.

7	31.74	8.69	Light, greenish, sandy shale, highly micaceous, massive in parts. Lamination and thin bedding. Pinstripe.
8	38.32	6.58	Light, gray shale similar to the shale in unit 7, but it has less mica and less sand and is poorly laminated, almost massive. Pinstripe.
9	38.45	0.13	Coal bed (coal smut).
10	54.58	16.13	Light greenish paleosol. Structureless. Some very thin laminae of organic material at the bottom.
11	63.76	9.18	Shale, very thin lamination, the shale becomes darker with increasing depth, horizontal bedding. It contains black spots of organic material. The laminae and the beds become thicker with increasing depth. Transition to underlying coal bed.
12	65.5	1.74	Coal bed, partings and layers of mud.
13	66.22	0.72	Paleosol

14	71.24	5.02	Light-colored shale, lamination, pinstripe, few deformation structures.
*15	99.29	28.05	Alternations of dark mud and light sand, pinstripe, laminations, deformation structures. At the top of the unit the sand and the mud ratio is almost the same; but then, the mud ratio starts to dominate the unit.
**16	101.06	30.2	Mostly massive mudstone with some deformation structures. Pinstripes. Thin lamination.
17	147.06	17.57	Very thin planar lamination with no deformation zones. The thickest sand laminae are about 0.2 mm or less, mud dominated unit.

***Description of subunits of unit 15 (Mechaskey)**

Unit No.	Thickness (feet)	Deformation Zone(s)	Thickest Sand (cm)	Thickest Mud (cm)
15-1	1.94	4	2	5
15-2	1.80	1	2.5	6
15-3	2.02	0	1.4	1.5
15-4	1.92	3	2	10
15-5	1.81	1	1	3
15-6	1.86	2	1.5	6
15-7	1.91	0	0.7	3
15-8	1.94	1	0.9	2.7

15-9	1.74	0	1.1	10.2
15-10	1.68	0	0.8	8
15-11	1.77	0	0.8	3
15-12	1.89	2	1.5	6.5
15-13	1.92	4	0.4	14
15-14	1.9	2	0.5	1.7
15-15	1.95	3	0.3	1

**** Description of subunits of unit 16 (Mechaskey)**

Unit No.	Thickness (feet)	DZ	Thickest Sand (cm)	Thickest Mud (cm)	Remarks
16-1	1.77	1	--	--	Massive mudstone, no sand
16-2	1.84	2	--	--	Mud
16-3	1.92	0	0.2	0.5	Lamination at the bottom
16-4	1.74	0	0.2	2	Lamination and Pinstripe
16-5	1.89	2	0.3	The rest of the core	Pinstripe
16-6	3.8	0	--	--	Mud dominated with some pinstripes

16-7	5.52	1	--	--	Mud dominated. Pinstripe
16-8	11.72	0	--	--	Massive mud with few pinstripes.

(2) Aelschlaeger Core Description

Unit No.	Thickness (feet)	Depth (feet)	Description
1	1.97	0 – 1.97	Highly fossiliferous Packstone, mostly Pelecypods and brachiopods. It contains grains, clasts, and some deformation structures.
2	1.15	3.12	Coarse sandstone with some fossils, mainly Pelecypods. Moderately sorted.
3	2.12	5.24	Medium to coarse sandstone. Some fossils. Micaceous. Moderate to well sorted. Structureless, oolitic in some parts.
4	1.02	6.26	Fine to coarse sandstone, no fossils, fine at the top and coarse at the bottom, well sorted to moderately sorted, Structureless (Massive).
5	1.97	8.23	Coarse gray sandstone, massive, micaceous, well sorted, no fossils.
6	0.36	8.59	Very deformed paleosol.
7	0.54	9.13	Massive, coarse

			sandstone, no fossils, moderately micaceous, well sorted.
8	0.74	9.87	Fine to medium sandstone, highly micaceous, some fossils, massive
9	3.1	12.97	Muddy, silty weathered sandstone.
10	26.5	39.47	Silty mudstone, light to dark in color, mostly massive, not well laminated.
11	0.6	40.07	Very dark shale, rich in organic material.
12	1.05	41.12	Black coal
13	0.3	41.42	Carbonaceous shale contains many clasts.
14	0.1	41.52	Massive shale, some clasts.
15	7.9	49.42	Well developed paleosol.
16	0.7	50.12	Thinly laminated shale.
17	2.4	52.52	Sandy mudstone.
18	1.2	53.72	Well sorted sandstone with some shale laminae at the top of the unit.
19	0.7	54.42	Fine to medium sandstone, well sorted, very highly micaceous, cross-bedded and laminated, interbedded with some very thin shale laminae.
20	6.9	61.32	Very coarse sandstone, very well

			to well sorted almost massive, silica as cement.
21	2	63.32	Coarse to very coarse laminated sandstone, well sorted, micaceous, high amount of iron oxide (Patches of iron oxides), cross-bedded at the top.
22	3	66.32	Medium sandstone, massive to laminated, very well sorted.
23	2.2	68.52	Medium to fine sandstone, highly micaceous, well-developed mud drapes, some ripples, very well sorted.
24	1.9	70.42	Very coarse sandstone, massive, very high amount of iron oxide as patches, well sorted.
25	3	73.42	Massive coarse sandstone, some iron oxide patches, well sorted.
26	1.2	74.62	Medium laminated sandstone, well sorted, cross-bedded.
27	3.5	78.21	Very coarse brownish sandstone, moderately to poorly sorted, rich in iron oxides. Contains clasts, cross-bedded to massive, some organic material.
28	2	80.21	Medium sandstone, very well to well

			sorted, massive to rippled and laminated in some parts, very thin laminae of organic material.
29	0.6	80.81	Brown coarse sandstone, very poorly sorted, some clasts, very thin coal laminae.
30	1.2	82.02	Conglomerate
31	0.3	82.32	Fine to very coarse sandstone, well to poorly sorted, interbedded with coal laminae.
32	0.4	82.72	Very coarse sandstone, very poorly sorted, silica-cemented, mud at the bottom of the unit.
33	4	86.72	Coarse sandstone, very well sorted, some shale, silica as a cement, massive, traces of mica.
34	0.8	87.52	Coarse laminated sandstone, very well sorted, silica as a cement, massive, high amount of organic material as layers.
35	8.7	96.22	Coarse sandstone, very well sorted, mostly massive with some laminae in some parts.
36	8.9	105.12	Coarse sandstone, very well sorted, partly laminated, very thin organic laminae (coal).
37	0.5	105.62	Sandstone

			interbedded with conglomerate.
38	0.6	106.22	Conglomerate
39	0.1	106.32	Calcareous shale
40	0.7	107.02	Well developed mudstone.
41	3.2	110.22	Gray wackstone, fossils mostly brachiopods and Pelecypods,
42	1.4	111.62	Gray sandstone
43	2.1	113.72	Flaser bedding, deformation structures (load casts).
44	4.9	118.62	Gray to greenish paleosol.
45	15.9	134.52	Massive wackstone, stylolite, beds and layers of mud.
46	3.6	138.12	Fine black shale, very rich in organic material.

APPENDIX C

Data Stations of the Turnagain Arm, Alaska, USA

Station Number	Latitude	Longitude	Description
1702	61.0764	-149.8269	Rabbit Creek (discharge data)
1700	61.0508	-149.7955	State Park Headquarters
1692	61.0302	-149.7617	slow vehicle turnout
1690	61.0166	-149.7331	McHugh creek trailhead
1686	61.0071	-149.6948	Beluga Point
1684	60.9996	-149.6501	camera spot
1672	60.9233	-149.6500	Porcupine Campground (south side)
1670	60.9083	-149.6417	Hope (south side)
1668	60.9847	-149.6091	2nd camera spot
1666	60.9844	-149.5757	Falls Creek trailhead
1664	60.9849	-149.4994	Indian Creek
1653	60.9739	-149.4664	Bird Creek bridge
1652	60.9689	-149.4564	flats at Bird Creek campground
1600	60.9291	-149.3464	Bird Point (beluga statues)
1540	60.9325	-149.3232	Tidal bore lookout. 1 st pull off east. All American road/Scenic surroundings/Turnagain's formative years signs
1530	60.9361	-149.2887	Tidal bore lookout with rock. 2 nd pulloff. Tower in middle. Follow the breeders/Whale depleted signs
1520	60.9369	-149.2654	Tidal bore lookout. 3 rd pulloff. Gray water/Tricky mudflats/Boring tide never signs
1510	60.9387	-149.2405	Tidal bore lookout with rock island. 4 th pulloff. Tower on side. Great quake sign
1500	60.9421	-149.2113	Tidal bore lookout with flats. 5th pulloff. Rivers of ice/Glacial dimensions signs
1410	60.9446	-149.1889	Tidewater Slough bridge
1400	60.9426	-149.1816	Girdwood dead spruce (west end)
1300	60.9392	-149.1686	Glacier Creek bridge
1200	60.9321	-149.1538	Virgin Creek
1180	60.9071	-149.0834	Chugach Nat. Forest sign
1130	60.8857	-149.0485	Peterson Creek
1110	60.8559	-149.0102	Beluga lookout (no pull off)

1100	60.8462	-148.9907	20 Mile River bridge
1090	60.8172	-148.9889	Placer River bridge
1050	60.8266	-148.9771	Portage Creek 2
1040	60.8186	-148.9653	Portage Creek 1
1010	60.7917	-148.9017	Portage River (turbidity mixing area, braided)
1002	60.7859	-148.8438	Portage River (headwaters, below lake)
1000	60.7834	-148.8410	Portage Lake (icebergs)

